의학박사 학위논문

Molecular mechanisms of UV-induced skin responses

자외선에 의한 피부 반응의 분자기전

2018 년 2 월

서울대학교 대학원

의과학과 의과학전공

이 석 진

A thesis of the Degree of Doctor of Philosophy

자외선에 의한 피부 반응의 분자기전

Molecular mechanisms of UV-induced skin responses

February 2018

The Department of Biomedical Science

Seoul National University

College of Medicine

Seok-jin Lee

Molecular mechanisms of UV-induced skin responses

by

Seok-Jin Lee

A thesis submitted to the Department of Biomedical Science in partial fulfillment of the requirements for the Degree of Doctor of Philosophy in Medical Science at Seoul National University College of Medicine

December 2017

Approved by Thesis Committee:

Professor _____ **Chairman**

Professor _____ **Vice chairman**

Professor _____

Professor _____

Professor _____

ABSTRACT

Molecular mechanisms of UV-induced skin responses

Seok-Jin Lee

Department of Biomedical Science

Seoul National University College of Medicine

Ultraviolet radiation (UVR) can profoundly affect human skin as it functionally naked unlike other furred animals. UV-irradiated skin exhibits several unique features, including sunburn and tanning responses at the acute level, an increased risk of developing skin cancer, immunosuppression and photoaging at the chronic level. Among these, tanning (melanogenesis), sunburn and wrinkles are being actively investigated in the clinical and cosmetic fields.

The first chapter discusses the molecular mechanism of anti-melanogenic effects of 4-n-butylresorcinol investigated. 4-n-butylresorcinol is a competitive inhibitor of tyrosinase and has been used as an anti-melanogenic agent. However, its anti-melanogenic mechanism(s) in cell is not fully understood. In this study, it was discovered that 4-n-butylresorcinol regulates tyrosinase protein level, but not its mRNA level, through promotion of the proteolytic degradation of tyrosinase. Moreover, 4-n-butylresorcinol-mediated activation of p38 MAPK was observed, which promotes ubiquitination of tyrosinase. Treating B16F10 cells with E64 or proteasome inhibitors restores 4-n-

butylresorcinol-mediated decrease of tyrosinase. These findings will assist with the development new, effective and safe agents for the treatment of hyperpigmentation disorders.

The second and third chapters discuss the role of transglutaminase 2 (TG2) in UV-irradiated epidermal and dermal tissues investigated. TG2 catalyzes the posttranslational modification of substrate proteins, including crosslinking, polyamination and deamidation. While epidermal keratinocytes and dermal fibroblasts have been known to express TG2, there still is lack of knowledge regarding this enzyme's role in regulation of skin homeostasis.

Chapter 2 discusses the role of TG2 in UV-induced acute skin inflammation was investigated through the use of human and mouse keratinocytes as well as TG2-deficient mice. TG2-deficient mice exhibited reduced UV-induced skin inflammatory phenotypes, including decreased erythema, edema, dilation of blood vessels, immune cell infiltration and expression of inflammatory cytokines. Using HaCaT cells and primary mouse keratinocytes, it was observed that TG2 is activated following UV irradiation without increase of its protein level and that UV-induced phospholipase C activation followed by ER calcium release was a prerequisite for TG2 activation. Moreover, activated TG2 enhanced transcriptional activity of NF-κB which leads expression of inflammatory cytokine genes such as interleukin-6, -8 and TNF-α. These results not only indicate that TG2 serve as a critical mediator of cytokine expression in the UV-induced inflammatory response of keratinocytes, but also suggest that TG2 inhibition might be a useful target for the prevention of sunburn.

Chapter 3 discusses the role of fibroblasts TG2 in UV-exposed fibroblasts investigated by using primary human and mouse dermal fibroblasts and *ex vivo* mouse skin culture model. In this study, it was revealed that human matrix metalloproteinase (MMP) -1 and -3, and mouse MMP-13 expressions are regulated by UV-induced activation of TG2 as well as its protein level. It was also found that TG2 regulates MMP gene transcription through NF-κB rather than AP-1 pathway. This study provides a new insight that TG2 can be a new therapeutic target for the treatment for UV-induced skin disorders like photoaging.

In summary, all of above studies have focused on elucidating molecular mechanisms of responses in UV-irradiated skin cells, including melanocytes, keratinocytes and fibroblasts, and suggest new molecular mechanisms that can be considered in treating of UV-induced skin damages.

Keywords: 4-n-butylresorcinol, melanogenesis, tyrosinase, transglutaminase 2, inflammatory cytokines, matrix metalloproteinase 1, NF-κB, ultraviolet radiation

Student Number: 2008-22006

*** Chapter 1 and 2 are published in International Journal of Cosmetic Science (2016) and Cell Death & Disease (2017), respectively.**

CONTENTS

LIST OF TABLES AND FIGURES

Chapter 1

Chapter 2

Chapter 3

General Discussion

LIST OF ABBREVIATIONS

2-APB: 2-aminoethyl diphenylborinate

4BR: 4-n-butylresorcinol

ANOVA: analysis of variance

AP-1: activator protein-1

CBA: cytokine bead array

CE: cornified envelope

DAG: diacylglycerol

Endo H: endoglycosidase H

ER: endoplasmic reticulum

H&E: hematoxylin and eosin stain

HDFs: human dermal fibroblasts

IHC: immunohistochemistry

IL-6: interleukin 6

IL-8: interleukin 8

IP_3: inositol triphosphate

IP_3R: inositol triphosphate receptor

IκBα: nuclear factor of kappa light polypeptide gene enhancer in B-cell inhibitor, alpha

MDFs: mouse dermal fibroblasts

MITF: microphthalmia-associated transcription factor

MMP-1: matrix metalloproteinase-1

MMP-13: matrix metalloproteinase-13

MMP-3: matrix metalloproteinase-3

MNEKs: mouse neonatal epidermal keratinocytes

NF-κB: nuclear factor kappa light chain enhancer of activated B cells

PIC: proteasome inhibitor cocktail

PIP_2: phosphatidylinositol 4,5-bisphosphate

PLC: phospholipase C

PNGase F: peptide:N-glycosidase F

QRT-PCR: quantitative real-time PCR

ROS: reactive oxygen species

SEM: standard error of mean

TG2: transglutaminase 2

TNF-α: tumor necrosis factor alpha

TRP-1: tyrosinase-related protein 1

TRP-2: tyrosinase-related protein 2

TUNEL: Terminal deoxynucleotidyl transferase dUTP nick end labeling

Ub: ubiquitin

αMSH: alpha melanocyte stimulating hormone

General Introduction

Human skin is a stratified tissue which consists of four layers; the stratum corneum, the viable epidermis, the dermis and the hypodermis. Furthermore, skin is a heterogeneous organ since it contains four types of independent mini-organs, such as nails, pilosebaceous follicles and hair, eccrine sweat glands and apocrine sweat glands. Skin performs various functions such as self-maintenance, self-repair, protection against physical/chemical/biological insults, sensory function, regulating body temperature, ossification, immune function and even socio-psychological functions (1). Furthermore, recent evidence indicates that this organ is hardwired into the body's key neuro-immuno-endocrine axis (2, 3).

Unlike non-human primates, most of the surface of human body is naked except for the scalp, armpit and groin. Human lineages lost their hair throughout the evolutionary history and instead acquired efficient thermoregulation systems through the use of eccrine sweat glands (4). This advanced cooling system led to increased human activities during hot daytime. However, loss of body hair brought not only considerable advantages, but also a notable disadvantage, namely, the protective function of hair.

Among many insults that could have been protected by hair, human skin can be tremendously affected by ultraviolet radiation (UVR) which is subdivided into three classes, according to wavelength; UVA (400 ~ 320 nm) constitutes 90 ~ 95% of total UVR which can reach onto the ground; UVB (320 ~ 290 nm) occupies the remaining 5 ~ 10% which varies, depending on the seasons,

latitude and time; UVC (290 ~ 100 nm) possesses the most intensive energy, but its effects on human skin is negligible since the radiation with this wavelength is mostly absorbed by the ozone layer. In other words, UVA and UVB are the wavelength classes of UVR that can affect the homeostasis of human skin.

Human skin responds in various ways upon exposure to UVR. As a short-term response, UV-exposed skin shows an acute inflammatory response that is caused by the increased production of inflammatory cytokines (5), and tanning response to protect against further UVR penetration into the skin by synthesizing melanin, a natural sunscreen (6). When skin is exposed to UVR over a long period of time, the chances of the development of skin cancer and wrinkle formations are increased by accumulated UV-induced DNA damage and the degradation of skin extracellular matrix (ECM) proteins, respectively (7). This study focused on elucidating the molecular mechanisms of responsiveness of skin cells consequence to UV irradiation.

The UV irradiation onto skin induces the tanning response attributed to melanogenesis, increased synthesis of the melanin pigment (6). Furthermore, repeated exposure to UVR contributes to the development of pigmentary disorders, such as melasma, ephelides and solar lentigines on sun-exposed lesions (8, 9). Since these pigmentary disorders are not favored in cosmetic and clinical perspectives, there are considerable interests in the development of anti-melanogenic agents. Chapter 1 discusses the mechanisms of anti-melanogenic effect of 4-n-butylresorcinol. 4-n-butylresorcinol is a derivative

of resorcinol, which is commercially used in the cosmetic industry for whitening application. However, the only known mechanism of this agent is as an inhibitor of tyrosinase and tyrosinase-related protein-1 (TYRP-1) (10). In this study, cellular tyrosinase protein levels in B16F10 melanoma cells were observed to have decreased following 4-n-butylresorcinol treatment. This phenomenon was associated with the accelerated proteolytic degradation of tyrosinase. This result is expected to suggest a new mechanism of 4-n-butylresorcinol and to contribute to the development of more effective derivatives of 4-n-butylresorcinol which can be used to treat hyperpigmentary disorders.

Another important feature of UV-exposed skin is sunburn which is caused by UV-damaged epidermal keratinocytes (5). Chapter 2 discusses the role of transglutaminase 2 (TG2) investigated in UVB-induced acute skin inflammation using human keratinocytes and TG2-deficient mice. Although keratinocytes express TG2, its roles in maintaining keratinocytes homeostasis are poorly understood. In this study, it was discovered that UV-irradiated keratinocytes induce the activation of TG2. Additionally, it was concluded that the PLC-IP_3-IP_3R axis plays a central role in activating TG2. The enzymatic activation of TG2 further promoted activation of NF-κB which is a well-known master transcription factor for inflammatory cytokine genes. This ultimately leads to skin inflammation by inducing immune cell infiltration, erythema, edema and dilation of blood vessels in the UV-exposed lesions. This study

suggests that the regulation of TG2 activity following UV irradiation may serve as a new therapeutic target for treating UV-induced acute skin inflammation.

UV irradiation on the dermal skin causes remodeling of dermal ECM, leading to skin aging. One of the prominent features of chronically UV-damaged skin is the formation of deep and coarse wrinkles which are distinct from the fine wrinkles present in chronologically aged skin. One of the causes of skin wrinkles is alterations in skin ECM structure (7). A set of proteins construct a dynamic structure of the ECM- fibrous proteins (collagens and elastin fibers), glycoproteins (fibronectins and laminins) and proteoglycans (7). Collagen constitutes major families of ECM proteins, thereby playing a pivotal role in wrinkle formation. Homeostasis of collagen is maintained by synthetic and degradative pathways which can be disturbed by intrinsic and extrinsic factors. MMP family proteins have a critical role in the degradative pathway of ECM proteins such as collagen and elastin (2). MMPs are zinc-dependent endopeptidases which are subdivided into several groups including collagenase, gelatinase, stromelysin and matrilysin, according to their substrates specificity (11). It is MMP-1 that plays a significant role in initiating the wrinkle formation of human skin as it is capable of degrading intact fibrillar collagen (12). Chapter 3 introduces the role of TG2 in regulating the expression of MMPs in dermal fibroblasts. The role of TG2 in regulating the expression of human MMP-1 and -3, and mouse MMP-13 was investigated in this study. Similar to chapter 2, UVB irradiation induces the activation of fibroblast TG2, followed by NF-κB activation that further facilitates MMP-1 expression at transcriptional level.

This indicates that regulation of TG2 activity in dermal fibroblasts may be a new strategy for the alleviation of UV-mediated wrinkle formation at the chronic level by preventing the degradation of dermal collagen.

The responses of UVR stimulated skin cells, such as melanocytes, keratinocytes and fibroblasts, were investigated by performing the studies described above. Since UVR is one of the most prominent exogenous stresses for skin, understanding the biochemical influences of the UV on human is critical in proceeding toward the prevention of UV-induced skin damage clinically and cosmetically. These studies will provide new insights in the development of strategies for anti-aging agents based on molecular mechanisms, which will be distinct from conventional treatment.

CHAPTER 1

4-n-butylresorcinol enhances proteolytic degradation of tyrosinase in B16F10 melanoma cells

1.1 INTRODUCTION

Melanins are brown or black pigments in the skin that are synthesized in melanosomes, transferred to keratinocytes, and distributed around cell nuclei (13). These processes of pigmentation are influenced by UV irradiation, inflammatory cytokines secreted from keratinocytes and fibroblasts, and hormonal status (6, 14-17). Of these, UV irradiation is the most critical factor to increase pigmentation by stimulating melanin synthesis, proliferation of melanocytes and transfer of melanosomes, known as tanning response (6). Melanin pigments absorb and scatter UV irradiation, thereby protecting epidermal keratinocytes from UV-induced DNA damage. On the other hand, aberrantly stimulated melanin production by UV irradiation is thought to cause common hypermelanotic skin disorders on sun-exposed areas in the face, such as melasma, ephelides and solar lentigines (8, 9).

In melanosomes, eumelanin, and pheomelanin are synthesized from tyrosine through a series of oxidative reaction, including the conversion of L-tyrosine to 3,4-dihydroxyphenylalanine catalyzed by tyrosinase, a rate-limiting step of melanin biosynthesis (Fig. 1-1) (6, 18). Thus the expression level of tyrosinase is a critical determinant for melanin production. At the transcriptional level, tyrosinase mRNA is upregulated by microphthalmia-associated transcriptional factor (MITF), a master regulator of genes involved in the proliferation, differentiation and melanogenesis of melanocytes (19, 20), while MITF expression is increased by α-melanocyte stimulating hormone (αMSH)-mediated, cAMP-dependent CREB phosphorylation (21). Because UV

irradiation increases αMSH secretion from keratinocytes through the p53-dependent signaling pathway (14), tyrosinase levels depend on the activities of p53 and cAMP signals in keratinocyte and melanocyte, respectively (Fig. 1-2). At the post-translational level, tyrosinase is glycosylated in the endoplasmic reticulum (ER), and further matured in the Golgi (22-24). The protein level of tyrosinase is also regulated by two degradation systems, the proteasomal and endosomal/lysosomal systems for proteolysis of misfolded of unfolded proteins during maturation processing (25-27).

Regulation of tyrosinase activity and protein level is a target for treating hyperpigmentation disorders and for whitening skin after sunburn. A number of compounds, including kojic acid, arbutin, hydroquinone, and akylresorcinols, namely 4-n-butylresorcinol, 4-n-hexylresorcinol and 4-(1-phenylethyl)-resorcinol, are known to inhibit tyrosinase activity and are currently utilized for cosmetic purpose (28-33). On the other hand, several agents, such as linoleic acid, 25-hydroxycholesterol, phynylthiourea, and 1-phenyl-3-(2-thiazolyl)-2-thiourea, inhibit tyrosinase by decreasing its protein level through accelerating the degradation system (22, 23, 34, 35)

On these, 4-n-butylresorcinol is a derivative of resorcinol and inhibits tyrosinase and tyrosinase-related protein-1 (TRP-1) *in vitro* as well as in B16 cell line (10). In clinical studies, topical application of 4-n-butylresorcinol showed a significant decrease of the melanin index in patients with melasma (36-38). In this study, we found that 4-n-butylresorcinol reduces the protein level of tyrosinase with no change in its mRNA level. Analyses with

glycosidase digestion and protease inhibitors showed that 4-n-butylresorcinol enhances tyrosinase degradation not by interfering with its maturation processing, but by increasing the activities of the proteasomal and eondosomal/lysosomal degradation systems. Our results indicate that enhancement of proteolytic degradation is a new mechanism by which 4-n-butylresorcinol inhibits tyrosinase in melanocytes. It would be interesting to know if this mechanism is also applicable to other two commercially available akylresorcinols – hexylresorcinol and phenylethylresorcinol.

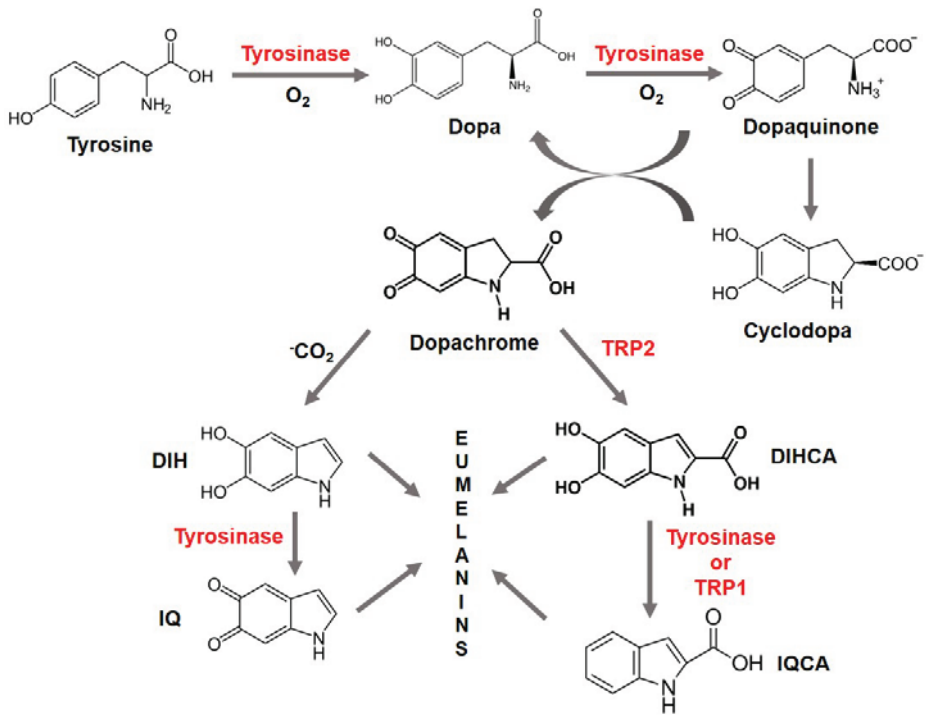

Figure 1-1. The mammalian eumelanogenic pathway. Tyrosinase is a rate-limiting enzyme of melanogenesis. TRP1 and TRP2 determine the type and amount of eumelanins. DIH: 5,6-dihydroxyindole; IQ: 5,6-indolequinone; DIHCA: DHI-2-carboxylic acid; IQCA: indole-2-carboxylic acid-5,6-quinone. Modified image from reference (39).

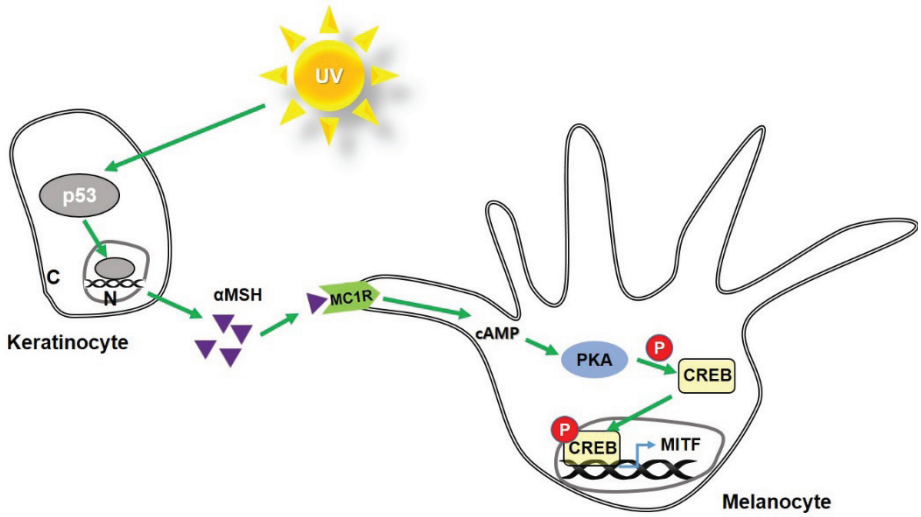

Figure 1-2. Signaling pathway of UV-induced melanogenesis. UV-exposed keratinocytes secret αMSH through the p53 dependent pathway. Secreted αMSH binds with MC1R which is expressed on melanocyte plasma memebrane. This receptor-ligand binding increases cytosolic cAMP level and followed by PKA-dependent phosphorylation of CREB. Phosphorylated CREB translocates to the nucleus and initiates MITF transcription, a master transcription factor of melanogenesis. N: nucleus; C: cytosol, P: phosphorylation.

1.2 MATERIALS AND METHODS

1.2.1 Cell culture

B16F10 cells were cultured in Dulbecco's modified Eagles's medium (DMEM, Welgene, Gyeongsan, South Korea) containing 10% heat-inactivated fetal bovine serum (Hyclone), 100 U/ml of penicillin and 100 μg/ml of streptomycin sulfate (GIBCO) under 5% CO_2 atmosphere at 37°C. To examine the effect of 4-n-butylresorcinol on melanin synthesis, cells were treated with 4-n-butylresorcinol (Enprani, Incheon, South Korea), αMSH (Sigma-Aldrich Co., St Louis, MO, USA), E64 (Sigma-Aldrich Co., St Louis, MO, USA), and/or proteasome inhibitor cocktail (Enzo Life Sciences, San Diego, CA, USA) for t he indicated period.

1.2.2 Tyrosinase activity assay

Mushroom tyrosinase (10 U, Sigma-Aldrich Co., St Louis, MO, USA) was incubated with various concentrations of 4-n-butylresorcinol in a reaction buffer (80 mM potassium phosphate, pH 6.8 and 200 μM L-tyrosine) at 37°C for 30 min. Tyrosinase activity was estimated by measuring the absorbance at 475 nm.

To assess the effect of 4-n-butylresorcinol on tyrosinase activity in live cells, B16F10 cells (1.5 x 10^5/well) were cultured in 6-well plate for 18 h, and then treated with 5 nM αMSH and/or 10 μM 4-n-butylresorcinol for 2 days. Cells were washed twice with phosphate buffered saline (PBS) and lysed in 0.1 M

potassium phosphate buffer, pH 6.8 with 1% Triton X-100, followed by centrifugation for 10 min (10,000 ×*g*) at 4°C. After quantification of protein concentrations with the BCA method, L-DOPA (0.5 mM, Sigma-Aldrich Co., St Louis, MO, USA) was added to the supernatant, and the mixture was incubated at 37°C. Tyrosinase activity was estimated by measuring the absorbance at 475 nm. For comparison, tyrosinase activity in the cell lysates prepared from untreated B16F10 cells was determined in the presence of 5 nM αMSH and/or 10 μM 4-n-butylresorcinol.

1.2.3 Measurement of melanin content

B16F10 cells (1.5 x 10^5) were cultured in 6 well plate for 18 h. Cells were washed twice with PBS and treated with αMSH and 4-n-butylresorcinol diluted in phenol red-free culture media for 2 days. Media was collected from each well and centrifuged for 5 min (1,500 x g) at 4°C to remove cellular debris. Melanin content in the medium was determined by measuring the absorbance at 405 nm. To quantify cellular melanin content, the cells were washed twice with PBS, detached by treatment with trypsin, and centrifuged for 5 min (1,500 x g) at 4°C. Cell pellets were lysed in the dissolving buffer (1 N NaOH and 10% dimethyl sulfoxide) by boiling for 1 h. Melanin content in each sample was determined by measuring the absorbance at 470 nm. The melanin standard curve was prepared with synthetic melanin (Sigma-Aldrich Co., St Louis, MO, USA) in the range of 1-40 μg/ml. Melanin content was normalized using cell numbers.

1.2.4 Melanosome isolation

Melanosomes were isolated as described previously (27) with slight modifications. Cells (1 x 10^7) were washed twice with PBS and exposed to repeated freeze-thaw in a buffer containing 250 mM sucrose, 20 mM Tris-HCl, pH 7.2, 150 mM NaCl, and 1 mM EDTA, followed by centrifugation for 5 min (1000 × *g*) at 4°C. The supernatant was carefully separated and layered over an equal volume of 1.5 M sucrose in 20 mM Tris-HCl, pH 7.2, 150 mM NaCl and 1 mM EDTA, followed by centrifugation for 30 min (50,000 x g) at 4°C. The supernatant and pellet were collected for the cytoplasmic and melanosome fraction, respectively. The pellet was resuspended in 60 mM Tris-HCl, pH 6.8, 100 mM dithiothreitol, and 2% sodium dodecyl sulfate (SDS). To check the purity of each fraction, immunoblotting analysis was performed using anti-PMEL17 and anti-calregulin antibodies for the melanosome and cytoplasm, respectively.

1.2.5 Western blot analysis

Cells were lysed in buffer (10 mM Tris-HCl, pH 7.5, 1 mM EDTA, 150 mM NaCl, 1% Triton X-100, protease inhibitor cocktail (Roche, Indianapolis, IN, USA)) and centrifuged at 12,000 x g for 10 min at 4°C. After quantitating the protein concentration of each cell extract using the BCA method, samples were boiled in a loading buffer (50 mM Tris-HCl, pH 6.8, 2% SDS, 0.14 M 2-mercaptoehthanol, 10% glycerol, and 0.2% bromophenol blue) for 5 min, separated on SDS-PAGE, and transferred onto nitrocellulose membranes. The membranes were washed with Tris-buffered saline containing 0.1% Tween-20

(TBS-T), blocked with 5% skim milk in TBS-T, and probed with monoclonal antibodies specific for tyrosinase, TRP-1, TRP-2, PMEL17, MART-1, calregulin, ubiquitin (Santa Cruz Biotechnologies, Santa Cruz, CA, USA), p38, p-p38 (Cell Signaling Technology, Beverly, MA, USA), and beta-actin (Sigma, St. Louis, MO, USA). After washing three times with TBS-T, the membranes were incubated with a 1:2000 diluted secondary antibody coupled to horseradish peroxidase (Thermo Scientific Pierce, Rockford, IL, USA) for 1 h, and washed five times with TBS-T. The immunoreactive proteins were visualized with enhanced chemiluminescence detection (ECL, Thermo Scientific Pierce). For immunoprecipitation, cells were lysed in RIPA buffer with proteasome inhibitor cocktails. Extracted proteins (0.5 mg) were used in each immunoprecipitation with an anti-ubiquitin antibody. Prepared samples were subjected to western blot analysis using an anti-tyrosinase antibody.

1.2.6 QRT-PCR

RNA of B16F10 cells was purified with Total RNA Kit I (OMEGA Bio-Tek, Norcross, GA, USA). One μg of purified RNA was reverse transcribed using SuperScript II Reverse Transcriptase (Invitrogen, NY, USA). QRT- PCR was performed with EvaGreen qPCR Mastermix (abm, Richmond, CA, USA) using an iCycler RT-PCR instrument (Bio-Rad, Hercules, CA, USA). The following specific primers were used.

Species	Genes	Forward	Reverse
Mouse	GAPDH	GGACCTCATGGCCTACATGG	TAGGGCCTCTCTTGCTCAGT
	Tyrosinase	AATGGCTGCGAAGGCACCGC	TCCCACCAGTGCTGCCCCAA

Levels of tyrosinase mRNA were estimated by the $2^{-\Delta\Delta Ct}$ method (40) and normalized to GAPDH levels.

1.2.7 Glycosylation assay

B16F10 cells were lysed by sonication in PBS containing protease inhibitor cocktail (Roche, Indianapolis, IN, USA) and centrifuged at 12,000 x g for 5 min at 4°C. After quantitating the protein concentration of the supernatants by BCA assay, a glycosylation assay was performed with 10 μg of proteins per sample using Endo H and PNGase F (New England BioLabs, Ipswich, MA, USA), in accordance with the manufacturer's procedure.

1.2.8 Confocal microscopy

B16F10 cells were cultured on microscope cover glasses. Cells were fixed with 4% formaldehyde for 20 min at room temperature, washed twice with PBS, and permeabilized with 0.1% Triton X-100 in PBS (PBST) for 5 min. Cover glasses were blocked with 1% bovine serum albumin in PBST for 30 min, probed with mouse anti-MART1 or rabbit anti-tyrosinase antibody (Santa Cruz Biotechnologies, Santa Cruz, CA, USA), followed by Alexa Fluor 488-conjugated goat anti-rabbit IgG (H+L) antibody (Molecular Probes, Inc., Eugene, OR, USA) or Alexa Fluor 488 donkey anti-rabbit antibody (Invitrogen).

Cells were mounted with GEL/MOUNTTM (Biomeda corp.) and observed with a FluoView 1000 confocal microscope (Olympus, Tokyo, Japan). The nucleus was detected using 4,6-diamidino-2-phenylindole (DAPI, Roche, Palo Alto, CA, USA).

1.2.9 UVB induced hyperpigmentation and immunohistochemical analysis

Five weeks old female brown guinea pigs were purchased from Oriental Yeast Co., LTD (Tokyo, Japan). These animals were housed under standard experimental conditions (22±1 ℃, 55±5% humidity, 12-hour light and 12-hour dark cycle) and were fed on a standard diet (Guinea pig Diet, Cargill Agri Purina Inc, Seongnam, Korea) with freely available water. Animal experiments were conducted in accordance with the Guide for the Care and Use of Laboratory Animals (NIH Publication No. 85-23, 1996) and approved by the Korea Conformity Laboratories Institutional Animal Care and Use Committee (Approval No.: IA12-00036). The dorsal skin was shaved with an electric shaver and was subsequently exposed to 500mJ/cm^2 of UVB (per exposure) (Sankyo Denki, Tokyo, Japan) following on a week of adaptation. The UVB irradiation was repeated over three successive days. Subsequent to UVB irradiation vehicle, 2% arbutin or 0.3% 4-n-butylresorcinol cream, were topically applied to the UVB irradiated skin (1.5 cm x 1.5 cm) every two days for four weeks, respectively. The creams were kindly provided by Enprani (Incheon, Korea). A Mexameter (Courage and Khazaka, Cologne, Germany)

was employed to determine the delta L values.

For immunohistochemical analysis, the guinea pigs were euthanized by CO_2 asphyxiation, after which the skin was harvested and fixed in 4% paraformaldehyde. The skin samples were sent for hematoxylin & eosin staining or Masson-Fontana staining, to the Korea Conformity Laboratories (Incheon, Korea)

1.2.10 Statistical analysis

Statistical evaluations were conducted with Prism 5 software (GraphPad, San Diego, CA) using one-way or two-way ANOVA. $P < 0.05$ was considered significant.

1.3 RESULTS

1.3.1 Intact cell is required for 4-n-butylresorcinol to effectively inhibit B16F10 cell tyrosinase

4-n-butylresorcinol is a well-known tyrosinase inhibitor (10). We first determined the effective dose of 4-n-butylresorcinol for inhibiting purified mushroom tyrosinase. 4-n-butylresorcinol reduced tyrosinase activity in a concentration dependent manner, and 10 μM 4-n-butylresorcinol was found to completely inhibit mushroom tyrosinase (Fig. 1-3A). To evaluate the inhibitory capacity of 4-n-butylresorcinol in αMSH-stimulated melanogenesis, we compared this effective dose with that for tyrosinase in B16F10 melanoma cells. Addition of 10 and 50 μM 4-n-butylresorcinol to the lysate of αMSH-treated B16F10 cells reduced tyrosinase activity to 60% and 20% of the control level, respectively, and 100 μM of 4-n-butylresorcinol completely inhibited B16F10 cell tyrosinase (Fig. 1-3B), indicating that B16F10 cell tyrosinase is more resistant than mushroom tyrosinase to 4-n-butylresorcinol. By contrast, when B16F10 cells were cultured with αMSH and 10 μM 4-n-butylresorcinol for 2 days, tyrosinase activity was reduced to 35% of αMSH-induced activity (Fig. 1-3C), suggesting that an intact cell is required for 4-n-butylresorcinol to inhibit B16F10 cell tyrosinase. To confirm these results, we examined the effect of 4-n-butylresorcinol on αMSH-stimulated melanin synthesis. Treatment with αMSH caused a 40% increase in extracellular melanin secreted from B16F10 cells (Fig. 1-3D), and an approximately three-fold increase in melanin content

per cell (Fig. 1-3E). Under the same experimental conditions, 10 μM 4-n-butylresorcinol reduced the amount of melanin to the control levels (Fig. 1-3D–F). These results suggest that 4-n-butylresorcinol may suppress intracellular tyrosinase through unidentified mechanism(s) in addition to direct inhibition of tyrosinase activity.

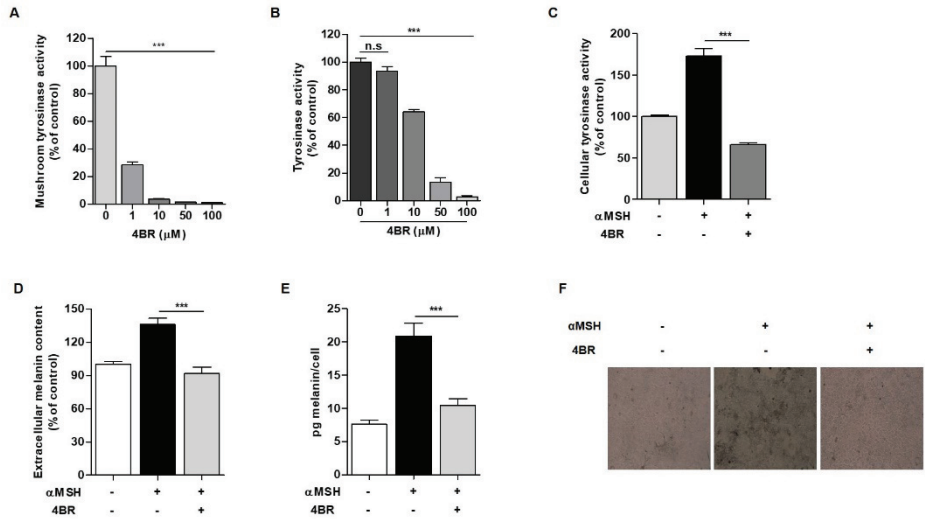

Figure 1-3. 4-n-butylresorcinol inhibits αMSH-induced tyrosinase activity and melanin synthesis to the level of αMSH-untreated cells. (A) Mushroom tyrosinase was incubated with various concentrations of 4-n-butylresorcinol at 37°C for 30 min and then tyrosinase activity was measured. (B) B16F10 cell lysates were incubated with 5 nM αMSH and various concentrations of 4-n-butylresorcinol at 37°C for 30 min and then tyrosinase activity was measured. (C–E) B16F10 cells were cultured with 5 nM αMSH in the presence or absence of 10 μM 4-n-butylresrocinol for 48 h. After cell lysis, tyrosinase activity was measured (C), concentration of secreted melanin was determined in cultured media (D) and concentration of intracellular melanin was measured in the cell lysates (E). Results are presented as the mean ± s.e.m. Data are representative of at least three experiments. (F) Microscopy images showed melanin deposition in 4-n-butyl-resorcinol-treated B16F10 cells. Magnification x100, *** $P< 0.001$ compared with control.

1.3.2 4-n-butylresorcinol reduces protein levels of tyrosinase in B16F10 cells

To explore the inhibitory mechanism of 4-n-butylresorcinol for intracellular tyrosinase, we tested whether 4-n-butylresorcinol could affect the tyrosinase expression in B16F10 cells. In control and αMSH-treated cells, 4-n-butylresorcinol had no effect on the levels of MITF mRNA and protein (data not shown). Consistent with these results, the mRNA levels of tyrosinase were not changed by treatment with 4-n-butylresorcinol (Fig. 1-4A). By contrast, western blot analysis revealed that the protein level of tyrosinase was decreased by treatment with 4-n-butylresorcinol in both control and αMSH-treated B16F10 cells, whereas the protein levels of TRP-1, TRP-2 and Pmel17, which are known to be MITF-dependent, were not significantly changed by 4-n-butylresorcinol treatment (Fig. 1-4B). These results suggest that 4-n-butylresorcinol negatively regulates the protein level of tyrosinase in a tyrosinase-specific manner

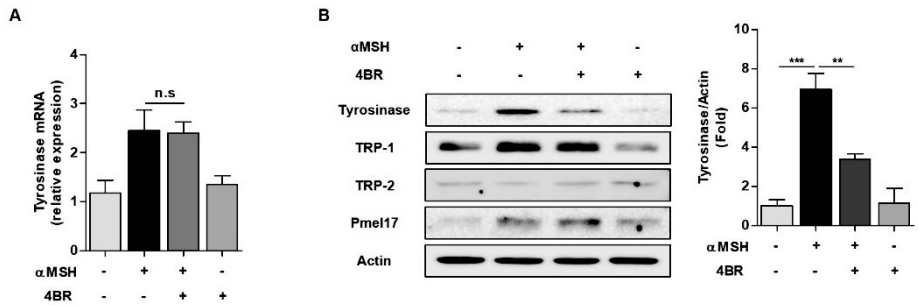

Figure 1-4. 4-n-butylresorcinol reduces level of tyrosinase protein but not mRNA. (A) B16F10 cells were cultured in media containing 5 nM αMSH and 10 μM 4-n-butylresrocinol for 6 h. Cell lysate was prepared and mRNA level of tyrosinase was estimated by QRT-PCR. (B) B16F10 cell lysate was subjected to western blot analyses using antibodies specific for tyrosinase, TRP-1, TRP-2, and PMEL17. Right panel shows protein level of tyrosinase estimated by densitometric analysis. Results are presented as the mean ± s.e.m. Data are representative of at least three experiments. $^{**}P<0.01$, $^{***}P < 0.001$ compared with control.

1.3.3 4-n-butylresorcinol has no effect on glycosylation and maturation of tyrosinase

A newly synthesized tyrosinase is glycosylated and further maturated in the endoplasmic reticulum (ER) and Golgi, and then transported to melanosome (41). Tyrosinase glycosylation helps to facilitate correct folding and trafficking to melanosome; thus aberration of glycosylation causes the retention of tyrosinase in the ER that leads to degradation (42). To determine whether 4-n-butylresorcinol could inhibit these processing, we examined the tyrosinase levels in the melanosome. In control and αMSH-treated B16F10 cells, 4-n-butylresorcinol treatment caused a decrease in tyrosinase co-localization with MART-1, a melanosomal marker protein (Fig. 1-5A). Moreover, western blotting analysis also showed a decrease of melanosomal tyrosinase in 4-n-butylresocinol treated cells (Fig. 1-5B), indicating an involvement of 4-n-butylresocinol in the post-translational processing of tyrosinase.

We then investigated the location where glycosylation processing is hampered. To this end, cell lysates obtained after 4-n-butylresorcinol treatment were digested with Endo H and PNGase F glycosidase. Endo H cleaves sugar chains of tyrosinase processed in the ER but not in the Golgi, whereas PNGase F cleaves sugar chains processed both in the ER and in the Golgi, producing deglycosylated tyrosinase. Western blotting analysis revealed that most of tyrosinase was not digested by Endo H, indicating that tyrosinase in the 4-n-butylresorcinol treated cells is fully matured and not retained in the ER (Fig. 1-5C, left). In addition, the protein level of PNGase F-digested tyrosinase was

reduced by 4-n-butylresorcinol to a similar extent with the control cell lysates (Fig. 1-5C, right). These results indicate that glycosylation processing of tyrosinase, which occurred in the ER, is not affected by 4-n-butylresorcinol.

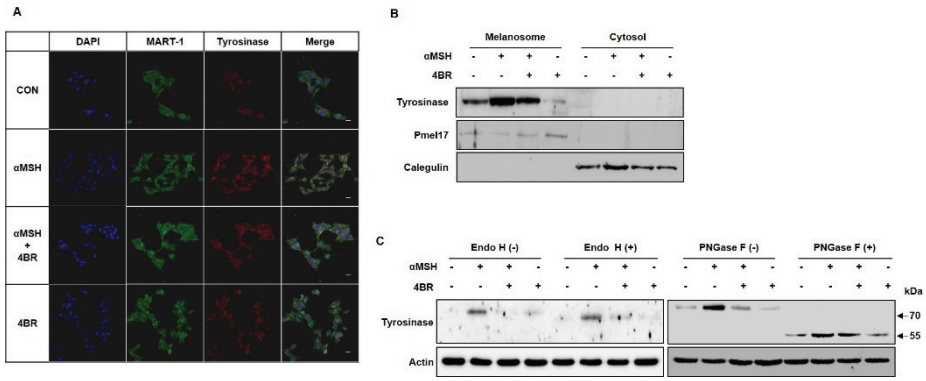

Figure 1-5. 4-n-butylresorcinol does not inhibit glycosylation processing of tyrosinase. (A) Confocal microscopy images show B16F10 cells immunostained with anti-tyrosinase or anti-MART-1 antibody. Cells were cultured in media containing 5nM αMSH and 10 μM 4-n-butylresrocinol for 6 h. MART-1 was used as a marker for melanosomes. DAPI staining showed nuclei. Scale bar, 20 μm. (B) Melanosomal and cytoplasmic fractions were isoloated from B16F10 cells. The level of tyrosinase in each fraction was assessed by western blot analysis with anti-tyrosinase antibody. Pmel17 and calregulin were used as a marker for melanosome and cytosol, respectively. (C) Lysates from B16F10 cells treated with Endo H (left panel) or PNGase F (right panel) were immunoblotted with the anti-tyrosinase antibody. Upper and lower bands indicate matured (glycosylated) and nascent (unglycosylated) forms of tyrosinase, respectively.

1.3.4 4-n-butylresorcinol enhances the degradation of tyrosinase

The protein level of tyrosinase is regulated by a balance between production and degradation. Misfolded or unassembled tyrosinase is ubiquitinated and subsequently proteolyzed by proteasomes (34, 43-45). Moreover, tyrosinase is also degraded by lysosomal enzymes after Golgi maturation (22). Therefore, we tested if 4-n-butylresorcinol was involved in the proteolytic process of tyrosinase by using E64, a lysosomal protease inhibitor, and proteasome inhibitor cocktail (PIC). Western blot analysis showed that treatment of B16F10 cells with E64 or PIC restored the protein levels of tyrosinase decreased by 4-n-butylresorcinol (Fig. 1-4A). In accordance with these results, E64 or PIC treatment increased the levels of secreted extracellular melanin (Fig. 1-6B) and melanin content per cell (Fig. 1-6C) in 4-n-butylresorcinol-treated B16F10 cell s , showing that E64 and PIC abrogated the inhibitory effect of 4-n-butylresorcinol on melanin synthesis. In addition, because activation of p38 MAPK induced proteasomal degradation of tyrosinase (46), we examined the phosphorylation levels of p38 MAPK in B16F10 cells. As shown in Fig. 1-6D, 4-n-butylresorcinol increased whereas αMSH decreased the phosphorylation of p38 MAPK. Moreover, when lysates were immunoprecipitated with an anti-tyrosinase antibody, there was a significant increase in ubiquitinated tyrosinase in 4-n-butylresorcinol-treated cells (Fig. 1-6E). These results indicate that 4-n-butylresorcinol inhibits tyrosinase via the acceleration of proteasomal, as well as lysosomal, degradation.

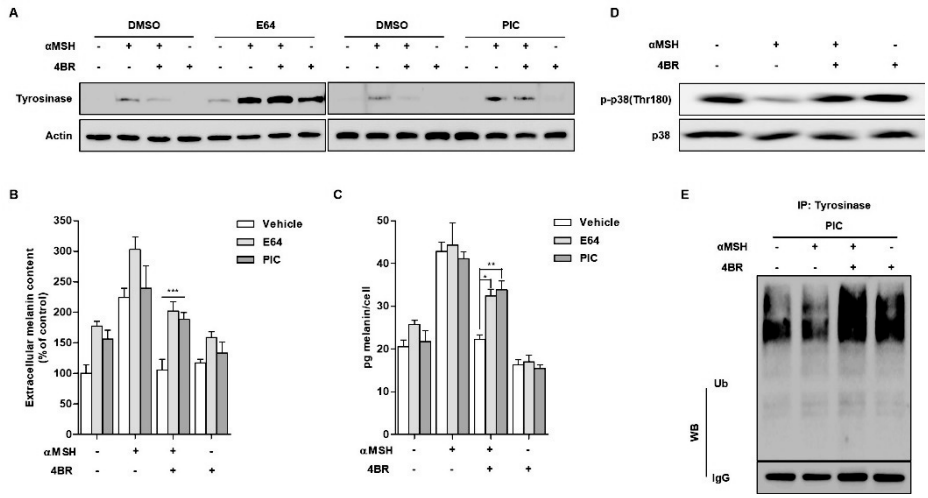

Figure 1-6. 4-n-butylresorcinol promotes lysosomal and proteasomal degradation of tyrosinase. (A) B16F10 cells were cultured for 48 h in media containing 5 nM αMSH and 10 μM 4-n-butylresrocinol in the presence of 50 μM E64 (left panel) or proteasome inhibitor cocktail (0.5 x PIC, right panel). Total cell extracts were immunoblotted with anti-tyrosinase antibody. (B and C) Concentration of melanin was determined in the media (B) and in the cell lysates (C). Results are presented as the mean ± s.e.m. Data are representative of at least three experiments. *$P < 0.05$, **$P < 0.01$, ***$P < 0.001$. (D) Lysates prepared from B16F10 cells cultured for 48 h in the presence of 5 nM αMSH and 10 μM 4-n-butylresrocinol were immunoblotted with anti-phospho p38 antibody. Total p38 protein was used as a loading control. (E) Lysates prepared from B16F10 cells cultured for 24 h in the presence of 5 nM αMSH, 10 μM 4-n-butylresrocinol and PIC were immunoprecipitated with anti-tyrosinase antibody, and immunoblotted with anti-ubiquitin antibody and anti-IgG antibody

1.3.5 4-n-butylresorcinol attenuates UVB-induced melanogenesis in Guinea pig skin

Lastly, we investigated the *in vivo* efficacy of 4-n-butylresorcinol in a model animal system. A brown guinea pig was selected as an animal model of pigmentation, since they express active melanocytes in the basal layer of the interfollicular epidermis, which is similar to human skin. Furthermore, this animal has the ability to tan in response to UV radiation.

Following the induction of the tanning response, vehicle or 2% arbutin or 0.3% 4-n-butylresorcinol creams were applied to the UVB-irradiated lesions. Arbutin, which is a commercially using agent for whitening purposes (47), was used to compare efficacy with 4-n-butylresorcinol. Following four weeks of applications, the skin lesions were analyzed via Masson-Fontana staining to visualize the melanin deposition. UVB irradiation induced the formation of melanin deposit on the basal epidermis of only the vehicle applied lesion (Fig. 1-7A). However, this melanin deposition was inhibited in the 2% arbutin or 0.3% 4-n-butylresolcinol applied lesions, without changes to the skin structures (Fig. 1-7A). Additionally, we measured the ΔL value to quantify the deposited melanin content in the skin. As shown in Fig. 1-7B, UVB irradiation induced the darkening of the skin at an approximately three-fold high rate than for the un-irradiated lesions. The 2% arbutin cream slightly decreased the melanin content, however it was not statistically significant. However, the application of 0.3% 4-n-butylresorcinol cream almost completely blocked melanin synthesis, which was comparative to un-irradiated skin lesions. Furthermore,

the 0.3% 4-n-butylresorcinol cream showed more superior effects for whitening in comparison with the 2% arbutin cream. These results suggest that 4-n-butylresorcinol is a more potent agent for *in vivo* whitening than arbutin.

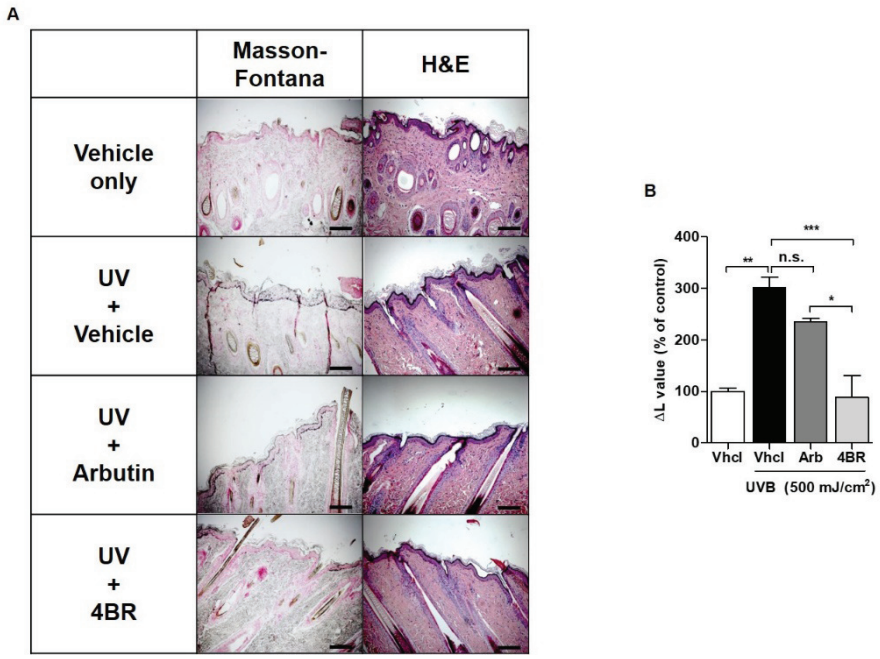

Figure 1-7. *in vivo* Whitening effect of 0.3% 4-n-butylresorcinol cream. Following the induction of tanning response on Guinea pig skin, vehicle or 2% arbutin or 0.3% 4-n-butylresorcinol creams were applied on the irradiated lesions for 4 weeks. (A) Histology of guinea pig skin. Scale bar, 200 μm. (B) Delta L value was determined by Mexameter (n=3). Arb, arbutin. n.s., not significant, *$P < 0.05$, **$P < 0.01$, ***$P < 0.001$.

1.4 DISCUSSION

4-n-butylresorcinol is a resorcinol derivative that is known to exhibit anti-melanogenic activity via direct inhibition of tyrosinase, a rate-limiting enzyme in melanogenesis (10, 37, 48). Its efficacy and safety have been proven in clinical studies (36-38). In the present study, we found that 4-n-butylresorcinol inhibits tyrosinase in intact cells more effectively than in cell lysates, suggesting that it inhibits tyrosinase by another mechanism in addition to direct inhibition of enzyme activity. QRT-PCR and western blot analysis showed that treatment with 4-n-butylresorcinol had no effect on mRNA levels of tyrosinase, but decreased its protein levels in a tyrosinase-specific manner in B16F10 cells. Therefore, we attempted to elucidate the mechanism through which 4-n-butylresorcinol may influence the protein level of tyrosinase. Experiments using glycosidases and inhibitors for proteolytic enzymes revealed that 4-n-butylresorcinol showed no effect on glycosylation processing or trafficking to melanosome, but accelerated proteasomal and lysosomal degradation. Moreover, we found that increased ubiquitination of tyrosinase by 4-n-butylresorcinol is associated with activation of p38 MAPK. Our results indicate that 4-n-butylresorcinol reduces the total amount of tyrosinase probably through p38 activation. To our knowledge, enhancing proteolytic degradation is a new mechanism for 4-n-butylresorcinol to inhibit tyrosinase.

The protein level of tyrosinase in melanocytes is regulated by the balance between its synthesis and degradation. De novo synthesized tyrosinase is glycosylated and matured in the ER and Golgi, respectively, and transported to

melanosome (41). Aberration of glycosylation resulted in ER retention of tyrosinase that leads to proteolysis by proteasome, which is known as ER-associated degradation (ERAD) (25-27). In addition, mature forms of tyrosinase are also degraded by ERAD via retrograde transport to the ER or by the endosomal/lysosomal system in an ubiquitination-independent manner (22, 49). Our results showed that the effect of 4-n-butylresorcinol on the protein level of tyrosinase was not associated with maturation processing, but with enhanced proteolytic enzyme activities (Fig. 1-8). Considering the quality control function of both proteasomal and lysosomal systems by removing misfolded or unfolded proteins, these findings suggest that the binding of 4-n-butylresorcinol may induce the unfolding of mature tyrosinase, thereby increasing proteolytic degradation of tyrosinase. In supporting this mechanism, we have shown that 4-n-butylresorcinol reduces the protein level of tyrosinase, but not of TRP-1. As revealed in a previous report, 4-n-butylresorcinol has more than two-fold higher binding affinity for tyrosinase than TRP-1 (10). Therefore, 4-n-butylresorcinol more effectively destabilizes tyrosinase than TRP-1, leading to unfolding of tyrosinase.

A number of agents are known to inhibit tyrosinase by accelerating its degradation, including linoleic acid, 25-hydroxycholesterol, 12-O-tetradecanoylphorbol-13-acetate (TPA), 2,2′-dihydroxy-5,5′-dipropyl-biphenyl, phenylthiourea, and 1-phenyl-3-(2-thiazolyl)-2-thiourea (22, 23, 34, 35, 46). Of these, linoleic acid, TPA, and 1-phenyl-3-(2-thiazolyl)-2-thiourea enhance tyrosinase degradation in a proteasom e -dependent manner, whereas 25-

hydroxycholesterol and phenylthiourea enhance in a proteasome-independent, but endosome/lysosome-dependent manner. In addition, linoleic acid and phenylthiourea induces tyrosinase-specific degradation, with no effect on the protein level of TRP-1. As shown in the present study, 4-n-butylresorcinol enhances tyrosinase degradation in a proteasome- and endosome/lysosome-dependent manner, and this effect on protein degradation is specific to tyrosinase. Interestingly, both 4-n-butylresorcinol and phenylthiourea are phenol derivatives and tyrosinase-specific inhibitors, but show different dependency for the tyrosinase degradation system. Therefore, it seems likely that selection of a degradation pathway for tyrosinase might be related to the inhibition mechanism of each agent.

Melanin synthesis is stimulated by αMSH secreted from keratinocytes and melanocytes in response to UV irradiation or skin inflammation (14). However, it also has been shown that melanin synthesis is inhibited by UV-induced inflammatory cytokines, such as IL-1α, IL-6, TNFα, and TGFβ, through the reduction of both protein and mRNA levels of tyrosinase (17, 50). Intriguingly, a recent study showed that p38 MAPK, one of downstream effector kinases activated by these cytokines, negatively regulates melanin synthesis through decreasing tyrosinase stability (51). Thus, these observations indicate that an increase of p38 MAPK phosphorylation is associated with the activation of ubiquitin-mediated proteasomal degradation. We have demonstrated that the phosphorylation level of p38 MAPK is increased in 4-n-butylresorcinol-treated cells, suggesting that an increase of unfolded tyrosinase might activate p38

MAPK, though a causal relationship between protein stability and p38 phosphorylation remains to be determined.

Finally, we compared the *in vivo* whitening efficacy of 4-n-butylresorcinol using an animal model. In our experiment, 4-n-butylresorcinol almost completely blocked UVB-induced melanin deposition and demonstrated more potent inhibitory activity than arbutin which is commercially used for anti-melanogenic purposes. Although, arbutin showed a slight, but not significant decrement of melanin content in the skin, which may have been attributed to our small sample size (n=3). Nevertheless, since 4-n-butylresorcinol exhibited a significant decrement of melanin content in contrast to arbutin, it may be concluded that it is a more potent whitening agent than arbutin.

In summary, 4-n-butylresorcinol is known to inhibit tyrosinase through competitive binding to its active site, and has been used as an anti-melanogenic agent. In this study, we reported a new mechanism by which 4-n-butylresorcinol inhibits melanin synthesis, and these findings may contribute to the development of an effective 4-n-butylresorcinol derivative.

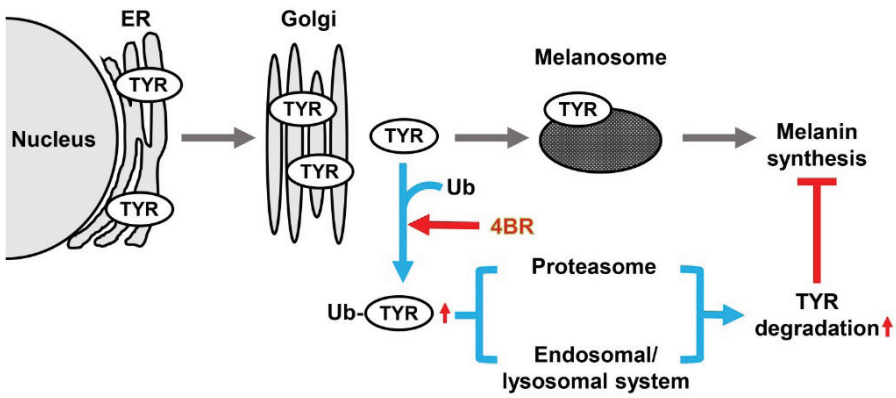

Figure 1-8. Action mechanism of 4-n-butylresorcinol. Schematic model shows that 4-n-butylresorcinol affects ubiquitination of tyrosinase which leads proteasomal and endosomal/lysosomal degradation of tyrosinase.

*** This study is published in International Journal of Cosmetic Science (2016) except for animal study.**

CHAPTER 2

Transglutaminase 2 mediates UV-induced skin inflammation by enhancing inflammatory cytokine production

2.1 INTRODUCTION

Transglutaminases (TGs) are a calcium-dependent enzyme family that produces crosslinked, polyaminated, or deamidated proteins by catalyzing the acyl-transfer reaction between glutamine and lysine residues of substrate proteins or polyamines (Fig. 2-1) (52, 53). Several proteins are crosslinked by TGs, such as loricrin, involucrin, cystatin A, filaggrin, trichohyalin, small proline-rich proteins, and keratins, which are components of the cornified envelope (CE), a barrier structure found in terminally differentiated keratinocytes (54). In the skin, 6 isozymes among 9 members of TG family are expressed, TG1–TG5 and factor XIIIa (55). Since TG isozymes share a common active-site structure and catalytic mechanism, isozyme-specific functions in the skin have been elucidated only by using isozyme-null mice and genetic analyses of congenital skin diseases.

TG1-null mice displayed defective CE formation in their stratum corneum and impaired skin barrier function leading to death within 4–5 h after birth due to dehydration (56). Moreover, TG1 mutations are the most common cause of autosomal recessive congenital ichthyosis in humans (57), indicating that crosslinking activity of TG1 plays a crucial role in epidermal barrier formation. Mice lacking TG3 showed thinner hair with markedly decreased crosslinking of hair proteins (58), and showed increased contact hypersensitivity elicited by FITC sensitization (59) and increased apoptosis induced by UV radiation (60). Mutations in TG3 have been associated with uncombable hair syndrome (61), indicating that TG3 contributes to hair development as well as CE formation.

TG5 is expressed in the upper layer of the human epidermis (54, 62), and TG5 mutations cause acral peeling skin syndrome in humans (63), indicating the role of TG5 in cell to cell adhesion in the uppermost layer of epidermis. TG4 is expressed in glandular epithelia but not in epidermal keratinocytes, and TG4-deficient mice showed no altered skin phenotypes (64). Factor XIIIa-deficient mice showed delayed and defective wound healing, indicating that the crosslinking activity of factor XIIIa plays a role in wound repair and remodeling (65). Unlike these TG isozymes, TG2-null mice showed no obvious altered skin phenotypes, despite its expression in epidermal keratinocytes (66). Moreover, there is no report of human skin disease associated with TG2. Thus, the role of TG2 in skin pathophysiology remains unknown.

UV irradiation causes acute inflammatory responses in the skin by inducing synthesis and release of proinflammatory cytokines, such as tumor necrosis factor-α (TNF-α) and IL-6, from keratinocytes (5). Mechanistically, UV radiation generates reactive oxygen species (ROS) and DNA damage in keratinocytes, which activate the NF-κB signaling pathway responsible for cytokine release (67, 68). However, the mechanism linking UV radiation with the activation of NF-κB signaling remains unclear. Previously, we showed that intracellular TG2 is normally inactive, but activated under various stress conditions, including UV radiation, oxidative stress, hypoxia, and DNA damage, through mobilization of calcium (69-73). In cultured cells, stress-induced TG2 activation results in enhancement of cell survival by crosslinking IκB and caspase-3 (70, 74). In mouse models, activation of TG2 is reportedly

involved in the development of cataract formation, tissue injury-induced lung fibrosis, and resistance to cancer chemotherapy by aberrantly increasing crosslinked proteins (52). These findings indicate that TG2 functions as a stress responsive enzyme, modulating cellular functions through modification of various substrate proteins (71).

Herein, we determined whether TG2 mediated inflammatory responses in UV-exposed skin, and showed that UV-induced TG2 activation is crucial for NF-κB-dependent expression of proinflammatory cytokines. In this process, PLC/IP_3/IP_3R-mediated ER calcium release acts as an upstream signal for activation of TG2. These results indicate that TG2 is a critical regulator that mediates acute cutaneous inflammation in response to UV radiation.

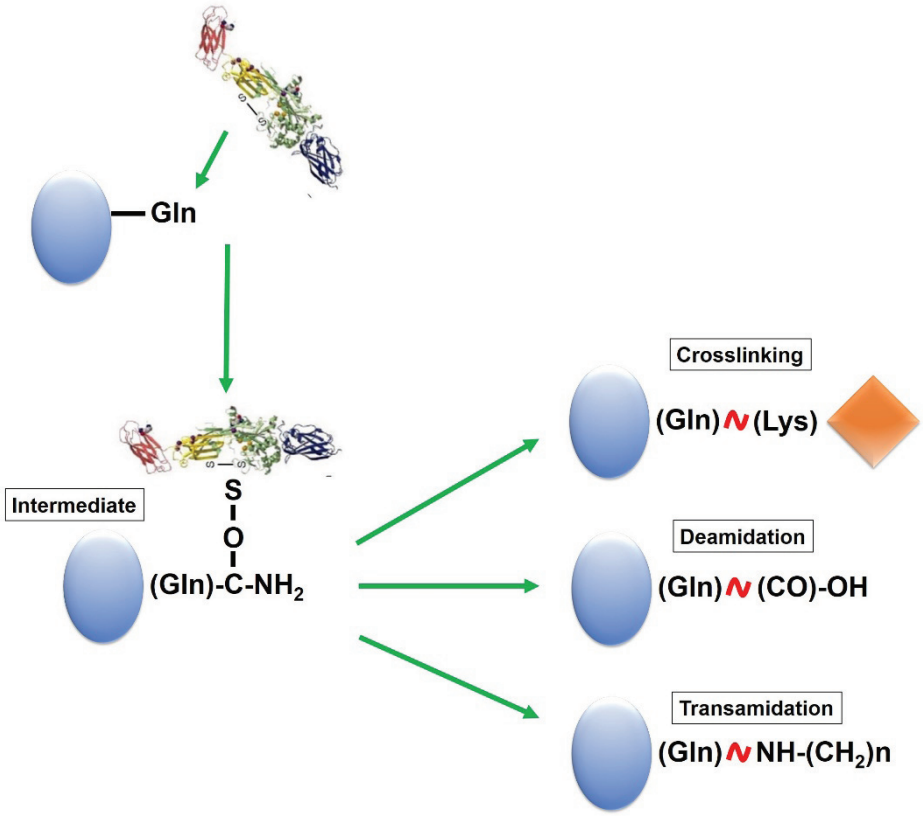

Figure 2-1. Catalytic reactions by TGs. The thiol group located in the cysteine residue of the activated TG forms intermediate with γ-carboxamide group of the glutamine residue. This intermediate reacts with lysine residue of the other protein (corsslinking) or primary amine (transamidation) or water molecule (deamidation). Modified image from the reference (53).

2.2 MATERIALS AND METHODS

2.2.1 Mice

$TG2^{-/-}$ mice (66) were backcrossed 12 times on C57BL/6J background. Female WT and $TG2^{-/-}$ littermates (8-week-old) were used for all experiments. All mice were bled and kept in our animal facility at Seoul National University College of Medicine, Seoul, South Korea, under standard conditions (22 ± 1°C, 55 ± 5 % humidity, 12-h light and 12-h dark cycle). Animal experiments were approved by the Seoul National University Institutional Animal Care and Use Committee (IACUC No. SNU-130103-1-5). The dorsal skin was shaved and chemically depilated by Veet Cream (Oxy-Reckitt Benskiser, Slough, UK) 48 h before UV irradiation.

2.2.2 Immunohistochemical analysis

Mouse skin tissues were fixed in 4% paraformaldehyde for 24 h, embedded in paraffin, and processed to get at 4 μm thick sections for hematoxylin & eosin staining or immunohistochemical analysis. The sections were dewaxed in xylene (Junsei Chemical Co.,Ltd., Tokyo, Japan), unmasked with heat mediated antigen retrieval EDTA (pH 9), and incubated in 0.3% H_2O_2 in methanol for 30 min at room temperature to eliminate endogenous peroxidase activity. The sections were then blocked for 60 min at room temperature in blocking serum in PBS, incubated in anti-TG2 polyclonal antibody (Thermo Fisher Scientific Inc., Rockford, IL, USA, RB-060-P) or primary antibody rabbit anti-CD11b

(Abcam, Cambridge, MA, USA, ab133357), and equilibrated at 4°C overnight. The next day, sections were incubated in each biotinylated secondary antibody (secondary and blocking serum in PBS) for 30 min at room temperature. The secondary antibody was visualized using Vectastain ABC Elite Reagent (Vector Laboratories Inc., Burlingame, CA, USA) and 3,3'-diaminobenzidine (Dako, Denmark) according to the manufacturer's instructions. TUNEL staining was carried out according to the manufacturer's protocol in the 'ApopTag Peroxidase In Situ Apoptosis Detection Kit' manual (Chemicon International, Inc., MA, USA). Mayer's Hematoxylin was used as a counterstain. Coverslips were mounted and sealed with Tissue Tek Glas Mounting Media (Sakura, Torrance, CA, USA). Bright-field imaging was performed using a Leica-microscope (Leica Microsystems, Bensheim, Germany), and images were captured using Microscope Imaging Software (Leica Microsystems, Bensheim, Germany). For *in situ* TG2 activity assay in mice exposed to UV irradiation (200 mJ/cm^2), BP (0.1 mg/g) was administered 5 h after irradiation by intraperitoneal injection. Mice were sacrificed 3 h later, and skin tissues were embedded in Tissue-TEK OCT compounds (Sakura, Torrance, CA, USA), reacted with streptavidin-488 (Thermo Fisher Scientific Inc., Rockford, IL, USA) and visualized using a FluoView 1000 confocal microscope (Olympus, Tokyo, Japan).

2.2.3 Immunohistochemistry on cryosections

Mice were euthanized by CO_2 asphyxiation. The skin was harvested, embedded

in Tissue-Tek OCT compound (Sakura Finetek, Inc., Torrance, CA, USA), and snap-frozen in liquid nitrogen. Frozen sections (10 μm) were cut from OCT-embedded tissues and fixed in cold acetone for 10 min and dried in air for 1 h. The sections were blocked with H_2O_2 and subsequently treated with 10% goat serum at room temperature for 20 min. They were then incubated with anti-loricrin polyclonal antibody (Abcam, Cambridge, MA, USA, ab85679), involucrin polyclonal antibody (Abcam, Cambridge, MA, USA, ab28057), and filaggrin polyclonal antibody (Abcam, Cambridge, MA, USA, ab24584) at 4°C for 18 h, followed by staining the proteins with Alexa Fluor 488-conjugated goat anti-rabbit IgG (H+L) secondary antibody (Molecular Probes, Inc., Eugene, OR, USA) in accordance with the manufacturer's instructions. The sections were mounted with fluorescent mounting medium (Dako North America, Inc., Carpinteria, CA, USA) and observed using a FluoView 1000 confocal microscope (Olympus, Tokyo, Japan).

2.2.4 Cell culture

HaCaT cells were cultured in Dulbecco's Modified Eagle's Medium (DMEM, Welgene, Gyeongsan, South Korea) containing 10% heat-inactivated fetal bovine serum (Hyclone, Logan, UT, UK), 100 U/mL of penicillin, and 100 μg/mL of streptomycin sulfate (Gibco, Carlsbad, CA, USA) under 5% CO_2 at 37°C. The TG2-deficient HaCaT cell line was generated by transfection with TG2 CRISPR/Cas9 vector (Santa Cruz Biotechnologies, Santa Cruz, CA, USA) and sorted by FACS. For generating short hairpin RNA (shRNA) expressing

vectors, the following forward and reverse oligonucleotides were annealed in annealing buffer (100 nM Tris, pH 7.5, 1 M NaCl, 1 Mm EDTA) by heating the mixture at 100°C for 5 min and cooling to room temperature.

Genes	Forward	Reverse
GFP	GATCCCCGCAAGCTGACCCTGAAGTTCTTCAAGAGAGAACTTCAGGGTCAGCTTGCTTTTTGGAAA	AGCTTTTCCAAAAAGCAAGCTGACCCTGAAGTTCTCTCTTGAAGAACTTCAGGGTCAGCTTGCGGG
TG2 (Human)	GATCCCCGATGGGATCCTAGACATCTTTCAAGAGAAGATGTCTAGGATCCCATCTTTTGGAAA	AGCTTTTCCAAAAAGATGGGATCCTAGACATCTTCTCTTGAAAGATGTCTAGGATCCCATCGGG

The annealed oligos were ligated into linearized pSuper plasmid (75) by HindIII and BglII enzyme digestion. The shRNA HaCaT cell lines were generated by co-transfection with pcDNA3 and pSuperGFP or pSuperTG2 vector. HaCaT cells over-expressing $TG2^{WT}$ or $TG2^{C277S}$ were generated by transfection with WT or C277S mutant cDNA in pcDNA vector, respectively. All cells were selected with G418 (1 mg/mL, Sigma-Aldrich, St Louis, MO, USA) for 1 week. All cell lines were regularly tested to exclude mycoplasma contamination.

MNEKs were prepared from neonatal skin as previously described with minor modifications (76). Briefly, mice were euthanized with CO_2 two days after birth. Mice were washed twice with betadine and then rinsed with phosphate buffered saline (PBS). The skin of neonates was removed and soaked in PluriSTEM™ Dispase-II solution (Merck Millipore, Darmstadt, Germany) for 12 h at 4°C. The skin was then separated to epidermis and dermis. The epidermal layer was incubated in 1 mL of TrypLE™ (Gibco, Grand Island, NY, USA) for 10 min at 37°C, then 1 mL of fetal bovine serum was added to inactivate TrypLE™. The epidermal tissues were vortexed for 10 min followed

by centrifugation for 3 min at 1 000 x *g* at room temperature. The cell pellet was resuspended in keratinocyte proliferation media (1:1 mixture of KGM-Gold and calcium free KGM-Gold kit media, Lonza, Lyon, France). MNEKs were used at passage 1.

2.2.5 UV irradiation

G20T10E UVB lamp (Sankyo, Denki, Japan) was used for UV irradiation. UVB was measured using a UV light meter, UV-340A (Lutron Electronic Enterprise Co. LTD, Taipei, Taiwan). Cells and mice were exposed to a single dose of UVB radiation (10 mJ/cm^2 for cells and 200 mJ/cm^2 for mice). Cells in a 6-well plate were washed twice with PBS after removal of culture media, 500 µL PBS was added, and they were exposed to UVB radiation.

2.2.6 Western blot analysis

Sample preparation and SDS-PAGE were performed as previously described (35). The following primary antibodies were used: anti-β-actin (Sigma-Aldrich, St Louis, MO, USA, A5441), TG2 (77), p65 (Santa Cruz Biotechnology, Santa Cruz, CA, USA, sc-8008), p-p65^{Ser536} (Cell Signaling Technology, Beverly, MA, USA, #3031), IκBα (Cell Signaling Technology, Beverly, MA, USA, sc-847). After reaction with horseradish peroxidase-conjugated secondary antibody (Santa Cruz Biotechnology, Santa Cruz, CA, USA, sc-2004 or sc-2005), immunoreactive proteins were visualized by SuperSignal™ West Pico Chemiluminescent Substrate (Thermo Fisher Scientific Inc., Rockford, IL,

USA). The bands were quantified using ImageJ (http://rsb.info.nih.gov/ij/).

2.2.7 QRT-PCR

Total RNA extraction and QRT-PCR were carried out using a CFX96™ Real-Time system (Bio-Rad, Hercules, CA, USA) as previously described (78). The following specific primers were used.

Species	Genes	Forward	Reverse
Mouse	GAPDH	GGACCTCATGGCCTACATGG	TAGGGCCTCTCTTGCTCAGT
	IL-6	TGATTGTATGAACAACGATGATGC	GGACTCTGGCTTTGTCTTTCTTGT
	TNF-α	TTCCCAAATGGCCTCCCTCTCATC	TCCTCCACTTGGTGGTTTGCTAC
Human	36B4	GCCAATAGACAGGAGCGCTATC	AAAGACGATGTCACTTCCACGAG
	IL-6	CTATGAACTCCTTCTCCACAAGCG	GGGCGGCTACATCTTTGGAATC
	IL-8	TCTGCAGCTCTGTGTGAAGGTG	TGTGGTCCACTCTCAATCACTCTC
	TNF-α	AGCCTGTAGCCCATGTTGTAGC	ATCTCTCAGCTCCACGCCATTG
	TG1	TCATCTCTGCCATGGTGAACTCC	ACCAGACCAGTTCCCAATCAGG
	TG2	AGAAGAGCGAAGGGACGTACTG	AGTCTACCACGTCGGCATTGAC
	TG3	TGGCAGGTACATCAGCACCAAG	TGTCTTTCCTGGTCAGAGCCTTC
	TG5	TCATCTTCGTGGTTGAAACTGGAC	ATTGGTCTCCAGCCAGGCAATC

Levels of mRNA were estimated by the $2^{-\Delta\Delta Ct}$ method and normalized to GAPDH or 36B4 levels.

2.2.8 Cytometric bead array (CBA)

Secreted human TNF-α, IL-6, and -8 protein levels were measured by BD CBA (Thermo Fisher Scientific Inc.). Briefly, 4.5 x 10^5 HaCaT cells were seeded on 6-well plates and incubated for 24 h. Then, culture medium was collected 6 h after UVB irradiation and analyzed according to the manufacturer's instructions. The MAGPIX Multiplexing System (Komabiotech, Seoul, Korea) was used to measure the protein levels of mouse IL-6 and TNF-α.

2.2.9 Luciferase reporter assay

HaCaT cells and MNEKs were co-transfected with the 3κB-luciferase construct and pRL-TK vector as an internal control. Luciferase reporter activity was measured by a luciferase assay kit (Promega, Madison, WI, USA) 9 h after UVB irradiation.

2.2.10 *in situ* TG activity assay

Six h after UVB irradiation, HaCaT cells were incubated with 1 mM EZ-link Pentylamine-Biotin (BP) (Thermo Fisher Scientific Inc., Rockford, IL, USA) as TG2 substrate in serum-free DMEM for 1 h. These cells were subjected to *in situ* TG activity assay as previously described (70).

2.2.11 Statistical analysis

Statistical evaluations were performed with GraphPad Prism 5.0 statistical software (GraphPad Software, La Jolla, CA, USA) using Student's t-test, or one-way or two-way ANOVA. $P<0.05$ was considered statistically significant. All error bars represent mean ± SEM. The data are representative of at least 3 independent experiments.

2.3 RESULTS

2.3.1 TG2-deficient mice show reduced UV-induced skin inflammation

The crosslinking activity of TG1 and TG3 is crucial for CE formation during terminal differentiation of epidermal keratinocytes (54). To test whether TG2 is also involved in this process, we examined the skin barrier function of $TG2^{-/-}$ mice. In wild-type (WT) mice, TG2 is expressed in all epidermal layers (Fig. 2-2A). Histochemical staining of skin sections showed no differences between WT and $TG2^{-/-}$ mice in gross structure of the skin and expression of differentiation markers, such as loricrin, involucrin, and filaggrin in epidermal keratinocytes (Fig. 2-2A and B). Functional evaluation of skin permeability with toluidine blue staining revealed no difference between WT and $TG2^{-/-}$ mice (Fig. 2-2C). These results indicate that TG2 activity is not required for differentiation or CE formation of epidermal keratinocytes.

TG2 is activated under various ROS-producing conditions, including UV irradiation (72). To determine whether TG2 is involved in UV-induced skin inflammation, we compared the effects of UV irradiation on the skin of WT and $TG2^{-/-}$ mice. After 48 h of UVB irradiation, $TG2^{-/-}$ mice showed reduced skin redness (Fig. 2-2D), significantly decreased swelling of the skin (Fig. 2-2E), reduced infiltration of immune cells to the UV-irradiated skin (Fig. 2-2F and G), reduced vasodilation in UV-irradiated lesions (Fig. 2-2I) compared with those of WT littermates. On the other hand, UV-irradiated WT and $TG2^{-/-}$ mice

exhibited no significant difference in the number of TUNEL-positive skin cells (Fig. 2-2H), indicating that TG2 may be not involved in UV-induced skin cell apoptosis. These skin phenotypes of $TG2^{-/-}$ mice suggest a causal role of TG2 in UV-induced acute inflammation.

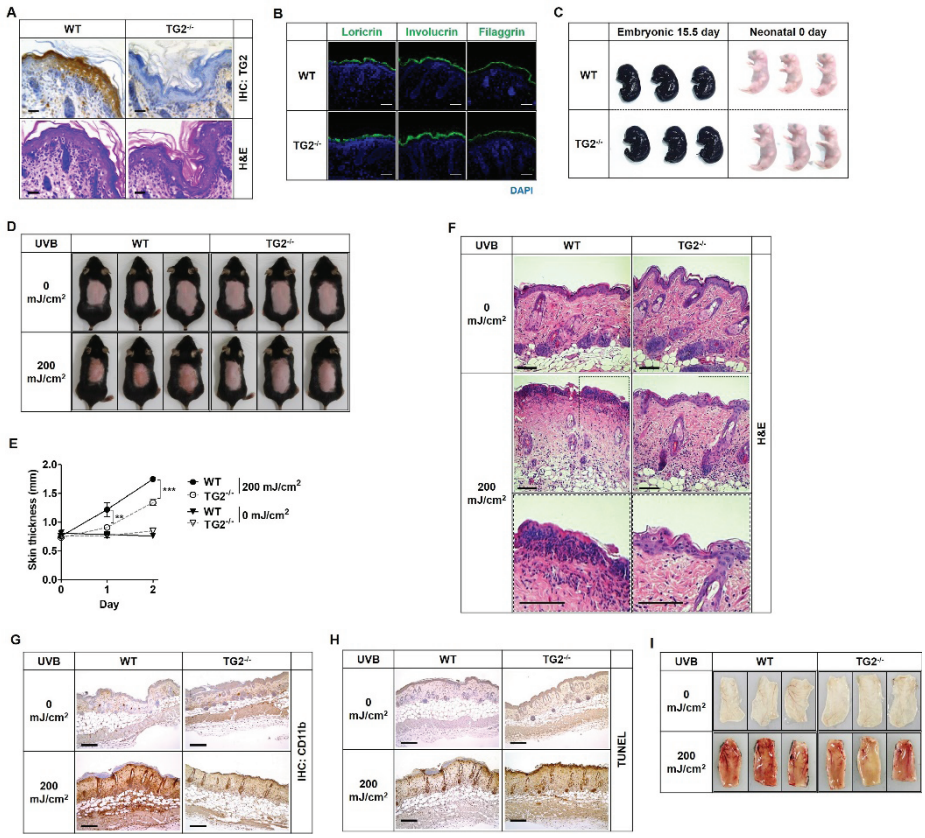

Figure 2-2. TG2$^{-/-}$ mice exhibit reduced skin inflammation in response to UV irradiation without any alterations for keratinocyte differentiation and skin barrier function. (A) Histology of skin from WT and TG2$^{-/-}$ littermates (8-week-old, female). Skin sections were stained with anti-TG2 antibody and hematoxylin & eosin (H&E). (B) Skin sections prepared from WT and TG2$^{-/-}$ neonates were immunostained with antibodies specific for loricrin, involucrin, and filaggrin. DAPI staining was used for localization of nuclei. Scale bar, 50 μm. (C) WT and TG2$^{-/-}$ neonates (birth day 0) or embryos (E15.5) were stained with toluidine blue. (D) Representative photographs of mice skin after 48 h of UV exposure (200 mJ/cm^2 UVB). (**E**) Skin thickness measured by caliper at

indicated times. Data are shown as mean ± SEM. (F-H) Histology and immunohistochemistry of skin from WT and $TG2^{-/-}$ littermates after 48 h of UV irradiation (200 mJ/cm^2 UVB), skin sections were stained with H&E (F), CD11b (G), and TUNEL (H). (I) Vasculature of the UV-irradiated skin after 96 h of UV-exposure. Scale bars, 100 μm. *, $P<0.05$; **, $P<0.01$; ***, $P<0.001$.

2.3.2 TG2 mediates UV-induced production of inflammatory cytokines in keratinocytes

UV irradiation stimulates the production and release of inflammatory cytokines in epidermal keratinocytes, which elicits skin inflammation. To test whether TG2 mediates UV-induced cytokine production, we compared the ability of WT and $TG2^{-/-}$ mice to produce inflammatory cytokines in response to UV irradiation. In the UV-exposed skin from WT mice, there was a 30- and 6-fold increase in the mRNA levels of TNF-α and IL-6, respectively, whereas there was no change in the expression levels of both cytokines in the skin of $TG2^{-/-}$ mice (Fig. 2-3A). MAGPIX Multiplexing revealed that protein levels of both TNF-α and IL-6 were significantly reduced in $TG2^{-/-}$ compared to those in the skin of WT mice in response to UV irradiation (Fig. 2-3B). To confirm the role of TG2 in keratinocytes, we prepared mouse neonatal epidermal keratinocytes (MNEKs) and examined the TNF-α and IL-6 expression levels. MNEKs from $TG2^{-/-}$ mice showed significantly reduced levels of TNF-α and IL-6 mRNA after UVB exposure compared with those from WT mice (Fig. 2-3C).

To test the role of TG2 in human keratinocytes, we generated $TG2^{-/-}$ and knockdown HaCaT cell lines by using the CRISPR-Cas9 system and small hairpin RNA (shRNA) transfection, respectively, and compared the levels of cytokine expression. In control HaCaT cells, mRNA levels of TNF-α, IL-6, and IL-8 rapidly increased after UV irradiation, remained constant for 2–4 h, and decreased thereafter to basal levels. In contrast, in $TG2^{-/-}$ and knockdown HaCaT cells, mRNA levels were significantly suppressed (Fig. 2-3D). The

protein levels of TNF-α, IL-6, and IL-8 secreted from UV-irradiated HaCaT cells were also significantly reduced in $TG2^{-/-}$ and knockdown cells (Fig. 2-3E). These results indicate that UV irradiation induces the production of inflammatory cytokines through regulation of TG2 in epidermal keratinocytes.

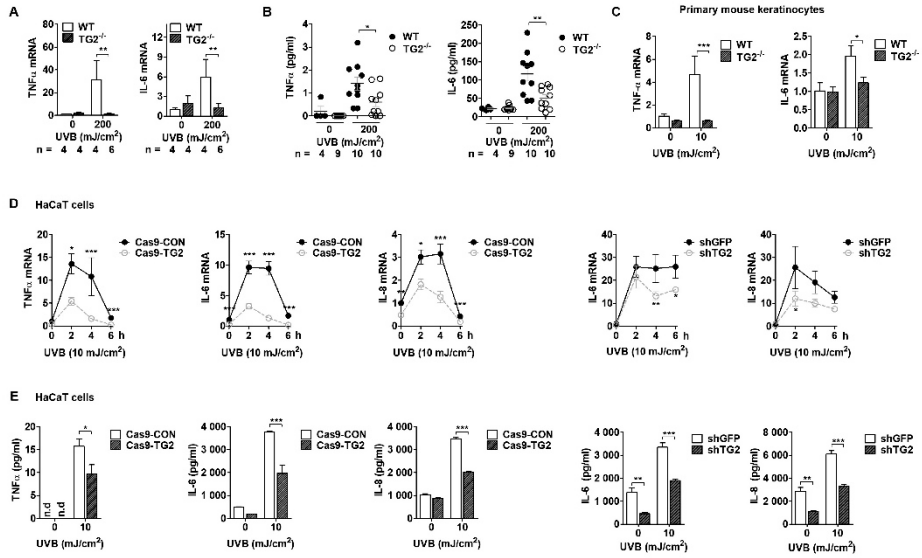

Figure 2-3. TG2 is required for expression of inflammatory cytokines in UV-irradiated keratinocytes. (A and B) Skin tissues were obtained from WT and TG2$^{-/-}$ littermates after 48 h of UV irradiation (200 mJ/cm^2). Levels of mRNA (A) and protein (B) for mouse IL-6 and TNF-α were determined by QRT-PCR and MAGPIX Multiplexing assay, respectively. (C) Primary mouse keratinocytes from WT and TG2$^{-/-}$ littermates were cultured and exposed to UV irradiation (10 mJ/cm^2). After 6 h, mRNA levels of mIL-6 and mTNF-α were determined by QRT-PCR (n = 3). (D, E) TG2-deficient or TG2-knock down HaCaT cells exposed to UV irradiation (10 mJ/cm^2). After 6 h, levels of mRNA (D, n = 3) and secreted protein (E, n = 3) for TNF-α, IL-6, and IL-8 were measured by QRT-PCR and by CBA method, respectively. All data are represented as mean ± SEM. *, P<0.05; **, P<0.01; ***, P<0.001.

2.3.3 UV irradiation increases TG2 activity but not its protein level

To gain evidence that TG2 is regulated by UV irradiation, we monitored the TG2 protein level and intracellular transamidation activity in UV-exposed HaCaT cells. Western blot analysis showed that there were no changes in the protein level of TG2 for 12 h after UV irradiation (Fig. 2-4A), even with increased dosage (Fig. 2-4B). Moreover, the mRNA levels of TG2, were not affected by UV irradiation (Fig. 2-4C). By contrast, UV irradiation induced a time- (Fig. 2-4A) and dose-dependent (Fig. 2-4B) increase of *in situ* TG activity, which paralleled mRNA levels of TNF-α, IL-6, and IL-8 in a time-dependent (Fig. 2-4D) and dose-dependent manner (Fig. 2-4E), indicating that UV-induced cytokine production is correlated with *in situ* TG activity but not with TG2 protein level.

In addition to TG2, TG1, 3, and 5 are also expressed in epidermal keratinocytes (54), and the current TG assay method is not able to discriminate TG isozymes. To test whether UV irradiation activates TG2 only, we compared *in situ* TG activity in the skin of $TG2^{-/-}$ mice with that of WT mice. $TG2^{-/-}$ mice showed no increase in TG activity in the epidermis in response to UV irradiation, whereas WT mice exhibited substantially increased TG activity (Fig. 2-4F). Similar results were observed in the TG2-deficient HaCaT cell line (Fig. 2-4G), indicating that an increase in *in situ* TG activity can be attributed to UV-induced TG2 activation.

To confirm these results, we examined the effect of KCC009, an inhibitor

of TG (79), on UV-induced cytokine expression. In HaCaT cells exposed to UV irradiation, KCC009 treatment significantly suppressed *in situ* TG activity (Fig. 2-5A and B), and concomitantly reduced the mRNA (Fig. 2-5C) and protein levels of TNF-α, IL-6, and IL-8 compared with control cells (Fig. 2-5D). To further confirm TG2-specific activation by UV irradiation, we established HaCaT cell lines overexpressing WT TG2 ($TG2^{WT}$) or active-site mutant of TG2 ($TG2^{C277S}$). When these cells were exposed to UV irradiation, *in situ* TG activity was increased in proportion to TG2 protein levels. By contrast, HaCaT cells expressing $TG2^{C277S}$ failed to increase *in situ* TG activity (Fig. 2-5E), mRNA levels (Fig. 2-4F), and protein levels of proinflammatory cytokines compared with cells overexpressing $TG2^{WT}$ (Fig. 2-5G). These results indicate that UV irradiation promotes cytokine production through TG2 activation, but not through upregulation of TG2 expression.

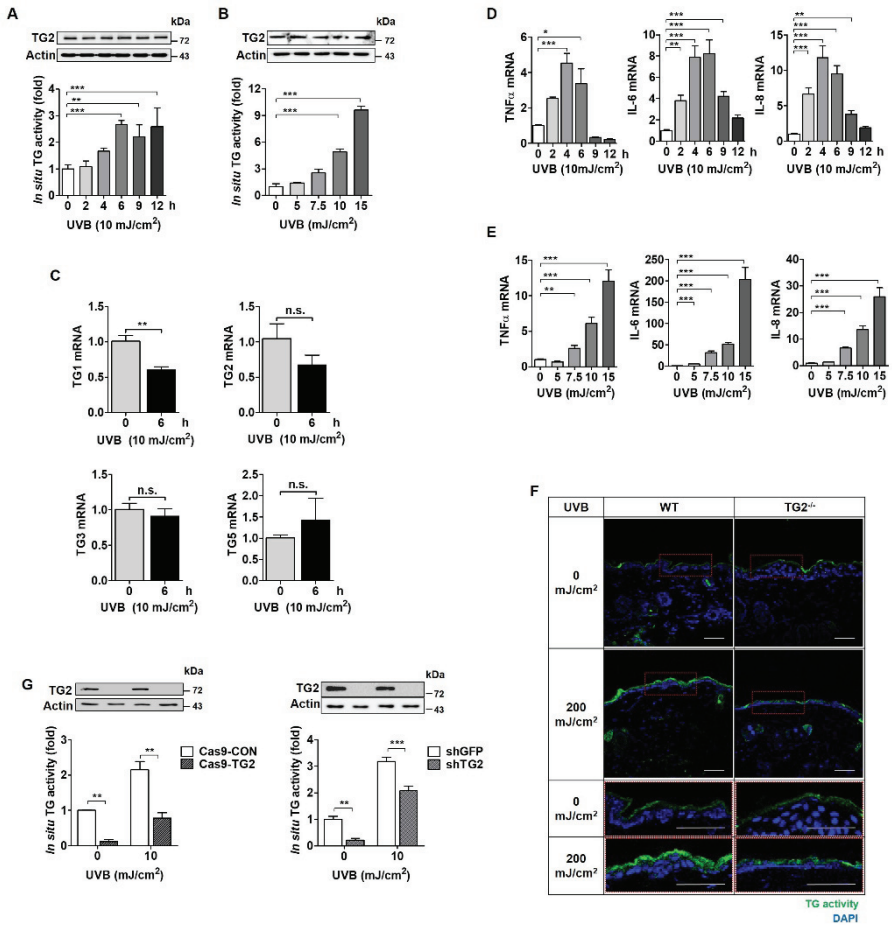

Figure 2-4. UV irradiation activates keratinocyte TG2. (A and B) Levels of TG2 protein and *in situ* TG activity in HaCaT cells were determined by Western blot analysis and biotinylated pentylamine (BP) incorporation assay, respectively. HaCaT cells were exposed to UV irradiation (A, 10 mJ/cm^2, n = 4; B, doses indicated, n = 4) and harvested at the time indicated (A) or after 6 h of UV irradiation (B). (C) **.** HaCaT cells were exposed to UV irradiation (10 mJ/cm^2), and mRNA levels of TG1, TG2, TG3, and TG5 were determined by QRT-PCR (n = 3). (D and E) mRNA levels of TNF-α, IL-6, and IL-8 were determined by QRT-PCR in HaCaT cells exposed to UV irradiation as (A) and

(B) (n = 3). (F) *in situ* TG activity in skin from UV-irradiated WT and $TG2^{-/-}$ littermates (n = 3). (G) *in situ* TG activity in TG2-deficient (Cas9–TG2) and TG2-knock down (shTG2) HaCaT cells after 6 h of UV irradiation (10 mJ/cm^2). All data are represented as mean ± SEM. *, $P<0.05$; **, $P<0.01$; ***, $P<0.001$.

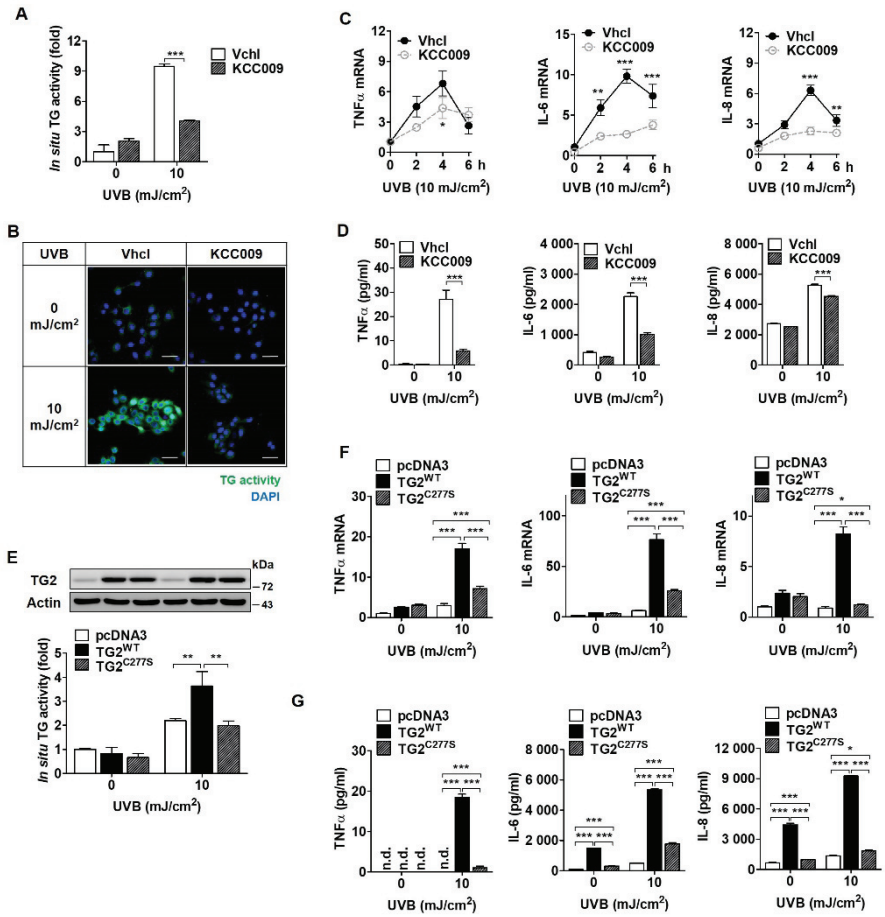

Figure 2-5. TG inhibition suppresses the production of cytokines in UV-irradiated keratinocytes. (A and B) HaCaT cells were pretreated with KCC009 (250 μM) or vehicle (Vhcl) 1 h before UV irradiation (10 mJ/cm^2). Cells were incubated for 6 h after UV irradiation in the same media. *in situ* TG activity was measured by BP incorporation assay (A, n = 3) and visualized by confocal microscopy (B). Scale bars, 50 μm. (C and D) Levels of mRNA (C, n = 3) and proteins (D, n = 3) for TNF-α, IL-6, and IL-8 were measured in KCC009-pretreated and UV-irradiated HaCaT cells at the times indicated (C) or 6 h after UV irradiation (D). (E) Levels of TG2 protein and *in situ* TG activity

were measured in HaCaT cell lines expressing pcDNA3, WT ($TG2^{WT}$), or active-site mutant TG2 ($TG2^{C277S}$) established by transfection and selection (n = 4). (F and G) Levels of mRNA (F, n = 4) and proteins (G, n = 4) for TNF-α, IL-6, and IL-8 were measured in HaCaT cell lines expressing pcDNA3, WT ($TG2^{WT}$) or active-site mutant TG2 ($TG2^{C277S}$) at 6 h after UV irradiation. All data are represented as mean ± SEM. *, $P<0.05$; **, $P<0.01$; ***, $P<0.001$.

2.3.4 UV irradiation activates TG2 through endoplasmic reticulum (ER) calcium release

We next investigated the mechanism by which UV irradiation activates TG2 in epidermal keratinocytes. Since TG2 is a calcium-dependent enzyme, we considered the role of calcium in activating TG2 in UV-irradiated keratinocytes. UV irradiation increases cytosolic Ca^{2+}, which is released from the ER through activation of the PLC-IP_3 signaling pathway (80). To determine whether PLC activation is required for UV-induced increase of TG2 activity, we examined the effect of U73122, a pan-PLC inhibitor, on *in situ* TG activity. In HaCaT cells exposed to UV irradiation, pretreatment with U73122 suppressed *in situ* TG activity, and mRNA expression of TNF-α, IL-6, and IL-8, whereas pretreatment with its inactive analogue U73343 showed no effect (Fig. 2-6A and B). Treatment with 2-aminoethyl diphenylborinate, an IP_3R inhibitor, also exhibited suppressed *in situ* TG activity and cytokine mRNA expression (Fig. 2-6C and D). To confirm the role of ER calcium in activating TG2, we evaluated the effect of thapsigargin treatment in HaCaT cells, which increased *in situ* TG activity and mRNA levels of inflammatory cytokines (Fig. 2-6E and F). These results indicate that TG2 is activated by UV-induced release of ER calcium through the PLC-IP_3 signaling pathway.

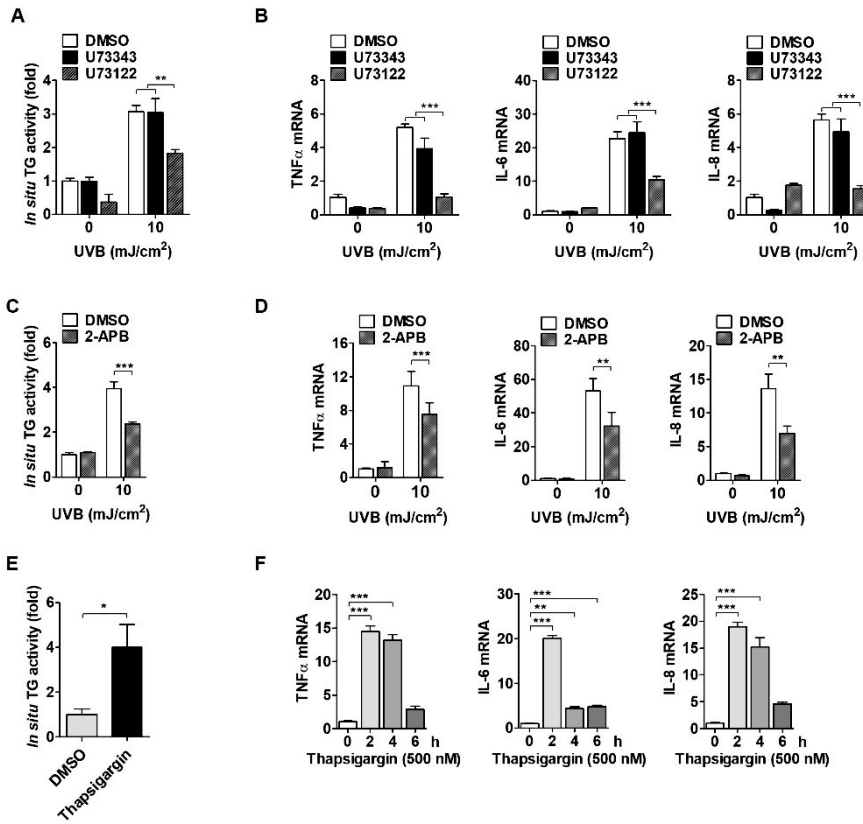

Figure 2-6. UV-induced release of ER calcium is responsible for TG2 activation. (A-D) HaCaT cells were pretreated with 20 μM U73122 or U73343 (A and B, n = 3) and with 100 μM 2-aminoethyl diphenylborinate (2-APB) (C and D, n = 3), and then exposed to UV irradiation (10 mJ/cm^2). After 6 h, levels of *in situ* TG activity and mRNA for TNF-α, IL-6, and IL-8 were measured by BP incorporation assay and QRT-PCR, respectively. (E and F) Effect of thapsigargin (500 nM) on *in situ* TG activity in HaCaT cells (E, n = 3) and expression of cytokines (F, n = 3) or in primary epidermal keratinocytes prepared from WT and TG2$^{-/-}$ littermates. All data are represented as mean ± SEM. *, P<0.05; **, P<0.01; ***, P<0.001.

2.3.5 Activation of TG2 enhances NF-κB transcriptional activity

The NF-κB signaling pathway plays a major role in the production of proinflammatory cytokines in response to UV irradiation (81), and TG2 is known to activate NF-κB signaling under oxidative stress; however, its molecular mechanism remains unclear (74, 82). To determine whether TG2 is involved in NF-κB activation under UV-irradiated conditions, we compared the ability to promote transcriptional activity of NF-κB in WT- and $TG2^{-/-}$-MNEKs transiently transfected with the 3κB-luciferase gene. $TG2^{-/-}$-MNEKs showed significantly reduced NF-κB reporter activity compared with WT-MNEKs after UV irradiation (Fig. 2-7A). In HaCaT cells stably expressing 3κB-luciferase, treatment with KCC009 or U73122 significantly inhibited UV-induced reporter activity of NF-κB (Fig. 2-7B and C), indicating that TG2 activity is required for UV-induced NF-κB activation.

To further analyze TG2-mediated NF-κB activation, we monitored the protein levels of IκBα and phosphorylated p65. Western blot analysis showed that IκBα levels were decreased after UV irradiation in a time-dependent manner in TG2 knockdown, KCC009-treated, and control HaCaT cells. By contrast, levels of phosphorylated p65 ($p\text{-}p65^{Ser536}$) were increased in control HaCaT cells, but decreased in TG2 knockdown and KCC009-treated cells (Fig. 2-7D and E), indicating that TG2 mediates NF-κB activation not by inducing IκBα degradation, but by promoting phosphorylation of p65 at Ser^{536}. These results indicate that UV irradiation activates TG2 through the PLC-IP_3 pathway,

which activates NF-κB signaling by promoting p65 phosphorylation, leading to increase in proinflammatory cytokine production.

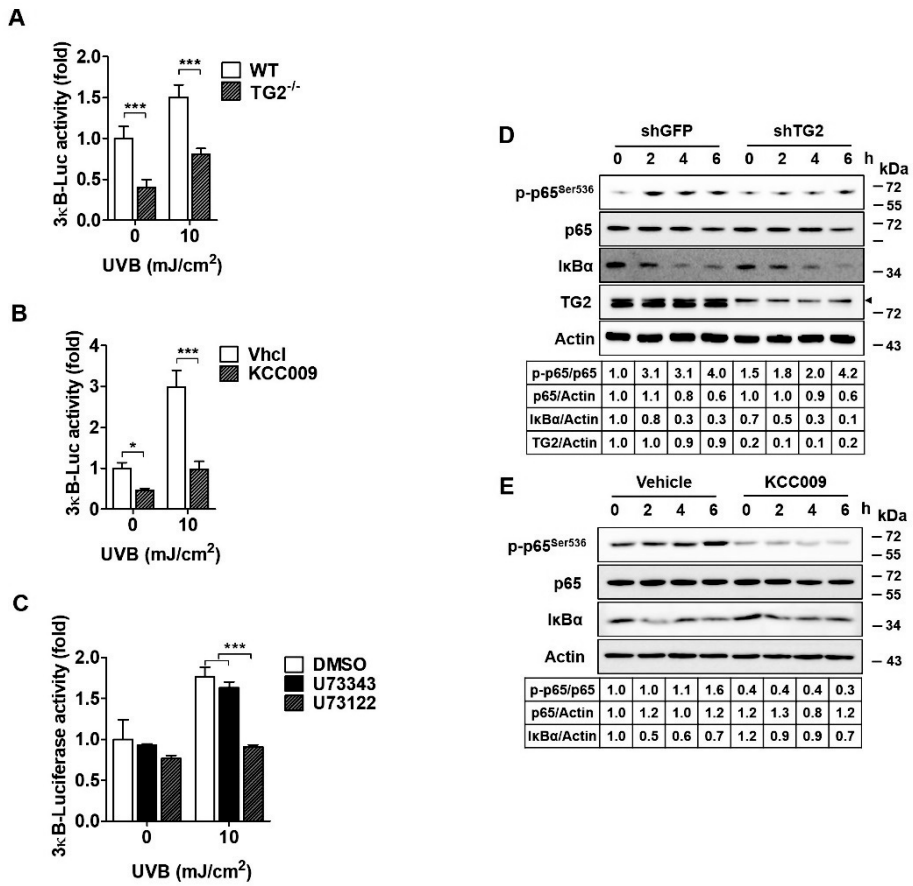

Figure 2-7. TG2 enhances transcriptional activity of NF-κB. (A-C) 3κB-luciferase reporter activity was assessed in primary epidermal keratinocytes prepared from WT and TG2$^{-/-}$ littermates (A, n = 3), or HaCaT cells (B and C, n = 3) 9 h after UV irradiation (10 mJ/cm^2). HaCaT cells were pretreated with 250 μM KCC009 (B), or with 20 μM U73122 or U73343 (C) 1 h before UV irradiation. Luciferase activity was normalized with co-transfected *Renilla* activity. Data are represented as mean ± SEM. *, P<0.05; **, P<0.01; ***, P<0.001. (D and E) Lysates prepared from TG2 knockdown HaCaT cells (D) or HaCaT cells treated with 250 μM KCC009 (E) were immunoblotted with

antibodies specific for IκBα, phosphorylated p65 at Ser536, p65, and TG2. Actin was used as a loading control. Arrowhead in the blot indicates a nonspecific band.

2.4 DISCUSSION

UV irradiation elicits a range of responses in the skin, including inflammatory and DNA damaging responses, which lead to the development of photoaging and skin cancer in chronically exposed skin (67). Of these, acute inflammatory reaction is mediated by UV-induced release of proinflammatory cytokines, such as TNF-α, IL-6, and IL-8. However, the signaling pathways responsible for cytokine production in UV-exposed keratinocytes have not been fully characterized. Herein, we show that keratinocyte TG2 is a critical mediator in UV-induced acute skin inflammation, based on a phenotype analysis of TG2-deficient mice. Moreover, our results identify the PLC-IP_3 pathway as an upstream pathway for UV-induced TG2 activation and the NF-κB pathway as a downstream pathway for TG2-induced release of proinflammatory cytokines. Collectively, these results indicate that TG2 is an effector enzyme that regulates NF-κB activity following UV irradiation in epidermal keratinocytes.

Skin barrier function and keratinization were impaired in autosomal recessive congenital ichthyosis 1 caused by TG1 mutation (56, 57), and skin barrier defects observed in $TG3^{-/-}$ mice caused the reduction of inflammatory threshold of skin exposed to UV irradiation (59). These observations indicate that the crosslinking activity of TG1 and TG3 in epidermal keratinocytes plays a critical role in the formation of the skin barrier, which in turn affects the inflammatory response to UV irradiation. In contrast, our data show that keratinization and skin barrier function were normal in $TG2^{-/-}$ mice. Consistent with these results, recent reports have shown no difference between $TG1^{-/-}$ and

TG1/TG2 double knockout mice in the structure of the epidermal CE (83). Thus, our results indicate that the reduced inflammatory response of $TG2^{-/-}$ mice to UV irradiation is not attributable to change in barrier function.

Our results provide insight into the role of PLC signaling in skin inflammation. PLC regulates cellular functions through hydrolysis of PIP_2 to DAG and IP_3, which bind with IP_3R on the ER membrane, leading to ER calcium release into the cytosol (84). In keratinocytes, PLC is a known regulator of inflammation. PLCε knock-out mice exhibited reduced UV-induced skin inflammation (85, 86), and reduced allergic contact hypersensitivity due to hampered expression of proinflammatory cytokines (87). Moreover, transgenic mice overexpressing PLCε in epidermal keratinocytes showed development of spontaneous skin inflammation (88). However, the pathway that mediates PLC-induced inflammation remains unknown. Our results demonstrate that TG2 is activated by increase in cytosolic calcium and it modulates NF-κB activity, thus indicating a pathway linking PLC signaling with skin inflammation. UV irradiation is also known to induce ER stress, triggering unfolded protein response by release of ER calcium (80, 89). Consistent with these findings, we showed that TG2 is activated by ER stress via oxidative stress-induced ER calcium release (71). Moreover, a recent report showed that TG2 crosslinks IP_3R-1, thereby inhibiting ER calcium release (90). This reaction might be a negative feedback mechanism to maintain intracellular calcium homeostasis and TG2 activity. These results imply that regulation of TG2 activity by ER calcium is a critical point of control in the inflammatory

response to UV irradiation.

TG2 is a calcium-dependent enzyme, and it is known that the EC_{50} of $[Ca^{2+}]_i$ required for activating TG2 is approximately 100–500 μM (91-95). At these calcium levels, TG isozymes expressed in epidermal keratinocytes, such as TG1 and TG3, can also be activated. Since it is not possible to evaluate TG isozyme-specific activity due to the lack of an effective assay method and isozyme-specific inhibitor, we used a genetic approach to assess UV-induced TG activation. Our results show that TG2 contributes > 90% of basal and 60% of UV-induced TG activity by comparison of *in situ* TG activity between WT and TG2-deficient HaCaT cells (Fig. 2-3G). Moreover, a majorly activated TG isotype in UV-irradiated mouse skin is TG2 in the upper layers of epidermis, where TG1 and TG3 are expressed, as well as in the lower layers of that by comparison of *in situ* TG activity between WT and $TG2^{-/-}$ mice (Fig. 2-3F). These results indicate that although TG1 and TG3 are also activated by UV irradiation, TG2 activation may account for most of the UV-induced increase of epidermal TG activity. In support of these data, proteolytic cleavage is required for TG1 and TG3 activation, in addition to increase in $[Ca^{2+}]_i$ during terminal differentiation of keratinocytes (96, 97). Nevertheless, UV irradiation upregulates TG1 expression through the NF-κB pathway (98), leading to restoration of damaged barrier function (99). TG3 has a protective role against photodamage, owing to its activity requirement in CE assembly (60). Thus, TG1 or TG3 inactivation might exacerbate UV-induced skin inflammation.

TG2 positively regulates NF-κB signaling in various cancer cell lines.

However, the substrate protein(s), whose function is altered by TG2-mediated modification, remains unidentified. Here, we tested two proposed mechanisms for activation of NF-κB signaling. First, TG2 is known to activate NF-κB through crosslinking of IκBα, which induces release and subsequent nuclear translocation of NF-κB (74). However, our results show that the protein level of monomeric IκBα was decreased by UV irradiation, even in TG2 knockdown, inhibitor-treated, and control HaCaT cells. Moreover, dimeric or multimeric forms of crosslinked IκBα were not observed in the same experimental conditions, indicating that IκBα crosslinking did not occur in TG2-mediated NF-κB activation. Second, TG2 reportedly facilitates nuclear translocation of NF-κB, regardless of its enzymatic activity in breast cancer cells (82). In contrast to this report, our data show that expression of enzymatically inactive TG2 failed to increase expression of proinflammatory cytokines after UV irradiation, demonstrating that transamidation activity of TG2 is required for UV-induced NF-κB activation. Instead, we show that $p65^{Ser536}$ phosphorylation was increased, but decreased in TG2 knockdown or inhibitor treated cells after UV irradiation (Fig. 2-6D and E). Since Ser536 is phosphorylated by IKK (100), and is a functionally important residue in regulating the transcriptional activity of p65 (101), our results imply that TG2 activates NF-κB signaling by increasing $p65^{Ser536}$ phosphorylation in UV-irradiated keratinocytes. However, there is no evidence that TG2 regulates kinase activity of IKKs. Moreover, it was reported that TG2 activates NF-κB signaling in an IKK-independent manner (102). Thus, further investigation of the molecular mechanism by

which TG2 regulates phosphorylation of $p65^{Ser536}$ is needed.

In summary, we have shown that keratinocyte TG2 plays a pivotal role in mediating UV-induced skin inflammation. TG2 is activated by UV-induced ER calcium release through the PLC-IP_3 signaling pathway, which in turn activates NF-κB signaling, leading to increase in proinflammatory cytokine production (Fig. 2-7A). These findings suggest that inhibition of keratinocyte TG2 might be a useful strategy in preventing UV radiation-related skin disorders, such as photoaging and skin cancer, which occur with chronic exposure to UV irradiation.

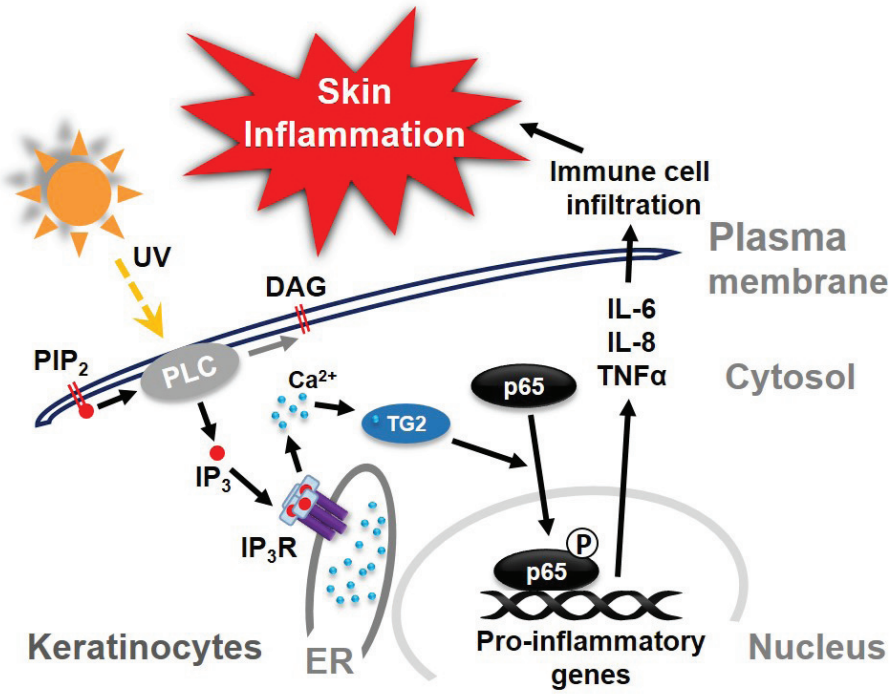

Figure 2-8. Schematic representation of TG2-dependent UV-induced inflammation. UVB-induced activation of PLC facilitates release of calcium from ER to cytosol. The cytosolic increment of free calcium ions induces activation of TG2, followed by transcriptional activation of NF-κB. Activated NF-κB initiates transcription of target genes such as IL-6, IL-8 and TNF-α, which are mediates skin inflammation.

*** This study is published in Cell Death & Disease (2017).**

CHAPTER 3

Transglutaminase 2 mediates UVB-induced matrix metalloprotease-1, -3 and -13 expression in dermal fibroblasts

3.1 INTRODUCTION

Transglutaminases (TGs) constitute a large family of enzymes that are responsible for the posttranslational modification of proteins by catalyzing acyl-transfer reaction between substrate proteins and polyamines in calcium-dependent fashion (52). Until now, nine members of the TG family proteins have been identified and six isozymes among the family are expressed in human skin including TG1-TG5 and factor XIIIa (55).

TG1, TG3 and TG5 are enzymes playing crucial role in maintaining epidermal barrier by mediating crosslinking of various cornified envelope (CE) components including loricrin, envoplakin, periplakin, involucrin, small proline-rich proteins (SPRs), and lipids (54). TG1 is the most critical enzyme for normal epidermal barrier formation in mouse and human. TG1-null mice die from dehydration due to defective in CE formation within 4-5 h after birth (56). Additionally, TG1 mutations in human cause autosomal recessive congenital ichthyosis (57). Skin TG3 participates in crosslinking of hair proteins (58), FITC-induced hypersensitivity (59) and UV-induced apoptosis (60) in mouse, and uncombable hair syndrome in human (61), indicating TG3 has roles in hair development as well as CE formation. TG5 mutations in human are associated with acral peeling syndrome (63), indicating TG5 regulates cell-to-cell adhesion in epidermis. In addition, crosslinking activity of factor XIIIa is considered to be important for wound repair since factor XIIIa-null mice showed impaired wound healing phenotype (65). Although TG4 is expressed in glandular epithelial cells, there are no reports on altered skin phenotype(s) of

TG4-null mice. Unlike these isozymes, TG2-null mice showed normal skin phenotype (66). Previously, we showed that UV irradiation induces enzymatic activation of intracellular TG2 through the calcium mobilization (72, 103). Additionally, TG2 activation is indispensable in UV-induced acute skin inflammation through mediating transcriptional activation of NF-κB and following expression of inflammatory cytokine genes (103). Furthermore, Victoria *et al.* (104) reported that TG2 abundance and its activity in mediating crosslinking of extracellular matrix (ECM) are crucial for pathogenesis of recessive dystrophic epidermolysis bullosa (RDEB). These results indicate that TG2 regulates skin homeostasis under pathogenic rather than normal condition.

Matrix metalloproteinases (MMPs) are a family of zinc-dependent endopeptidases that degrade various ECM components. At least 28 different types of MMPs have been discovered and they can be subdivided into several classes, based on their substrate specificities and structures (Table 3-1) (11). MMPs play critical roles in tissue remodeling during pathophysiological processes, including developmental morphogenesis, angiogenesis, tissue repair, arthritis, tumor invasion and metastasis and skin aging. Human fibroblasts express several different types of MMPs including MMP-1 (collagenase), MMP-2 and -9 (gelatinase) and MMP-3 (stromelysin) following various stresses, such as UV, infrared radiation and heat shock (105-108). UV irradiation induces MMP-1, -3, and -9 expressions through activation of AP-1 and NF-κB pathways (109, 110). In particular, MMP-1 is the most important MMP family proteins in maintaining ECM homeostasis of the skin since it is a

major collagenolytic enzyme responsible for UV-damaged human skin (111).

Herein, we determined whether TG2 mediates UV-induced human and mouse MMPs expressions, and showed that TG2-dependent NF-κB activation is crucial in this process through cell culture and *ex vivo* skin culture model. These results suggest that TG2 is a critical regulator that mediates MMPs expressions and remodeling of the skin in response to UV radiation.

Table 3-1. Classification of human metalloproteinases (11).

MMP subgroups	MMP number
Collagenase	MMP-1, MMP-8, MMP-13
Gelaninase	MMP-2, MMP-9
Stromelysins	MMP-3, MMP-10, MMP-11
Matrilysins	MMP-7, MMP-26
Membrane-type	MMP-14, MMP-15, MMP-16, MMP-17, MMP-24, MMP-25
Other types	MMP-12, MMP-19, MMP-20, MMP-21, MMP-22, MMP-23, MMP-28

3.2 MATERIALS AND METHODS

3.2.1 Cell culture and siRNA transfection

Human dermal fibroblasts (HDFs) were purchased form Gibco (Gibco, Carlsbad, CA, USA) and cultured in Dulbecco's Modified Eagle's Medium (DMEM, Welgene, Gyeongsan, South Korea) containing 10% heat-inactivated fetal bovine serum (FBS, Hyclone, Logan, UT, UK), 100 U/mL of penicillin, and 100 μg/mL of streptomycin sulfate (Gibco, Carlsbad, CA, USA) under 5% CO_2 at 37°C. For siRNA transfection, 1 x 10^5 cells were plated on 6-well plate and incubated 24 h. GFP and TG2 siRNAs (Santa Cruz Biotechnology, Santa Cruz, CA, USA, sc-45924, sc-37514) were transfected by using RNAiMAX (Invitrogen, NY, USA) in accordance with the manufacturer's instruction. All experimental procedures were performed 24 h after siRNA transfection. HDFs were used under passage 8.

3.2.2 Isolation of mouse dermal fibroblasts and *ex vivo* skin culture

Mouse dermal fibroblasts (MDFs) were prepared from neonatal mice skin as previously described with minor modifications (76). Briefly, mice were euthanized with CO_2 two days after birth and washed twice with betadine and then rinsed with phosphate buffered saline (PBS). After removing the skin from neonates, the skin was soaked in PluriSTEM™ Dispase-II solution (Merck Millipore, Darmstadt, Germany) for 12 h at 4°C. The skin was then separated

to epidermis and dermis. The dermal layer was incubated in 1 mL of TrypLE™ (Gibco, Grand Island, NY, USA) for 50 min at 37°C, then 1 mL of FBS was added to inactivate TrypLE™. The dermal tissues were vortexed for 10 min followed by centrifugation for 3 min at 1000 x *g* at room temperature. The cell pellet was resuspended and cultured in DMEM containing 10% FBS and 1% penicillin-streptomycin. MDFs were used under passage 3.

For *ex vivo* culture, the skin removed from neonate mice was divided into four pieces and incubated in DMEM containing 0.1% FBS and 1% penicillin-streptomycin for 24 h. Culture media changed (DMEM containing 10% FBS and 1% penicillin-streptomycin) after UVB irradiation and incubated as indicated times.

3.2.3 UV irradiation

G20T10E UVB lamp (Sankyo, Denki, Japan) was used for UV irradiation. To measure UVB, UV light meter, UV-340A (Lutron Electronic Enterprise Co. LTD, Taipei, Taiwan) was used. The cells and skins were exposed to a single dose of UVB radiation (10 mJ/cm^2 for cells and 200 mJ/cm^2 for skin). To irradiate cells, 3 x 10^5 cells were seeded on 6-well plate and incubated for 24 h. The cells were washed twice with PBS after removal of culture media, 500 μL PBS was added to prevent dry, and they were exposed to UVB radiation. Cycloheximide (Sigma-Aldrich Co., St Louis, MO, USA) or MG132 (Sigma-Aldrich Co., St Louis, MO, USA) were added to culture media according to the experimental conditions.

3.2.4 *in situ* TG activity assay

Six hours after UVB irradiation, HDFs were incubated with 1 mM EZ-link Pentylamine-Biotin (BP) (Thermo Fisher Scientific Inc., Rockford, IL, USA) in serum-free DMEM for 1 h. *In situ* TG activity was measured as previously described (70).

3.2.5 Gelatin zymography

Since gelatin is a partial substrate of MMP-1 (117), MMP-1 activity can be measured by gelatin zymography. The culture media were collected after 48 h of UV irradiation and mixed with the same volume of 2X sample buffer (122 mM pH7.4 Tris-HCl, 20% Glycerol, 4% SDS, 0.01% bromophenol blue). The mixture was loaded on 0.5% gelatin-acrylamide gel. After gel running, the gel was washed by 2.5% Triton X-100 solution for 20 min at room temperature with gentle agitation for two times then washed with distilled water. Then, the gel was incubated in incubation buffer (50 mM pH 7.4 Tris-HCl, 10 mM $CaCl_2$, 10 nM $ZnCl_2$, 0.01% NaN_3) for 18 h at 37°C. Enzymatic activity was visualized by coomassie staining and imaged by scanning the gel.

3.2.6. Cell *in situ* zymography

Cell *in situ* zymography was performed and quantified as previously described with minor modifications (112). Briefly, cells were incubated on the coverslip and then UVB irradiated. The cells were fixed by methanol for 15 min at -20°C

followed by incubation with 2 μg/ml DQ™ collagen, type I (Thermo Fisher Scientific Inc., Rockford, IL, USA) at 37°C for 1h. DQ™ collagen, type I was diluted with MMP reaction buffer (100 mM NaCl, 100 mM Tris-HCl pH7.5, 10 mM $CaCl_2$, 20 μM ZnCl, 0.05% Brij). After wash six times with 1X PBS, the coverslips were mounted on mounting medium (Dako North America, Inc., Carpinteria, CA, USA) and observed using a FluoView 1000 confocal microscope (Olympus, Tokyo, Japan). Corrected Total Cell Fluorescence (CTCF) was calculated using Image J software (http://rsb.info.nih.gov/ij/).

CTCF = Integrated density of selected cell – (Area of selected cell x Mean fluorescence of background)

3.2.7 Nuclear fractionation

The cells were seeded on 100 mm dishes between 95-100% confluency and incubated for 24 h. The cells were harvested by scraper and pelleted after UVB irradiation at indicated times. After removing supernatant, the pellets were gently mixed with 500 μl hypotonic buffer (20 mM pH7.5 Tris-HCl, 10 mM NaCl, 3mM $MgCl_2$ containing protease and phosphotase inhibitor cocktail) and incubated on ice for 15 min. Then, 21.5 μl of 10% NP-40 was added to each samples then vigorously vortexed for 10 secs and centrifuged for 10 min at 3,000 rpm, 4°C. The supernatant contains the cytoplasmic fraction. Nuclear pellets were lysed in 200 μl cell extraction buffer (100 mM pH7.5 Tris-HCl, 2 mM Na_3VO_4, 1 mM NaF, 100 mM NaCl, 1% Triton X-100, 10% glycerol, 1

mM EDTA, 1 mM EGTA, 0.5% sodium deoxycholate, 20 mM $Na_4P_2O_7$ containing protease and phosphatase inhibitor cocktail (Roche, Indianapolis, IN, USA)) followed by sonication and centrifuged for 30 min at 14,000 x *g*, 4°C. The supernatant contains the nuclear fraction. Each fractions were quantified by BCA method for western blotting.

3.2.8 Western blot analysis

Sample preparation and SDS-PAGE were performed as previously described (35). The following primary antibodies were used: anti-β-actin (Sigma-Aldrich, St Louis, MO, USA, A5441), TG2 (77), MMP-1 (Santa Cruz Biotechnology, Santa Cruz, CA, USA, sc-8834), MMP-13 (Thermo Fisher Scientific Inc., Rockford, IL, USA, MS-827-P1), Collagen 1 (Abcam, Cambridge, MA, USA, ab88147), p65 (Santa Cruz Biotechnology, Santa Cruz, CA, USA, sc-8008), p-p65^{Ser276} (Abcam, Cambridge, MA, USA, ab106129), p-p65^{Ser468} (Cell Signaling Technology, Beverly, MA, USA, #3039), p-p65^{Ser536} (Cell Signaling Technology, Beverly, MA, USA, #3031), c-Jun (Santa Cruz Biotechnology, Santa Cruz, CA, USA, sc-1694), phospho-c-Jun^{Ser63} (Cell Signaling Technology, Beverly, MA, USA, #2361), p38 (Santa Cruz Biotechnology, Santa Cruz, CA, USA, sc-728), phospho-p38$^{Thr180/182}$ (Cell Signaling Technology, Beverly, MA, USA, #9211), COX-1 (Santa Cruz Biotechnology, Santa Cruz, CA, USA, sc-1752), Lamin B (Santa Cruz Biotechnology, Santa Cruz, CA, USA, sc-6216). After reaction with horseradish peroxidase-conjugated secondary antibody (Santa Cruz Biotechnology, Santa Cruz, CA, USA, sc-2004 or sc-2005),

immunoreactive proteins were visualized by SuperSignal™ West Pico Chemiluminescent Substrate (Thermo Fisher Scientific Inc., Rockford, IL, USA). The bands were quantified by using ImageJ software (http://rsb.info.nih.gov/ij/).

3.2.9 QRT-PCR

Total RNA extraction and QRT-PCR were carried out using a CFX96™ Real-Time system (Bio-Rad, Hercules, CA, USA) as previously described (78). The following specific primers were used

Species	Genes	Forward	Reverse
Human	MMP-1	GGTGTCTCACAGCTTCCCAG	CCGCTTTTCAACTTCCCTCC
	MMP-3	GCATTCAGTCCCTCTATGGACCTC	AGGACAAAGCAGGATCACAGTTG
	Collagen1A1	CTCGAGGTCGACACCACCCT	CAGCTGGATGGCCACATCGG
	GAPDH	AACTTTGGCATTGTGGAAGG	GGATGCAGGGATGATGTTCT
Mouse	MMP-13	AGGAAGACCTTGTGTTTGCAGAGC	TTCAGGATTCCCGCAAGAGTCG
	36B4	GAGGCCACACTGAACAT	ATGCTGCCGTTGTCAAACAC

Relative mRNA expression was calculated by $2^{-\Delta\Delta Ct}$ method (40).

3.2.10 Luciferase reporter assay

For human MMP1 promoter-luciferase, AP-1-luciferase and 3κB-luciferase assay, MDFs were transfected with the human MMP1 promoter construct (113) or 3xAP1pGL3 vector (Addgene #40342) or 3κB-luciferase construct, respectively. pRL-TK vector was co-transfected to normalize luciferase activity. Luciferase reporter activity was measured by a luciferase assay kit (Promega, Madison, WI, USA) in accordance with the manufacturer's instruction.

3.2.11 Statistical analysis

GraphPad Prism 5.0 statistical software (GraphPad Software, La Jolla, CA, USA) was used for statistical evaluations. Two-way ANOVA was conducted for evaluation. $P<0.05$ was considered statistically significant. All error bars represent mean ± SEM.

3.3 RESULTS

3.3.1 UVB irradiation induces human MMP-1 and -3 and mouse MMP-13 expressions but not in TG2-deficient dermal fibroblast

In our previous studies we showed that UV induced ROS generation and increased cytosolic free calcium are critical factors for TG2 activation (72, 73). It is an indispensable process for UV-induced acute skin inflammation through regulating inflammatory cytokine expression (103). Since UVB can penetrate into upper dermal layer of skin (114), it is plausible that UVB activates TG2 of dermal fibroblasts. However, there is no research on the role of TG2 in fibroblasts after UVB irradiation.

MMPs are zinc-containing endopeptidases which mediate dermal remodeling through the degradation of broad range dermal matrix proteins (115). To investigate the role of TG2 in UV-induced dermal remodeling, we examined the TG2-dependent expressions of MMP proteins in human dermal fibroblasts (HDFs). HDFs treated with TG2 siRNA showed decreased level of MMP-1 mRNA expression as well as MMP-3 after UVB irradiation (Fig. 3-1A). Western blot analysis showed that increased MMP-1 secretion into the culture media of control-siRNA-treated HDFs after UVB irradiation, whereas TG2-siRNA-treated cells did not (Fig. 3-1B). Next, we further examined the role of TG2 in the expressions of MMPs using primary neonatal mouse dermal fibroblasts (MDFs). MMP-13 mRNA level was measured since it is a main

collagenase gene in mice (116). Similar with the data obtained from HDFs, MDFs obtained from $TG2^{-/-}$ mice failed to express MMP-13 mRNA as much as WT cells did (Fig. 3-1C). In addition, enzymatic activities of MMP-1 and MMP-13 were measured by zymography. As shown in Fig. 3-1D and E, it was observed that MMP-1 and MMP-13 activities decreased in TG2-siRNA-treated culture media and $TG2^{-/-}$ MDFs, respectively. Although we showed that TG2 is indispensable for expressing MMP proteins in the data above, it did not regulate the expression of collagen1A1, a major ECM protein of dermis (Fig. 3-1A and B). These results suggest that TG2 is essential for regulating human MMP-1, -3 and mouse MMP-13 expressions without affecting collagen gene expression.

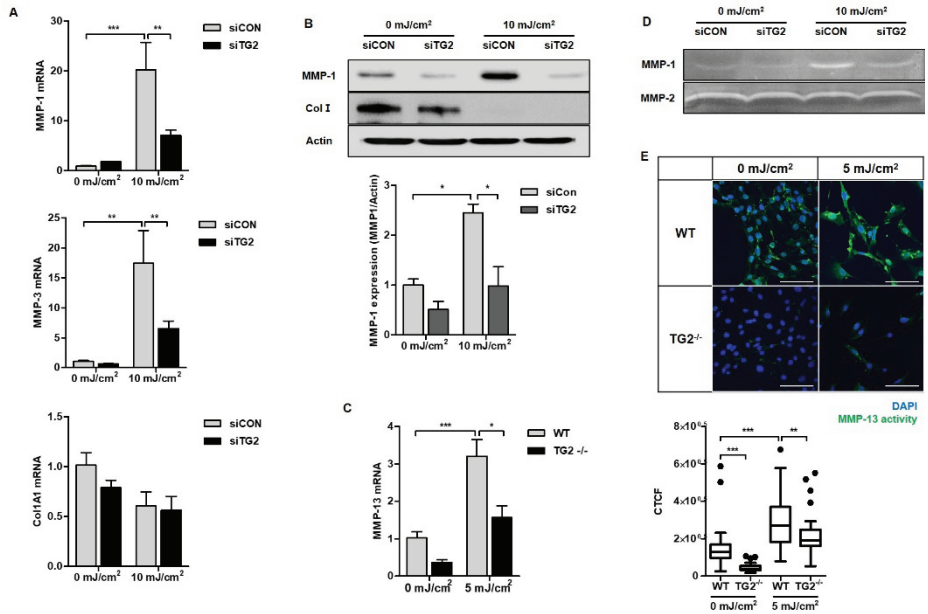

Figure 3-1. Reduced MMP-1, -3 and -13 expression in TG2-deficient fibroblasts after UVB irradiation. siRNA (control or TG2) was transfected to HDFs. Twenty-four hours after transfection, the cells were irradiated by UVB (10 mJ/cm^2). MMP-1, MMP-3 and collagen1A1 mRNA (A) and secreted protein (B) levels were measured 48 h after irradiation. Actin from un-quantified lysate was used for loading control. (C) Mouse MMP-13 mRNA expression was measured 24 h after UV irradiation. (D) After 48 h of UV irradiation, culture media were collected and used for gelatin zymography at non-reducing condition. (E) MMP-13 activity was measured using DQ™ collagen, type I. Scale bar, 100 μm. All data are represented as ± SEM. *, P<0.05; **, P<0.01; ***, P<0.001, CTCF, corrected total cell fluorescence.

3.3.2 KCC009 treated fibroblasts show decreased MMP-1 and -3 expressions after UVB irradiation

Previously, we showed that enzymatic activity of TG2 is a more important factor than its protein level in UVB-mediated acute skin inflammation (103). KCC009, an inhibitor of TG (79), was used to gain evidence for significance of enzymatic activity of TG2 in UV-mediated MMPs expressions.

First, UV-induced transamidation activity of TG2 in fibroblasts was measured. UV-irradiated HDFs showed two to four fold increase of transamidation activity, whereas we observed the activity was comparable in KCC009-treated and TG2 siRNA-treated HDFs with un-irradiated cells (Fig. 3-2A and B). In addition, KCC009-treated HDFs showed reduced MMP-1 and -3 mRNA expressions after UVB irradiation (Fig. 3-2C). As with its mRNA expression, there was reduced secretion of MMP-1 protein in the culture media of KCC009 treated HDFs (Fig.3-2D). Similar with TG2 siRNA treated HDFs, KCC009 treatment did not affect mRNA and protein level of collagen1A1 (Fig. 3-2C and D). These data indicate that the enzymatic activity of TG2 is also a critical factor as much as its protein level.

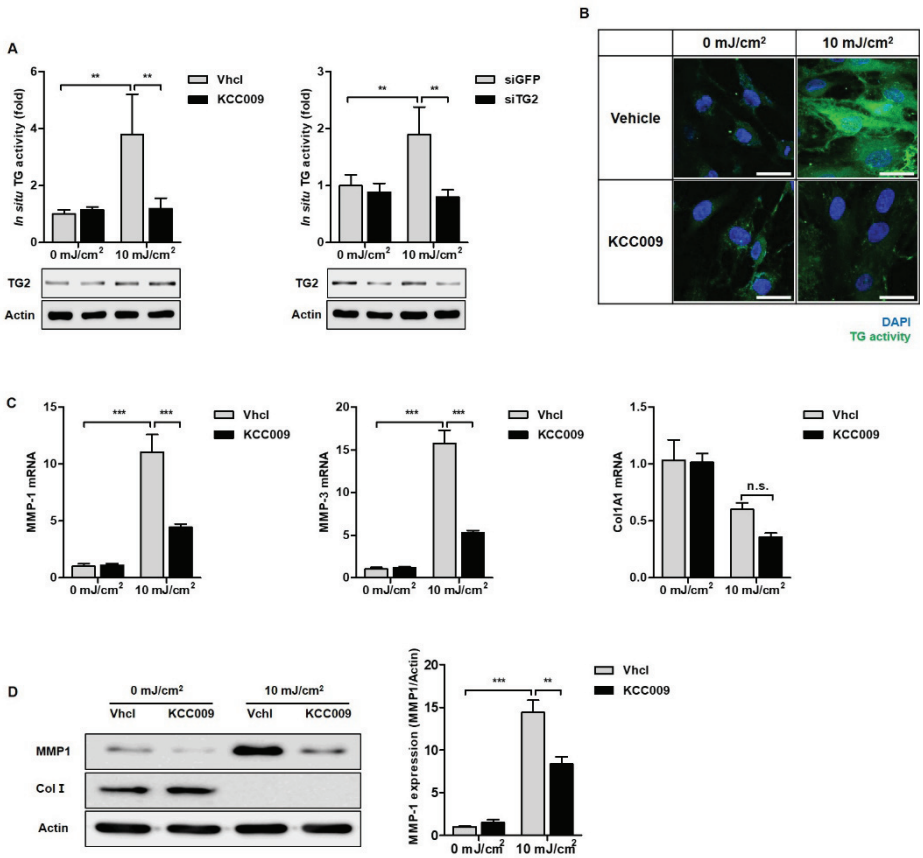

Figure 3-2. KCC009 treatment decreases MMP-1 and -3 expression after UVB irradiation. HDFs were pre-treated with KCC009 (250 μM) 1 h before UV irradiation (10 mJ/cm^2). (A) *In situ* TG activity was measured by BP incorporation in KCC009-treated (A, right panel) or TG2 siRNA-treated (A, left panel) HDFs 6 h after UV irradiation. (B) *In situ* TG activity was visualized by confocal microscopy. Scale bar, 30 μm. MMP-1, -3 and collagen1A1 mRNA (C) and protein levels (D) were measured 48 h after UV irradiation. All data are represented as ± SEM. **, P<0.01; ***, P<0.001. n.s., non-significant.

3.3.3 TG2 regulates MMP-1 expression at the transcriptional level through NF-κB rather than AP-1 pathway

MMPs can be regulated by transcription, inhibition of activated MMPs and activation of zymogen (118, 119). Fig. 3-1 and 3-2 show that TG2 regulates MMPs expressions at their transcriptional levels. To examine this, WT and $TG2^{-/-}$ MDFs were transiently transfected with human MMP-1 promoter. As shown in Fig. 3-3A, human MMP-1 promoter transfected WT MDFs showed about 1.5 times higher luciferase activity following UVB irradiation than un-irradiated WT cells. However, luciferase activity did not change in $TG2^{-/-}$ MDF regardless of UV irradiation. Furthermore, $TG2^{-/-}$ cells showed one third lower luciferase activity than WT cells at un-irradiated condition. This data indicate that TG2 regulates MMP-1 expression at basal condition as well as UV-irradiated situation.

It has been suggested that UV irradiation induces an excess generation of ROS such as singlet oxygen ($^1O_2$), superoxide anion (O_2^-), hydrogen peroxide (H_2O_2) and hydroxyl radicals ($OH\cdot$) (120). ROS activates the mitogen-activated protein kinase (MAPK) family including extracellular signal-regulated kinases (ERKs), p38 and c-Jun NH2-terminal kinase (JNK). These proteins are upstream kinases for activating activator protein-1 (AP-1) transcription factor. AP-1 is a class of dimeric transcription factors, which is composed of Jun (c-Jun, JunD, JunB), Fos (c-Fos, FosB, Fra-1, Fra-2), and ATF (ATF-2, ATFa) families (121). The heterodimeric form, made of c-Jun and c-Fos, is discovered

most commonly in the cells. ERK stimulates the expression of c-Fos, whereas p38 and JNK regulate expression of c-Jun (11). Regulation of c-Jun protein level is a critical factor in AP-1 activity as c-Fos is constitutively expressed in the cells (1). c-Jun protein level is important in regulating MMP transcription since most MMP gene promoters including MMP-1, MMP-3 and MMP-13 contain AP-1 binding site (122, 123). For these reasons, the relationship between TG2 and AP-1 transcription factor was examined by measuring AP-1 promoter luciferase activity and c-Jun protein level. However, as shown in Fig. 3-4A, we could not observe TG2-dependent changes of transcriptional activity of AP-1 in UV-irradiated WT and $TG2^{-/-}$ MDFs. Moreover, UV-irradiated HDFs and MDFs increased protein levels of c-Jun as well as p-c-Jun^{Ser63}, which indicates increased transcriptional activity (124). On the other hand, there was no difference in the protein levels of c-Jun and p-c-Jun^{Ser63} between TG2-siRNA-treated HDFs and $TG2^{-/-}$ MDFs, comparing to its control cells (Fig. 3-4B).

Besides AP-1, NF-κB is another transcription factor that regulates MMP-1, -3 and -13 expressions at transcriptional level (123, 125). In the previous study, we showed that UV irradiated keratinocytes have increased NF-κB activity in accordance with increase of TG2 activity (103). Furthermore, several researches concluded that TG2 positively regulates NF-κB activity (74, 82, 103), yet the regulating mechanism is still not clear. This has raised the question whether TG2-mediated NF-κB activity has a role in UV-induced MMP expression. As shown in Fig. 3-4C, $TG2^{-/-}$ MPFs failed to increase 3κB-

luciferase activity after UVB irradiation, whereas UVB-irradiated WT MPFs showed about three times higher level of 3κB-luciferase activity than non-irradiated cells. Next, we investigated nuclear translocation of p65, a subunit of NF-κB, which indicates NF-κB activity at the nucleus. We could not observe different nuclear translocation of p65 in TG2 knock-downed or inhibitor-treated cells comparing to the control cells. Instead, however, we observed increased p-p65^{Ser468} in the nucleus of TG2 abrogated cells, but there were no significant changes in other phosphorylation sites. Ser468 residue of p65 is phosphorylated by GSKβ and IKKβ and known to negatively regulates NF-κB function. (126, 127). Functionally, this phosphorylation site is required for COMMD1-dependent ubiquitination and target gene-specific proteasomal elimination of p65 (128). That is, increased p-p65^{Ser468} is a sign of p65 degradation in the nucleus. However, this degradation effect can be masked by resynthesized p65, as only a small fraction of p65 undergoes proteasomal degradation. To prevent resynthesis of the degraded protein, cycloheximide (CHX) was administrated into the culture media after UV irradiation. In this experimental condition, reduced nuclear p65 protein level was observed in KCC009-treated HDFs (Fig. 3-4E). These data imply that TG2 regulates transcriptional activity of NF-κB through phosphorylation of p65 at Ser468, thereby inducing target gene specific elimination of p65 rather than modulating nuclear translocation of p65. In summary, TG2 regulates MMP-1, -3 and -13 expressions via NF-κB activation rather than regulating AP-1 activity.

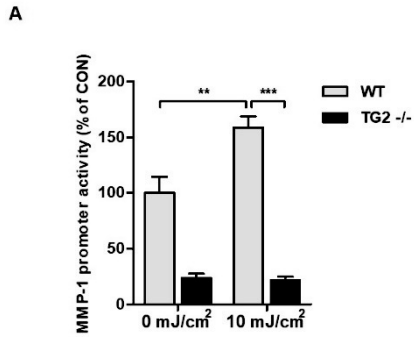

Figure 3-3. Human MMP-1 promoter activity in TG2-deficient MDFs after UVB irradiation. Human MMP1 activity was assessed in MDFs prepared from WT and $TG2^{-/-}$ littermates. MDFs were transfected with human MMP-1 promoter vector. After UV irradiation, the cells were incubated 24 h. Luciferase activity was normalized co-transfected *Renilla* activity. Data are represented as mean ± SEM. **, $P<0.01$; ***, $P<0.001$.

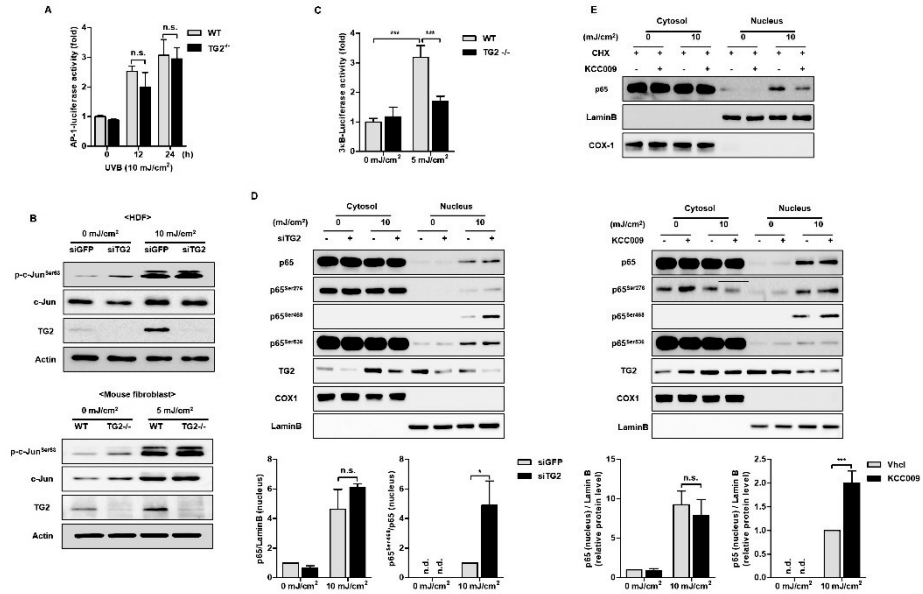

Figure 3-4. TG2 regulates NF-κB but not AP-1 activity. (A) MDFs were transfected with 3xAP1pGL3 vector. The cells were incubated 12 or 24 h after UV irradiation. Luciferase activity was normalized by co-transfected *Renilla* activity. (B) Six hours after UV irradiation, the cells were lysed and immunoblotted with indicated antibodies. As a loading control, actin was used. (C) 3κB-luciferase reporter activity was assessed 9 h after UVB irradiation (5 mJ/cm^2) in MDFs prepared from WT and TG2-/- littermates. Luciferase activity was normalized by co-transfected *Renilla* activity. (D) After 6 h of UV irradiation, the cells were separated into cytoplasm and nucleus. (E) After UV irradiation, the cells were incubated with 10 μg/ml CHX for 6 h and then fractionated. The fractions were immunoblotted with the indicated antibodies. Cox-1 and LaminB were used as marker proteins for cytoplasm and nucleus, respectively. All data are represented as ± SEM. *, P<0.05; **, P<0.01; ***, P<0.001. n.s., non-significant, n.d., not detected.

3.3.4 *ex vivo* cultured $TG2^{-/-}$ mice skin shows reduced MMP-13 expression after UVB irradiation

Skin is relatively easy to organ culture than other kind of organs (129, 130). When compared with cell-culture system, skin organ culture system shows characteristics of skin more clearly as the tissue architecture remains intact as well as cell-cell interactions are relatively undisturbed. Furthermore, it is also possible to minimize the infiltration of immune cells under inflammatory conditions such as UV irradiation, thereby helping to eliminate the effects of undesirable cell types. Therefore, it is a suitable method to explore various aspects of pathophysiology of skin biology.

Neonatal mouse skin was prepared and UV irradiated as described in Fig. 3-5A. Mouse MMP-13 protein level was measured 24 h after UV irradiation by western blotting. UV-irradiated WT skins showed increased expression of MMP-13 about 5 times higher than non-irradiated WT skin (Fig. 3-5B). However, the skins obtained from $TG2^{-/-}$ mice failed to express MMP-13 protein after UV irradiation (Fig. 3-5B). Although p-$p65^{Ser536}$ expression was reduced after UVB irradiation, it may be attributed to our late time point observation. In addition, the expression of IκBα, an inhibitory protein of NF-κB, was not different between the $TG2^{-/-}$ and WT skin. In previous data, it was concluded that TG2 does not regulate expression of c-Jun (Fig. 3-4A and B). Similar with this data, we could not observe different expression of c-Jun nor of p38, the upstream regulator of c-Jun, between the WT and $TG2^{-/-}$ skin. These results reinforce our conclusion that TG2 does not regulate human MMP-1 and

mouse MMP-13 expressions through AP-1 pathway.

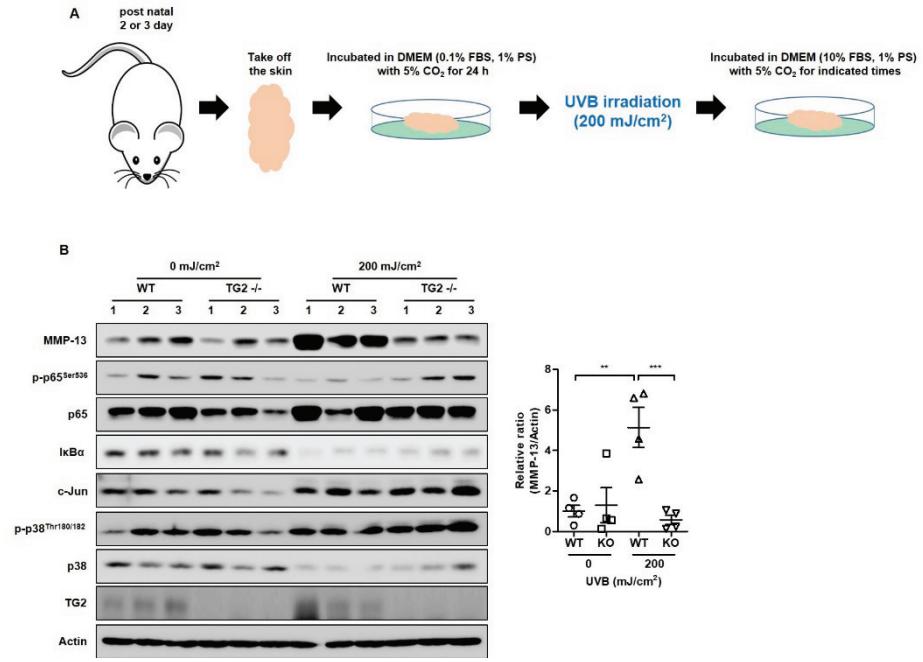

Figure 3-5. Reduced MMP13 expression in TG2 $^{-/-}$ mice skin after UVB irradiation. (A) Schematic figure of neonate mouse skin organ culture and UV irradiation. (B) Western blot analysis of the skin lysate 24 h after UV irradiation. Actin was used as a loading control. MMP-13 protein level were quantified by ImageJ software (Right panel, n=4). Data are represented as mean± SEM. **, P<0.01; ***, P<0.001.

3.4 DISCUSSION

Through the skin, organisms primarily interact with surrounding environments. It is simultaneously exposed to UV radiation on regular bases, which leads to the development of photoaging and skin cancer through inflammation, DNA damage and immune suppression (67). In the previous study, we clarified that TG2, expressed in epidermal keratinocytes, mediates UV-induced acute skin inflammation through regulation of expressions of inflammatory cytokines, such as IL-6, IL-8 and TNF-α (103). Besides epidermis, dermis also abundantly expresses TG2. Dermis provides mechanical characteristics of skin and primarily consists of fibroblasts. However, the role of fibroblast TG2 has not been fully characterized yet. Herein, we showed that fibroblast TG2 is a critical regulator of UV-induced MMPs expressions. Moreover, our results prove that TG2 regulates MMPs expression through NF-κB activation rather than AP-1 pathway. Collectively, these results indicate that TG2 is an enzyme that participates in dermal remodeling following UV-irradiation.

In this study, TG2 regulates MMPs expressions at transcriptional level. The major transcription factors that regulate MMPs expressions are AP-1 and NF-κB (122, 123, 125). In this respect, it can be presumed that TG2 is a regulator of AP-1 or NF-κB. AP-1 is a dimeric transcription factor composed of Jun (c-Jun, JunD, JunB), Fos (c-Fos, FosB, Fra-1, Fra-2), and ATF (ATF-2, ATFa) families and is involved in cellular proliferation, transformation and death (121). Among the various combinations, heterodimer of c-Jun/c-Fos is common in the cells. There is some research about the role of TG2 in regulating AP-1 pathway.

TG2 participates in Aβ1-42-induced inflammatory activation in monocytes via AP-1 pathway (131) and induces JNK activation, one of upstream kinases of c-Jun (132, 133). However, in this study, we observed that TG2 did not affect AP-1 activity and c-Jun protein level at cellular and at tissue levels following UV irradiation. These data indicate that TG2 regulates c-Jun in cell type- and stimulation-specific manner. Instead, several lines of evidence indicate that TG2 positively regulates NF-κB activity (74, 82, 103), however the exact regulatory mechanisms remain unidentified. Moreover, we observed that TG2 regulates transcriptional activity of NF-κB and affects phosphorylation status of p65 at Ser468 in the nucleus. It is suggested that phosphorylation of p65 at Ser468 negatively regulates NF-κB activity (126, 127), as this phosphorylation site is associated with proteolytic degradation of p65 (128). Consistent with these studies, TG2 knock-down and inhibitor treatment induced degradation of p65 in the nucleus. This implies that TG2-mediated NF-κB activation specifically modulates the target genes rather than the universal manner since p-p65^{Ser468} is known to be a marker of target gene specific degradation of p65 (128). This is supported by the observation of collagen gene expression. Although, NF-κB activation is known to inhibit collagen gene transcription (134, 135), TG2 did not affect the expression of collagen in this study. The concept of target gene specific regulation of TG2-NF-κB signaling could be demonstrated by comparing the status of p-p65^{Ser468} on MMP and collagen promoter through techniques such as chromatin immunoprecipitation (ChIP).

Although we observed TG2-mediated regulation of p-p65^{Ser468}, its molecular

mechanism is still unclear. It is known that some kinases target this phosphorylation residue. GSK3β is responsible for basal phosphorylation (127), TNF-α or IL-1 stimulation induces IKKβ-mediated phosphorylation (126) and IKKε is known to be responsible for phosphorylation of T cells (136). However, UV irradiation induces phosphorylation of GSK3β at Ser9 (137, 138) which inactivates its kinase activity. Furthermore, it is suggested that UV irradiation does not induce IKKβ activation (139, 140), instead IKKβ acts as an adaptor protein for IκBα degradation in the nucleus of UV-irradiated cells (141). There is no evidence about UV irradiation regulates IKKε activity at the present time. These data suggest that these kinases are not responsible for the p-p65^{Ser468} following UV irradiation. Besides kinases, phosphatases also target this phosphorylation residue (126, 127). UV radiation has been reported to decrease phosphatase 1 (PP1) activity (142). Moreover, it has also been reported that TG2 regulates JNK phosphorylation through downregulation protein phosphatase 2A (PP2A) (132). In this regard, it will be worth investigating whether TG2 regulates phosphorylation of p65 through modulating phosphatase activity or not.

In summary, we have shown that fibroblasts TG2 plays a critical role in regulating MMP-1, -3 and -13 expression under UV irradiation. UV-induced activation of TG2 promotes transcriptional activation of NF-κB but not AP-1, which leads to increased production of MMPs. These findings indicate that TG2 plays a pivotal role in MMPs-mediated skin remodeling induced by UV light and inhibition of fibroblast TG2 following UV irradiation will be a useful target

for the prevention of photoaging caused by MMPs which is induced by chronic UV exposure.

General Discussion

The development and evaluation of anti-melanogenic agents has been actively studied for not only alleviate pigmentary disorders cosmetically and medically, but also for melanoma treatment in which melanogenesis level is one of crucial factors for chemo-/radio- therapy as well as survival period of patients (143, 144). There are some strategies for anti-melanogenesis including tyrosinase inhibition, inhibition of melanosome transfer, acceleration of epidermal turnover and desquamation, and antioxidant application (145).

In chapter 1, a new anti-melanogenic mechanism of 4-n-butylresorcinol which is used as an inhibitor of tyrosinase was elucidated. Although, there are several cellular and clinical studies clarified the efficacy of 4-n-butylresorcinol, all of these studies focused on only the inhibitory ability against tyrosinase. In this study, it was observed that 4-n-butylresorcinol inhibits tyrosinase more effectively in live cell condition than in cell lysate. It suggests that there is another regulatory mechanism of 4-n-butylresorcinol in addition to the tyrosinase inhibitor. Indeed, 4-n-butylresorcinol treated cells decreased the expression of tyrosinase after αMSH stimulation without changes in its mRNA level. This means that 4-n-butylresorcinol regulates tyrosinase at posttranslational level. Tyrosinase is one of the representative proteins that undergoes glycosylation in the ER and Golgi, which is critical for its proper folding and trafficking to the melanosomes (41). Aberrant glycosylation of tyrosinase induces ER retention of the protein that leads proteasomal degradation of the protein which is known as ER-associated degradation

(ERAD) (25-27). Indeed, several agents are known to affect glycosylation of tyrosinase (27, 146, 147). However, we could not find any evidences for involvement of 4-n-butylresorcinol in this process. Instead, 4-n-butylresorcinol has been shown to accelerate the proteolytic degradation of tyrosinase through both of endosomal/lysosomal and proteasomal pathway, which is partially related to phosphorylation status of p38 MAPK. There are some possible hypotheses for explaining 4-n-butylresorcinol-mediated degradation of tyrosinase which is mentioned in the discussion section of Chapter 1, which should be tested.

Although, the degradative pathway of tyrosinase was focused in this study, it will be also worth investigating the antioxidant property of 4-n-butylresorcinol. Oxidative condition is favored to melanogenesis as tyrosinase prefers superoxide anion radical (O_2^-) over O_2 for its enzyme activity (148). Furthermore, redox agents can affect melanogenesis by interacting with active site copper of tyrosinase (149). Resorcinol and its derivatives, especially, are known to have antioxidant properties (150-152). Moreover, it was observed that 4-n-butylresorcinol actually acts as an antioxidant both *in vitro* and at the cellular level (unpublished data). These data indicate that 4-n-butylresorcinol can inhibit melanogenesis through multifunctional approaches.

Transglutaminase 2 mediates posttranslational modification of substrates proteins (52) and is activated by various factors including reactive oxygen species (ROS), UV, irradiation, hypoxia and etc. (153).

In chapter 2 and 3, the role of TG2 in UV-irradiated epidermal keratinocytes and dermal fibroblasts was investigated. In these studies, it was discovered that TG2 has central roles for the UV irradiation-mediated production of inflammatory cytokines and MMPs in keratinocyte and fibroblasts, respectively. Even though, it was known that UV irradiation activates TG2, the exact molecular mechanisms were not clear. From these studies, it was clarified that UV activates TG2 via activating PLC-IP_3-IP_3R pathway, followed by the ER calcium release. Furthermore, it was revealed that activated TG2 enhances transcriptional activity of NF-κB which is a critical player that mediates UV-induced production of inflammatory cytokines and MMPs in keratinocytes and fibroblasts, respectively. Although, there are explanations for the molecular mechanisms of TG2-induced NF-κB activation (74, 82), it is still controversial and more studies need to be done. In this study, it was observed that TG2 regulates the phosphorylation status of p65. Inhibition or knockdown of TG2 decreased phosphorylation of Ser536 which is related with transcriptional activity of p65 (101) in keratinocytes. Moreover, TG2 does not affect nuclear translocation of p65, but instead affects Ser468 phosphorylation followed by nuclear degradation of p65 in fibroblasts. This phosphorylation site is known as a residue for target gene specific degradation of p65 (128). That is, it seems that TG2 regulates NF-κB activity by regulating p65 stability in the nucleus rather than facilitating nuclear translocation of p65 following UV irradiation. However, it is uncertain how TG2 modulates phosphorylation status of p65 at the present stage. Phosphorylation of p65 is regulated by both of kinases and

phosphatases. Although GSK3β (127) and IKKβ (126) are responsible for the phosphorylation of p65 at Ser468, the possibility of TG2-mediated regulation of these kinases seems low, since UV radiation does not affect IKKβ activity (139, 140) and inhibits GSK3β activity (137, 138). Instead, protein phosphatases mediated mechanism seems more plausible since TG2 downregulates protein phosphatase 2A (PP2A) (132). Furthermore, it was suggested that UV irradiation inhibits phosphatase 1 (PP1) activity (142). The study about the relationship between TG2 and phosphatases might suggest a new insight for the molecular mechanism of TG2-mediated NF-κB activation.

Although, TG2 is an enzyme, the importance of enzyme activity of TG2 has been overlooked so far. UV irradiation to the cells induces generation of reactive oxygen species (ROS) (7) and ER calcium release into the cytoplasm (80) which are indispensable factors for TG2 activation. Chapter 2 and 3 discuss the importance of enzyme activity of TG2 in the production of inflammatory cytokines and MMPs following UV irradiation by using TG2 inhibitor, KCC009. Even though more studies need to be done to clarify the effector molecules of activated TG2 and their biological significance, these data indicate that enzyme activity of TG2 should be considered under conditions of stress which can activate TG2.

It has been suggested that cytokines can regulate skin ECM remodeling via paracrine and autocrine fashions (154). Since keratinocyte-derived cytokines can penetrate into the basement membrane (155), fibroblasts can be influenced by these cytokines. In chapter 2, we reported that UV-induced activation of

keratinocyte TG2 regulates inflammatory cytokines expressions such as IL-6, IL-8 and TNF-α (103). TNF-α mediates MMP-1 and MMP-3 expressions in various cell types (156-159) through NF-κB (160) and c-Jun (161) pathways. In addition, IL-6 induces MMP-1 induction in fibroblasts (105, 162, 163). Moreover, these cytokines induce infiltration of immune cells, such as neutrophils and macrophages. In particular, these immune cells are observed in the lesions of UV exposed skin (164, 165) and release MMPs to further degrade ECM at the irradiated sites (110, 164). $TG2^{-/-}$ mice showed reduced infiltration of immune cells into the UV-irradiated lesion, as discussed in chapter 2 (103). From these data, a hypothetical model of TG2-mediated remodeling of dermal ECM can be suggested (Fig. 4-1). First, TG2 directly regulates MMP-1, -3 and -13 expression through NF-κB-dependent pathway in UV-irradiated fibroblasts. Secondly, TG2 of UV-irradiated keratinocytes mediates secretion of inflammatory cytokines such as IL-6 and TNF-α (103). These cytokines might reach to the dermal fibroblasts and induce MMPs expressions via paracrine manner. Finally, keratinocyte-derived cytokines induce infiltration of immune cells. These immune cells release various matrix-degrading enzymes like MMPs. All of these situations will contribute to the pathological alterations of UV-damaged skin, such as inflammation, photoaging and photocarcinogenesis.

In conclusion, molecular mechanisms of skin cells, such as melanocyte, keratinocyte and fibroblast, were investigated after UV irradiation in this study. Research and understanding the influence of UV at molecular level are important for human health since we have ‘functionally naked’ skin. Through

this study, we will be able to broaden our understanding of skin responses after exposure to UV light at the molecular level and establish new strategies to control the harmful effects of UV light.

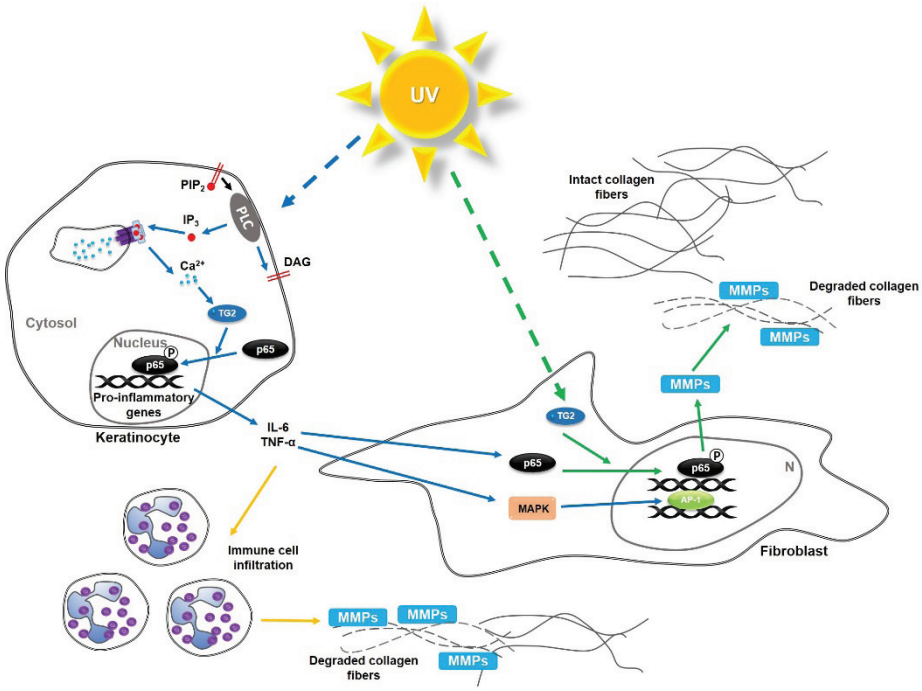

Figure 4-1. Hypothetical model of TG2-mediated dermal ECM remodeling.

In fibroblasts, UV-induced TG2 activation positively regulates NF-κB pathway followed by induction of its target genes including MMP-1, -3 and -13, directly (green arrow). Meanwhile, UV-irradiated keratinocytes release inflammatory cytokines in TG2-dependent fashion. These cytokines reach dermal fibroblasts and facilitate expression of MMP genes, indirectly (blue arrows). Finally, cytokines promote infiltration of immune cells to the UV-irradiated lesion. These immune cells release ECM degrading enzymes such as MMPs (orange arrows).

REFERENCES

1. Rittie L, Fisher GJ. Natural and sun-induced aging of human skin. Cold Spring Harb Perspect Med. 2015;5(1):a015370.

2. Tobin DJ. Introduction to skin aging. J Tissue Viability. 2017;26(1):37-46.

3. Fell GL, Robinson KC, Mao J, Woolf CJ, Fisher DE. Skin beta-endorphin mediates addiction to UV light. Cell. 2014;157(7):1527-34.

4. Jablonski NG. The evolution of human skin and skin color. Annu Rev Anthropol. 2004;33:585-623.

5. Barker JN, Mitra RS, Griffiths CE, Dixit VM, Nickoloff BJ. Keratinocytes as initiators of inflammation. Lancet. 1991;337(8735):211-4.

6. Costin GE, Hearing VJ. Human skin pigmentation: melanocytes modulate skin color in response to stress. FASEB J. 2007;21(4):976-94.

7. Kammeyer A, Luiten RM. Oxidation events and skin aging. Ageing Res Rev. 2015;21:16-29.

8. Lee AY. Recent progress in melasma pathogenesis. Pigm Cell Melanoma R. 2015;28(6):648-60.

9. Praetorius C, Sturm RA, Steingrimsson E. Sun-induced freckling: ephelides and solar lentigines. Pigment Cell Melanoma Res. 2014;27(3):339-50.

10. Katagiri T, Okubo T, Oyobikawa M, Futaki K, Shaki M, Kawai M. Novel melanogenic enzymes for controlling hyperpigmentation. 20th IFSCC International Congress. 1998;39:1-11.

11. Pittayapruek P, Meephansan J, Prapapan O, Komine M, Ohtsuki M. Role of Matrix Metalloproteinases in Photoaging and Photocarcinogenesis. Int J Mol Sci. 2016;17(6).

12. Krieg T, Hein R, Hatamochi A, Aumailley M. Molecular and clinical aspects of connective tissue. Eur J Clin Invest. 1988;18(2):105-23.

13. Wasmeier C, Hume AN, Bolasco G, Seabra MC. Melanosomes at a glance. J Cell Sci. 2008;121(24):3995-9.

14. Cui RT, Widlund HR, Feige E, Lin JY, Wilensky DL, Igras VE, et al. Central role of p53 in the suntan response and pathologic hyperpigmentation. Cell. 2007;128(5):853-64.

15. Lee HJ, Park MK, Kim SY, Choo HYP, Lee AY, Lee CH. Serotonin induces melanogenesis via serotonin receptor 2A. Brit J Dermatol. 2011;165(6):1344-8.

16. Hall PF. The influence of hormones on melanogenesis. Australas J Dermatol. 1969;10:125-39.

17. Viki B Swope ZA-M, Lina M Kassem, James J Nordlund. Interleukins 1α and 6 and Tumor Necrosis Factor-α Are Paracrine Inhibitors of Human Melanocyte Proliferation and Melanogenesis. Journal of Investigative Dermatology. 1991;96(2):180-5.

18. Kondo T, Hearing VJ. Update on the regulation of mammalian melanocyte function and skin pigmentation. Expert Rev Dermatol. 2011;6(1):97-108.

19. Yasumoto KI, Yokoyama K, Shibata K, Tomita Y, Shibahara S.

Microphthalmia-Associated Transcription Factor as a Regulator for Melanocyte-Specific Transcription of the Human Tyrosinase Gene. Mol Cell Biol. 1994;14(12):8058-70.

20. Carreira S, Goodall J, Aksan I, La Rocca SA, Galibert MD, Denat L, et al. Mitf cooperates with Rb1 and activates p21Cip1 expression to regulate cell cycle progression. Nature. 2005;433(7027):764-9.

21. Busca R, Ballotti R. Cyclic AMP a key messenger in the regulation of skin pigmentation. Pigment Cell Res. 2000;13(2):60-9.

22. Hall AM, Orlow SJ. Degradation of tyrosinase induced by phenylthiourea occurs following Golgi maturation. Pigment Cell Res. 2005;18(2):122-9.

23. Hall AM, Krishnamoorthy L, Orlow SJ. 25-hydroxycholesterol acts in the Golgi compartment to induce degradation of tyrosinase. Pigment Cell Res. 2004;17(4):396-406.

24. Ando H, Wen ZM, Kim HY, Valencia JC, Costin GE, Watabe H, et al. Intracellular composition of fatty acid affects the processing and function of tyrosinase through the ubiquitin-proteasome pathway. Biochem J. 2006;394(Pt 1):43-50.

25. Wang Y, Androlewicz MJ. Oligosaccharide trimming plays a role in the endoplasmic reticulum-associated degradation of tyrosinase. Biochem Biophys Res Commun. 2000;271(1):22-7.

26. Svedine S, Wang T, Halaban R, Hebert DN. Carbohydrates act as sorting determinants in ER-associated degradation of tyrosinase. J Cell Sci.

2004;117(Pt 14):2937-49.

27. Choi H, Ahn S, Chang H, Cho NS, Joo K, Lee BG, et al. Influence of N-glycan processing disruption on tyrosinase and melanin synthesis in HM3KO melanoma cells. Exp Dermatol. 2007;16(2):110-7.

28. Fujimoto N, Watanabe H, Nakatani T, Roy G, Ito A. Induction of thyroid tumours in (C57BL/6N x C3H/N)F1 mice by oral administration of kojic acid. Food Chem Toxicol. 1998;36(8):697-703.

29. Korner AM, Pawelek J. Dopachrome conversion: a possible control point in melanin biosynthesis. J Invest Dermatol. 1980;75(2):192-5.

30. Mishima Y, Hatta S, Ohyama Y, Inazu M. Induction of melanogenesis suppression: cellular pharmacology and mode of differential action. Pigment Cell Res. 1988;1(6):367-74.

31. Maeda K, Fukuda M. Arbutin: mechanism of its depigmenting action in human melanocyte culture. J Pharmacol Exp Ther. 1996;276(2):765-9.

32. Chaudhuri RK. Hexylresorcinol: Providing Skin Benefits by Modulating Multiple Molecular Targets. Cosmeceuticals and Active Cosmetics, Third Edition ed: CRC Press; 2015.

33. Won YK, Loy CJ, Randhawa M, Southall MD. Clinical efficacy and safety of 4-hexyl-1,3-phenylenediol for improving skin hyperpigmentation. Arch Dermatol Res. 2014;306(5):455-65.

34. Ando H, Watabe H, Valencia JC, Yasumoto K, Furumura M, Funasaka Y, et al. Fatty acids regulate pigmentation via proteasomal degradation of tyrosinase: a new aspect of ubiquitin-proteasome function. J Biol Chem.

2004;279(15):15427-33.

35. Kim YH, Park JI, Myung CH, Lee JE, Bang S, Chang SE, et al. 1-Phenyl-3-(2-thiazolyl)-2-thiourea inhibits melanogenesis via a dual-action mechanism. Arch Dermatol Res. 2016.

36. Kolbe L, Mann T, Gerwat W, Batzer J, Ahlheit S, Scherner C, et al. 4-n-butylresorcinol, a highly effective tyrosinase inhibitor for the topical treatment of hyperpigmentation. J Eur Acad Dermatol Venereol. 2013;27 Suppl 1:19-23.

37. Huh SY, Shin JW, Na JI, Huh CH, Youn SW, Park KC. Efficacy and safety of liposome-encapsulated 4-n-butylresorcinol 0.1% cream for the treatment of melasma: a randomized controlled split-face trial. J Dermatol. 2010;37(4):311-5.

38. Khemis A, Kaiafa A, Queille-Roussel C, Duteil L, Ortonne JP. Evaluation of efficacy and safety of rucinol serum in patients with melasma: a randomized controlled trial. Br J Dermatol. 2007;156(5):997-1004.

39. Garcia-Borron JC, Sanchez MCO. Biosynthesis of Melanins. In: Borovansky J, Riley PA, editors. Melanins and Melanosomes: Biosynthesis, Biogenesis, Physiological, and Pathological Functions: WIELY-BLACKWELL; 2011. p. 87.

40. Livak KJ, Schmittgen TD. Analysis of relative gene expression data using real-time quantitative PCR and the 2(-Delta Delta C(T)) Method. Methods. 2001;25(4):402-8.

41. Wang N, Hebert DN. Tyrosinase maturation through the mammalian

secretory pathway: bringing color to life. Pigm Cell Res. 2006;19(1):3-18.

42. Ando H, Kondoh H, Ichihashi M, Hearing VJ. Approaches to identify inhibitors of melanin biosynthesis via the quality control of tyrosinase. J Invest Dermatol. 2007;127(4):751-61.

43. Ando H, Wen ZM, Kim HY, Valencia JC, Costin GE, Watabe H, et al. Intracellular composition of fatty acid affects the processing and function of tyrosinase through the ubiquitin-proteasome pathway. Biochem J. 2006;394:43-50.

44. Jeong HS, Yun HY, Baek KJ, Kwon NS, Park KC, Kim DS. Okadaic acid suppresses melanogenesis via proteasomal degradation of tyrosinase. Biol Pharm Bull. 2013;36(9):1503-8.

45. Watabe H, Valencia JC, Yasumoto K, Kushimoto T, Ando H, Muller J, et al. Regulation of tyrosinase processing and trafficking by organellar pH and by proteasome activity. J Biol Chem. 2004;279(9):7971-81.

46. Nakamura K, Yoshida M, Uchiwa H, Kawa Y, Mizoguchi M. Down-regulation of melanin synthesis by a biphenyl derivative and its mechanism. Pigment Cell Res. 2003;16(5):494-500.

47. Jeon JS, Kim BH, Lee SH, Kwon HJ, Bae HJ, Kim SK, et al. Simultaneous determination of arbutin and its decomposed product hydroquinone in whitening creams using high-performance liquid chromatography with photodiode array detection: Effect of temperature and pH on decomposition. Int J Cosmet Sci. 2015;37(6):567-73.

48. Kim DS, Kim SY, Park SH, Choi YG, Kwon SB, Kim MK, et al.

Inhibitory effects of 4-n-butylresorcinol on tyrosinase activity and melanin synthesis. Biol Pharm Bull. 2005;28(12):2216-9.

49. Sprong H, Degroote S, Claessens T, van Drunen J, Oorschot V, Westerink BH, et al. Glycosphingolipids are required for sorting melanosomal proteins in the Golgi complex. J Cell Biol. 2001;155(3):369-80.

50. MartinezEsparza M, JimenezCervantes C, Beermann F, Aparicio P, Lozano JA, GarciaBorron JC. Transforming growth factor-beta 1 inhibits basal melanogenesis in B16/F10 mouse melanoma cells by increasing the rate of degradation of tyrosinase and tyrosinase-related protein-1. Journal of Biological Chemistry. 1997;272(7):3967-72.

51. Bellei B, Maresca V, Flori E, Pitisci A, Larue L, Picardo M. p38 regulates pigmentation via proteasomal degradation of tyrosinase. J Biol Chem. 2010;285(10):7288-99.

52. Iismaa SE, Mearns BM, Lorand L, Graham RM. Transglutaminases and disease: lessons from genetically engineered mouse models and inherited disorders. Physiol Rev. 2009;89(3):991-1023.

53. Hitomi K, Tatsukawa H. Preferred substrate structure of transgluataminases. In: Hitomi K, Kojima S, Fesus L, editors. Transglutaminases: Multiple Fuctional Modifiers and Targets for New Drug Discovery. 1st ed: Springer; 2015. p. 63.

54. Candi E, Schmidt R, Melino G. The cornified envelope: a model of cell death in the skin. Nat Rev Mol Cell Biol. 2005;6(4):328-40.

55. Iismaa SE, Aplin M, Holman S, Yiu TW, Jackson K, Burchfield JG, et

al. Glucose homeostasis in mice is transglutaminase 2 independent. PLoS One. 2013;8(5):e63346.

56. Matsuki M, Yamashita F, Ishida-Yamamoto A, Yamada K, Kinoshita C, Fushiki S, et al. Defective stratum corneum and early neonatal death in mice lacking the gene for transglutaminase 1 (keratinocyte transglutaminase). Proc Natl Acad Sci U S A. 1998;95(3):1044-9.

57. Farasat S, Wei MH, Herman M, Liewehr DJ, Steinberg SM, Bale SJ, et al. Novel transglutaminase-1 mutations and genotype-phenotype investigations of 104 patients with autosomal recessive congenital ichthyosis in the USA. J Med Genet. 2009;46(2):103-11.

58. John S, Thiebach L, Frie C, Mokkapati S, Bechtel M, Nischt R, et al. Epidermal transglutaminase (TGase 3) is required for proper hair development, but not the formation of the epidermal barrier. PLoS One. 2012;7(4):e34252.

59. Bognar P, Nemeth I, Mayer B, Haluszka D, Wikonkal N, Ostorhazi E, et al. Reduced inflammatory threshold indicates skin barrier defect in transglutaminase 3 knockout mice. J Invest Dermatol. 2014;134(1):105-11.

60. Frezza V, Terrinoni A, Pitolli C, Mauriello A, Melino G, Candi E. Transglutaminase 3 Protects against Photodamage. J Invest Dermatol. 2017;137(7):1590-4.

61. FB UB, Cau L, Tafazzoli A, Mechin MC, Wolf S, Romano MT, et al. Mutations in Three Genes Encoding Proteins Involved in Hair Shaft Formation Cause Uncombable Hair Syndrome. Am J Hum Genet. 2016;99(6):1292-304.

62. Candi E, Oddi S, Paradisi A, Terrinoni A, Ranalli M, Teofoli P, et al.

Expression of transglutaminase 5 in normal and pathologic human epidermis. J Invest Dermatol. 2002;119(3):670-7.

63. Cassidy AJ, van Steensel MA, Steijlen PM, van Geel M, van der Velden J, Morley SM, et al. A homozygous missense mutation in TGM5 abolishes epidermal transglutaminase 5 activity and causes acral peeling skin syndrome. Am J Hum Genet. 2005;77(6):909-17.

64. Dean MD. Genetic disruption of the copulatory plug in mice leads to severely reduced fertility. PLoS Genet. 2013;9(1):e1003185.

65. Inbal A, Lubetsky A, Krapp T, Castel D, Shaish A, Dickneitte G, et al. Impaired wound healing in factor XIII deficient mice. Thromb Haemost. 2005;94(2):432-7.

66. De Laurenzi V, Melino G. Gene disruption of tissue transglutaminase. Mol Cell Biol. 2001;21(1):148-55.

67. Svobodova A, Walterova D, Vostalova J. Ultraviolet light induced alteration to the skin. Biomed Pap Med Fac Univ Palacky Olomouc Czech Repub. 2006;150(1):25-38.

68. Valencia A, Kochevar IE. Nox1-based NADPH oxidase is the major source of UVA-induced reactive oxygen species in human keratinocytes. J Invest Dermatol. 2008;128(1):214-22.

69. Cho SY, Lee JH, Bae HD, Jeong EM, Jang GY, Kim CW, et al. Transglutaminase 2 inhibits apoptosis induced by calcium- overload through down-regulation of Bax. Exp Mol Med. 2010;42(9):639-50.

70. Jang GY, Jeon JH, Cho SY, Shin DM, Kim CW, Jeong EM, et al.

Transglutaminase 2 suppresses apoptosis by modulating caspase 3 and NF-kappaB activity in hypoxic tumor cells. Oncogene. 2010;29(3):356-67.

71. Lee JH, Jeong J, Jeong EM, Cho SY, Kang JW, Lim J, et al. Endoplasmic reticulum stress activates transglutaminase 2 leading to protein aggregation. Int J Mol Med. 2014;33(4):849-55.

72. Shin DM, Jeon JH, Kim CW, Cho SY, Kwon JC, Lee HJ, et al. Cell type-specific activation of intracellular transglutaminase 2 by oxidative stress or ultraviolet irradiation: implications of transglutaminase 2 in age-related cataractogenesis. J Biol Chem. 2004;279(15):15032-9.

73. Shin DM, Jeon JH, Kim CW, Cho SY, Lee HJ, Jang GY, et al. TGFbeta mediates activation of transglutaminase 2 in response to oxidative stress that leads to protein aggregation. FASEB J. 2008;22(7):2498-507.

74. Lee J, Kim YS, Choi DH, Bang MS, Han TR, Joh TH, et al. Transglutaminase 2 induces nuclear factor-kappaB activation via a novel pathway in BV-2 microglia. J Biol Chem. 2004;279(51):53725-35.

75. Brummelkamp TR, Bernards R, Agami R. A system for stable expression of short interfering RNAs in mammalian cells. Science. 2002;296(5567):550-3.

76. Lichti U, Anders J, Yuspa SH. Isolation and short-term culture of primary keratinocytes, hair follicle populations and dermal cells from newborn mice and keratinocytes from adult mice for in vitro analysis and for grafting to immunodeficient mice. Nat Protoc. 2008;3(5):799-810.

77. Jeon JH, Choi KH, Cho SY, Kim CW, Shin DM, Kwon JC, et al.

Transglutaminase 2 inhibits Rb binding of human papillomavirus E7 by incorporating polyamine. EMBO J. 2003;22(19):5273-82.

78. Lee SJ, Son YH, Lee KB, Lee JH, Kim HJ, Jeong EM, et al. 4-n-butylresorcinol enhances proteolytic degradation of tyrosinase in B16F10 melanoma cells. Int J Cosmet Sci. 2017;39(3):248-55.

79. Choi K, Siegel M, Piper JL, Yuan L, Cho E, Strnad P, et al. Chemistry and biology of dihydroisoxazole derivatives: selective inhibitors of human transglutaminase 2. Chem Biol. 2005;12(4):469-75.

80. Farrukh MR, Nissar UA, Afnan Q, Rafiq RA, Sharma L, Amin S, et al. Oxidative stress mediated Ca(2+) release manifests endoplasmic reticulum stress leading to unfolded protein response in UV-B irradiated human skin cells. J Dermatol Sci. 2014;75(1):24-35.

81. Abeyama K, Eng W, Jester JV, Vink AA, Edelbaum D, Cockerell CJ, et al. A role for NF-kappaB-dependent gene transactivation in sunburn. J Clin Invest. 2000;105(12):1751-9.

82. Kumar S, Mehta K. Tissue transglutaminase constitutively activates HIF-1alpha promoter and nuclear factor-kappaB via a non-canonical pathway. PLoS One. 2012;7(11):e49321.

83. Pitolli C, Pietroni V, Marekov L, Terrinoni A, Yamanishi K, Mazzanti C, et al. Characterization of TG2 and TG1-TG2 double knock-out mouse epidermis. Amino Acids. 2017;49(3):635-42.

84. Patterson RL, Boehning D, Snyder SH. Inositol 1,4,5-trisphosphate receptors as signal integrators. Annu Rev Biochem. 2004;73:437-65.

85. Oka M, Edamatsu H, Kunisada M, Hu L, Takenaka N, Dien S, et al. Enhancement of ultraviolet B-induced skin tumor development in phospholipase Cepsilon-knockout mice is associated with decreased cell death. Carcinogenesis. 2010;31(10):1897-902.

86. Oka M, Edamatsu H, Kunisada M, Hu L, Takenaka N, Sakaguchi M, et al. Phospholipase Cvarepsilon has a crucial role in ultraviolet B-induced neutrophil-associated skin inflammation by regulating the expression of CXCL1/KC. Lab Invest. 2011;91(5):711-8.

87. Hu L, Edamatsu H, Takenaka N, Ikuta S, Kataoka T. Crucial role of phospholipase Cepsilon in induction of local skin inflammatory reactions in the elicitation stage of allergic contact hypersensitivity. J Immunol. 2010;184(2):993-1002.

88. Takenaka N, Edamatsu H, Suzuki N, Saito H, Inoue Y, Oka M, et al. Overexpression of phospholipase Cepsilon in keratinocytes upregulates cytokine expression and causes dermatitis with acanthosis and T-cell infiltration. Eur J Immunol. 2011;41(1):202-13.

89. Mera K, Kawahara K, Tada K, Kawai K, Hashiguchi T, Maruyama I, et al. ER signaling is activated to protect human HaCaT keratinocytes from ER stress induced by environmental doses of UVB. Biochem Biophys Res Commun. 2010;397(2):350-4.

90. Hamada K, Terauchi A, Nakamura K, Higo T, Nukina N, Matsumoto N, et al. Aberrant calcium signaling by transglutaminase-mediated posttranslational modification of inositol 1,4,5-trisphosphate receptors. Proc

Natl Acad Sci U S A. 2014;111(38):E3966-75.

91. Begg GE, Holman SR, Stokes PH, Matthews JM, Graham RM, Iismaa SE. Mutation of a critical arginine in the GTP-binding site of transglutaminase 2 disinhibits intracellular cross-linking activity. J Biol Chem. 2006;281(18):12603-9.

92. Bergamini CM, Signorini M. Studies on tissue transglutaminases: interaction of erythrocyte type-2 transglutaminase with GTP. Biochem J. 1993;291 (Pt 1):37-9.

93. Kanchan K, Ergulen E, Kiraly R, Simon-Vecsei Z, Fuxreiter M, Fesus L. Identification of a specific one amino acid change in recombinant human transglutaminase 2 that regulates its activity and calcium sensitivity. Biochem J. 2013;455(3):261-72.

94. Lorand L, Conrad SM. Transglutaminases. Mol Cell Biochem. 1984;58(1-2):9-35.

95. Wilhelm B, Meinhardt A, Seitz J. Transglutaminases: purification and activity assays. J Chromatogr B Biomed Appl. 1996;684(1-2):163-77.

96. Kim IG, Gorman JJ, Park SC, Chung SI, Steinert PM. The deduced sequence of the novel protransglutaminase E (TGase3) of human and mouse. J Biol Chem. 1993;268(17):12682-90.

97. Kim SY, Chung SI, Steinert PM. Highly active soluble processed forms of the transglutaminase 1 enzyme in epidermal keratinocytes. J Biol Chem. 1995;270(30):18026-35.

98. Terazawa S, Mori S, Nakajima H, Yasuda M, Imokawa G. The UVB-

Stimulated Expression of Transglutaminase 1 Is Mediated Predominantly via the NFkappaB Signaling Pathway: New Evidence of Its Significant Attenuation through the Specific Interruption of the p38/MSK1/NFkappaBp65 Ser276 Axis. PLoS One. 2015;10(8):e0136311.

99. Biniek K, Levi K, Dauskardt RH. Solar UV radiation reduces the barrier function of human skin. Proc Natl Acad Sci U S A. 2012;109(42):17111-6.

100. Sakurai H, Chiba H, Miyoshi H, Sugita T, Toriumi W. IkappaB kinases phosphorylate NF-kappaB p65 subunit on serine 536 in the transactivation domain. J Biol Chem. 1999;274(43):30353-6.

101. Jiang X, Takahashi N, Matsui N, Tetsuka T, Okamoto T. The NF-kappa B activation in lymphotoxin beta receptor signaling depends on the phosphorylation of p65 at serine 536. J Biol Chem. 2003;278(2):919-26.

102. Mann AP, Verma A, Sethi G, Manavathi B, Wang H, Fok JY, et al. Overexpression of tissue transglutaminase leads to constitutive activation of nuclear factor-kappaB in cancer cells: delineation of a novel pathway. Cancer Res. 2006;66(17):8788-95.

103. Lee SJ, Lee KB, Son YH, Shin J, Lee JH, Kim HJ, et al. Transglutaminase 2 mediates UV-induced skin inflammation by enhancing inflammatory cytokine production. Cell Death Dis. 2017;8(10):e3148.

104. Kuttner V, Mack C, Gretzmeier C, Bruckner-Tuderman L, Dengjel J. Loss of collagen VII is associated with reduced transglutaminase 2 abundance and activity. J Invest Dermatol. 2014;134(9):2381-9.

105. Park CH, Lee MJ, Ahn J, Kim S, Kim HH, Kim KH, et al. Heat shock-induced matrix metalloproteinase (MMP)-1 and MMP-3 are mediated through ERK and JNK activation and via an autocrine interleukin-6 loop. J Invest Dermatol. 2004;123(6):1012-9.

106. Quan T, Little E, Quan H, Qin Z, Voorhees JJ, Fisher GJ. Elevated matrix metalloproteinases and collagen fragmentation in photodamaged human skin: impact of altered extracellular matrix microenvironment on dermal fibroblast function. J Invest Dermatol. 2013;133(5):1362-6.

107. Costa A, Eberlin S, Clerici SP, Abdalla BM. In vitro effects of infrared A radiation on the synthesis of MMP-1, catalase, superoxide dismutase and GADD45 alpha protein. Inflamm Allergy Drug Targets. 2015;14(1):53-9.

108. Kim HH, Lee MJ, Lee SR, Kim KH, Cho KH, Eun HC, et al. Augmentation of UV-induced skin wrinkling by infrared irradiation in hairless mice. Mech Ageing Dev. 2005;126(11):1170-7.

109. Rittie L, Fisher GJ. UV-light-induced signal cascades and skin aging. Ageing Res Rev. 2002;1(4):705-20.

110. Sardy M. Role of matrix metalloproteinases in skin ageing. Connect Tissue Res. 2009;50(2):132-8.

111. Brennan M, Bhatti H, Nerusu KC, Bhagavathula N, Kang S, Fisher GJ, et al. Matrix metalloproteinase-1 is the major collagenolytic enzyme responsible for collagen damage in UV-irradiated human skin. Photochem Photobiol. 2003;78(1):43-8.

112. Chhabra A, Jaiswal A, Malhotra U, Kohli S, Rani V. Cell in situ

zymography: an in vitro cytotechnology for localization of enzyme activity in cell culture. In Vitro Cell Dev Biol Anim. 2012;48(8):463-8.

113. Kim MK, Shin JM, Eun HC, Chung JH. The role of p300 histone acetyltransferase in UV-induced histone modifications and MMP-1 gene transcription. PLoS One. 2009;4(3):e4864.

114. Bruls WA, Slaper H, van der Leun JC, Berrens L. Transmission of human epidermis and stratum corneum as a function of thickness in the ultraviolet and visible wavelengths. Photochem Photobiol. 1984;40(4):485-94.

115. Quan T, Qin Z, Xia W, Shao Y, Voorhees JJ, Fisher GJ. Matrix-degrading metalloproteinases in photoaging. J Investig Dermatol Symp Proc. 2009;14(1):20-4.

116. Schorpp M, Mattei MG, Herr I, Gack S, Schaper J, Angel P. Structural organization and chromosomal localization of the mouse collagenase type I gene. Biochem J. 1995;308 (Pt 1):211-7.

117. Snoek-van Beurden PA, Von den Hoff JW. Zymographic techniques for the analysis of matrix metalloproteinases and their inhibitors. Biotechniques. 2005;38(1):73-83.

118. Liu P, Sun M, Sader S. Matrix metalloproteinases in cardiovascular disease. Can J Cardiol. 2006;22 Suppl B:25B-30B.

119. Gasche Y, Copin JC, Sugawara T, Fujimura M, Chan PH. Matrix metalloproteinase inhibition prevents oxidative stress-associated blood-brain barrier disruption after transient focal cerebral ischemia. J Cereb Blood Flow Metab. 2001;21(12):1393-400.

120. Chiang HM, Chen HC, Chiu HH, Chen CW, Wang SM, Wen KC. Neonauclea reticulata (Havil.) Merr Stimulates Skin Regeneration after UVB Exposure via ROS Scavenging and Modulation of the MAPK/MMPs/Collagen Pathway. Evid Based Complement Alternat Med. 2013;2013:324864.

121. Shaulian E, Karin M. AP-1 as a regulator of cell life and death. Nat Cell Biol. 2002;4(5):E131-6.

122. Benbow U, Brinckerhoff CE. The AP-1 site and MMP gene regulation: what is all the fuss about? Matrix Biol. 1997;15(8-9):519-26.

123. Vincenti MP, Brinckerhoff CE. Transcriptional regulation of collagenase (MMP-1, MMP-13) genes in arthritis: integration of complex signaling pathways for the recruitment of gene-specific transcription factors. Arthritis Res. 2002;4(3):157-64.

124. Pulverer BJ, Kyriakis JM, Avruch J, Nikolakaki E, Woodgett JR. Phosphorylation of c-jun mediated by MAP kinases. Nature. 1991;353(6345):670-4.

125. Bond M, Baker AH, Newby AC. Nuclear factor kappaB activity is essential for matrix metalloproteinase-1 and -3 upregulation in rabbit dermal fibroblasts. Biochem Biophys Res Commun. 1999;264(2):561-7.

126. Schwabe RF, Sakurai H. IKKbeta phosphorylates p65 at S468 in transactivaton domain 2. FASEB J. 2005;19(12):1758-60.

127. Buss H, Dorrie A, Schmitz ML, Frank R, Livingstone M, Resch K, et al. Phosphorylation of serine 468 by GSK-3beta negatively regulates basal p65 NF-kappaB activity. J Biol Chem. 2004;279(48):49571-4.

128. Geng H, Wittwer T, Dittrich-Breiholz O, Kracht M, Schmitz ML. Phosphorylation of NF-kappaB p65 at Ser468 controls its COMMD1-dependent ubiquitination and target gene-specific proteasomal elimination. EMBO Rep. 2009;10(4):381-6.

129. Sarkany I, Grice K, Caron GA. Organ Culture of Adult Human Skin. Br J Dermatol. 1965;77:65-76.

130. Beaven EP, Cox AJ, Jr. Organ Culture of Human Skin. J Invest Dermatol. 1965;44:151-6.

131. Curro M, Gangemi C, Giunta ML, Ferlazzo N, Navarra M, Ientile R, et al. Transglutaminase 2 is involved in amyloid-beta1-42-induced pro-inflammatory activation via AP1/JNK signalling pathways in THP-1 monocytes. Amino Acids. 2017;49(3):659-69.

132. Park MK, You HJ, Lee HJ, Kang JH, Oh SH, Kim SY, et al. Transglutaminase-2 induces N-cadherin expression in TGF-beta1-induced epithelial mesenchymal transition via c-Jun-N-terminal kinase activation by protein phosphatase 2A down-regulation. Eur J Cancer. 2013;49(7):1692-705.

133. Park MK, Lee HJ, Shin J, Noh M, Kim SY, Lee CH. Novel participation of transglutaminase-2 through c-Jun N-terminal kinase activation in sphingosylphosphorylcholine-induced keratin reorganization of PANC-1 cells. Biochim Biophys Acta. 2011;1811(12):1021-9.

134. Szoka L, Karna E, Palka JA. UVC inhibits collagen biosynthesis through up-regulation of NF-kappaB p65 signaling in cultured fibroblasts. J Photochem Photobiol B. 2013;129:143-8.

135. Kouba DJ, Chung KY, Nishiyama T, Vindevoghel L, Kon A, Klement JF, et al. Nuclear factor-kappa B mediates TNF-alpha inhibitory effect on alpha 2(I) collagen (COL1A2) gene transcription in human dermal fibroblasts. J Immunol. 1999;162(7):4226-34.

136. Mattioli I, Geng H, Sebald A, Hodel M, Bucher C, Kracht M, et al. Inducible phosphorylation of NF-kappa B p65 at serine 468 by T cell costimulation is mediated by IKK epsilon. J Biol Chem. 2006;281(10):6175-83.

137. Tang Q, Gonzales M, Inoue H, Bowden GT. Roles of Akt and glycogen synthase kinase 3beta in the ultraviolet B induction of cyclooxygenase-2 transcription in human keratinocytes. Cancer Res. 2001;61(11):4329-32.

138. Yang Y, Wang H, Wang S, Xu M, Liu M, Liao M, et al. GSK3beta signaling is involved in ultraviolet B-induced activation of autophagy in epidermal cells. Int J Oncol. 2012;41(5):1782-8.

139. Huang TT, Feinberg SL, Suryanarayanan S, Miyamoto S. The zinc finger domain of NEMO is selectively required for NF-kappa B activation by UV radiation and topoisomerase inhibitors. Mol Cell Biol. 2002;22(16):5813-25.

140. O'Dea EL, Kearns JD, Hoffmann A. UV as an amplifier rather than inducer of NF-kappaB activity. Mol Cell. 2008;30(5):632-41.

141. Tsuchiya Y, Asano T, Nakayama K, Kato T, Jr., Karin M, Kamata H. Nuclear IKKbeta is an adaptor protein for IkappaBalpha ubiquitination and

degradation in UV-induced NF-kappaB activation. Mol Cell. 2010;39(4):570-82.

142. Dedinszki D, Sipos A, Kiss A, Batori R, Konya Z, Virag L, et al. Protein phosphatase-1 is involved in the maintenance of normal homeostasis and in UVA irradiation-induced pathological alterations in HaCaT cells and in mouse skin. Biochim Biophys Acta. 2015;1852(1):22-33.

143. Brozyna AA, Jozwicki W, Carlson JA, Slominski AT. Melanogenesis affects overall and disease-free survival in patients with stage III and IV melanoma. Hum Pathol. 2013;44(10):2071-4.

144. Slominski RM, Zmijewski MA, Slominski AT. The role of melanin pigment in melanoma. Exp Dermatol. 2015;24(4):258-9.

145. Gillbro JM, Olsson MJ. The melanogenesis and mechanisms of skin-lightening agents--existing and new approaches. Int J Cosmet Sci. 2011;33(3):210-21.

146. Imokawa G, Mishima Y. Functional analysis of tyrosinase isozymes of cultured malignant melanoma cells during the recovery period following interrupted melanogenesis induced by glycosylation inhibitors. J Invest Dermatol. 1984;83(3):196-201.

147. Franchi J, Coutadeur MC, Marteau C, Mersel M, Kupferberg A. Depigmenting effects of calcium D-pantetheine-S-sulfonate on human melanocytes. Pigment Cell Res. 2000;13(3):165-71.

148. Wood JM, Schallreuter KU. Studies on the reactions between human tyrosinase, superoxide anion, hydrogen peroxide and thiols. Biochim Biophys

Acta. 1991;1074(3):378-85.

149. Briganti S, Camera E, Picardo M. Chemical and instrumental approaches to treat hyperpigmentation. Pigment Cell Res. 2003;16(2):101-10.

150. Hiasa M, Kurokawa M, Ohta K, Esumi T, Akita H, Niki K, et al. Identification and purification of resorcinol, an antioxidant specific to Awa-ban (pickled and anaerobically fermented) tea. Food Res Int. 2013;54(1):72-80.

151. Shimizu K, Kondo R, Sakai K, Takeda N, Nagahata T, Oniki T. Novel vitamin E derivative with 4-substituted resorcinol moiety has both antioxidant and tyrosinase inhibitory properties. Lipids. 2001;36(12):1321-6.

152. Cervellati R, Innocenti G, Dall'Acqua S, Costa S, Sartini E. Polyphenols from Polygala spp. and their antioxidant activity. Chem Biodivers. 2004;1(3):415-25.

153. Jeong EM, Kim I-G. Regulation of Transglutaminase 2 by Oxidative Stress. In: Hitomi K, Kojima S, Fesus L, editors. Transglutaminases: Springer.

154. Kondo S. The roles of cytokines in photoaging. J Dermatol Sci. 2000;23 Suppl 1:S30-6.

155. Kondo S, Kooshesh F, Sauder DN. Penetration of keratinocyte-derived cytokines into basement membrane. J Cell Physiol. 1997;171(2):190-5.

156. Agren MS, Schnabel R, Christensen LH, Mirastschijski U. Tumor necrosis factor-alpha-accelerated degradation of type I collagen in human skin is associated with elevated matrix metalloproteinase (MMP)-1 and MMP-3 ex vivo. Eur J Cell Biol. 2015;94(1):12-21.

157. Wong WR, Kossodo S, Kochevar IE. Influence of cytokines on matrix

metalloproteinases produced by fibroblasts cultured in monolayer and collagen gels. J Formos Med Assoc. 2001;100(6):377-82.

158. Hozawa S, Nakamura T, Nakano M, Adachi M, Tanaka H, Takahashi Y, et al. Induction of matrix metalloproteinase-1 gene transcription by tumour necrosis factor alpha via the p50/p50 homodimer of nuclear factor-kappa B in activated human hepatic stellate cells. Liver Int. 2008;28(10):1418-25.

159. Montier Y, Lorentz A, Kramer S, Sellge G, Schock M, Bauer M, et al. Central role of IL-6 and MMP-1 for cross talk between human intestinal mast cells and human intestinal fibroblasts. Immunobiology. 2012;217(9):912-9.

160. Sakai T, Kambe F, Mitsuyama H, Ishiguro N, Kurokouchi K, Takigawa M, et al. Tumor necrosis factor alpha induces expression of genes for matrix degradation in human chondrocyte-like HCS-2/8 cells through activation of NF-kappaB: abrogation of the tumor necrosis factor alpha effect by proteasome inhibitors. J Bone Miner Res. 2001;16(7):1272-80.

161. Lee J, Jung E, Lee J, Huh S, Hwang CH, Lee HY, et al. Emodin inhibits TNF alpha-induced MMP-1 expression through suppression of activator protein-1 (AP-1). Life Sci. 2006;79(26):2480-5.

162. Wlaschek M, Heinen G, Poswig A, Schwarz A, Krieg T, Scharffetter-Kochanek K. UVA-induced autocrine stimulation of fibroblast-derived collagenase/MMP-1 by interrelated loops of interleukin-1 and interleukin-6. Photochem Photobiol. 1994;59(5):550-6.

163. Irwin CR, Myrillas TT, Traynor P, Leadbetter N, Cawston TE. The role of soluble interleukin (IL)-6 receptor in mediating the effects of IL-6 on matrix

metalloproteinase-1 and tissue inhibitor of metalloproteinase-1 expression by gingival fibroblasts. J Periodontol. 2002;73(7):741-7.

164. Chung JH, Seo JY, Lee MK, Eun HC, Lee JH, Kang S, et al. Ultraviolet modulation of human macrophage metalloelastase in human skin in vivo. J Invest Dermatol. 2002;119(2):507-12.

165. Lee PL, van Weelden H, Bruijnzeel PL. Neutrophil infiltration in normal human skin after exposure to different ultraviolet radiation sources. Photochem Photobiol. 2008;84(6):1528-34.

Abstract in Korean

국 문 초 록

자외선에 의해 유도되는 피부 반응의 분자기전

서울대학교 대학원

의과학과 의과학전공

이 석 진

사람의 피부는 외부 환경에 직접적으로 노출되어 있기 때문에 다양한 환경적인 자극들에 의해 손상된다. 여러 자극들 중에서도 자외선이 가장 큰 영향을 미친다고 알려져 있다. 자외선에 노출된 피부는 급성 반응으로써 일광화상 (sunburn), 태닝반응 (tanning response)과 같은 특징을 나타내며, 자외선에 만성적으로 노출된 피부는 피부암 발병 위험의 증가, 면역 기능의 억제, 주름의 증가와 같은 병리적 특징을 보인다. 자외선에 의해 나타나는 여러가지 피부 반응들 중에서 태닝반응, 일광화상, 주름 생성과 같은 특징들은 임상과 미용 분야에서 활발히 연구되고 있는 주제이다.

제 1 장에서는, 4-n-butylresorcinol 에 의한 항-멜라닌합성의 분자기전을 연구하였다. 4-n-butylresorcinol 은 티로시네이즈(tyrosinase)의

억제제로 작용함으로써 항-멜라닌합성 물질로써 사용되고 있다. 하지만, 이 물질의 세포내 작용 기전에 대해서는 크게 알려진 바가 없다. 본 연구에서는, 4-n-butylresorcinol 이 티로시네이즈의 mRNA 수준에는 영향을 주지 않으면서, 단백질 분해는 촉진함으로써, 티로시네이즈의 단백질 양을 조절함을 관찰하였다. 4-n-butylresorcinol 은 p38 MAPK 를 활성화 시킴으로써 티로시네이즈의 ubiquitination 에 영향을 주었다. B16F10 흑색종 세포에 E64 또는 proteasome 억제제를 처리하자, 4-n-butylresorcinol 에 의해 감소된 티로시네이즈의 수준이 회복되는 것을 확인하였다. 본 연구를 통해 과색소형성 질환의 치료를 위한 좀 더 효과적이고, 안전한 새로운 물질 개발에 도움을 줄 수 것이다.

제 2 장과 3 장에서는 자외선에 노출된 표피와 진피에서의 트랜스글루타미네이즈 2 (transglutaminase 2 또는 TG2) 의 역할에 대해 규명하였다. TG2 는 기질 단백질의 crosslinking, polyamination, deamidation 과 같은 번역 후 변형 (posttranslational modification)을 조절하는 효소이다. 표피와 진피의 세포들은 TG2 를 발현하고 있음에도 불구하고, 현재까지 TG2 의 피부 항상성 조절 기전에 대한 연구는 이루어진 바 없다.

제 2 장에서는, 사람과 생쥐의 각질형성세포 (keratinocyte)와 TG2 가 결핍된 형질전환생쥐를 이용하여, 자외선에 노출된 피부의

급성 염증 반응에서 TG2 의 역할에 대해 규명하였다. TG2 가 결핍된 생쥐는 자외선에 노출 된 뒤, 홍반 (erythema), 부종 (edema), 혈관 확장 (dilation of blood vessels), 염증성 사이토카인의 발현 (inflammatory cytokines) 등과 같은 피부 염증의 특징들이 현저히 감소하였다. 불멸화된 인간 각질형성세포인 HaCaT 세포와, 생쥐에서 얻은 각질형성세포에 자외선을 조사하자 TG2 의 단백질 수준에는 영향을 미치지 않으면서 효소 활성이 증가하는 것을 관찰하였고, 이 과정에서 자외선에 의한 PLC-IP_3-IP_3R 신호전달계의 활성화와 뒤 이은 세포질로의 ER 내 칼슘이온 방출이 TG2 의 효소 활성을 유도하는데 있어 중요함을 확인하였다. 또한 활성화된 TG2 는 전사 인자인 NF-κB 의 전사 활성을 증가시킴으로써, IL-6, IL-8, TNF-α 와 같은 염증성 사이토카인의 발현을 유도하였다. 이러한 결과들은 TG2 가 자외선에 노출된 각질형성세포에서 사이토카인의 발현을 조절함으로써 염증반응을 매개하는 중요한 매개자임을 시사하며, TG2 의 억제가 일광 화상을 예방하는 데 있어 유용한 표적이 될 수 있음을 제시한다.

제 3 장에서는, 사람과 생쥐의 진피 섬유아세포 (dermal fibroblast)와 *ex vivo* 피부 배양 모델을 이용하여, 자외선에 노출된 섬유아세포에서 TG2 의 세포내 역할을 규명하였다. 본 연구에서, 자외선에 노출된 섬유아세포의 TG2 는 단백질 수준뿐만 아니라

효소 활성의 증가를 통해 사람의 MMP-1 과 MMP-3, 그리고 생쥐의 MMP-13 의 발현을 조절함을 확인하였다. 또한, TG2 는 AP-1 이 아닌, NF-κB 의 전사 활성을 증가시킴으로써 MMP 유전자의 발현을 조절하였다. 이 연구는 TG2 가 광노화와 같은 자외선에 의해 유발되는 피부질환의 치료를 위한 새로운 표적이 될 수 있음을 시사한다.

요약하면, 위의 연구들은 자외선에 노출된 멜라닌형성세포, 각질형성세포, 섬유아세포와 같은 피부 세포들의 반응을 분자수준에서 규명하는데 초점을 맞추어 진행되었다. 본 연구 결과들을 통해서 자외선에 의한 피부 손상의 치료를 위한 새로운 분자 기전을 제시할 수 있을 것이라 기대한다.

주요어: 4-n-butylresorcinol, 태닝반응, 티로시네이즈, 트랜스글루타미네이즈 2, 염증성 사이토카인, MMP, NF-κB, 자외선

학번: 2008-22006